



**WPI**

# Renewable Hybrid Optimized Microgrid Energy [RHOME]

A Major Qualifying Project  
Submitted to the Faculty of the  
WORCESTER POLYTECHNIC INSTITUTE  
in partial fulfillment of the requirements for the  
Degree of Bachelor of Science

by

Alexander Galvin  
Domenic Sena  
Elie DeLaville  
Thomas Rua  
Vincent Vu

Date:

March 25th, 2025

Report Submitted to:

Professor Gregory Noetscher - Worcester Polytechnic Institute

This report represents the work of WPI undergraduate students submitted to the faculty as evidence of a degree requirement. WPI routinely publishes these reports on its website without editorial or peer review. For more information about the projects program at WPI, please see

<http://www.wpi.edu/Academics/Projects>.

# Abstract

This MQP addresses global energy accessibility challenges and provides a simulation framework for hybrid renewable microgrids (MGs) in remote areas, using South Sudan as its main case study. Even though earth's renewable resources potential is substantial, a large percentage of the world population still lacks reliable access to electricity. Our project shows that sustainable energy solutions are cost competitive and cleaner than mainstream non-renewable energy alternatives at decentralized energy systems. The Renewable Hybrid Optimized Microgrid Energy (RHOME) model was developed using a dual simulation approach, merging high level techno-economic analysis with bottom-up power system functionality in MATLAB/Simulink. The model simultaneously includes multiple renewable and traditional energy sources. The model also describes their dynamic interactions in diverse scenarios. We find that appropriately designed hybrid MGs can achieve high levels of renewable penetration and meet reliability standards across all possible operating conditions. Training up to 2023 data, the RHOME model enables real-time visualization of the performance of a system and comparison of different scenarios, providing essential information for deploying sustainable energy solutions in marginalized areas. This research significantly tackles a key challenge in global development by carefully optimizing technical performance, cost-effectiveness, and environmental impact to enable universal electricity access that is reliable, affordable, and containable in underserved grid infrastructure contexts.

# Acknowledgments

Our team would like to thank the following individuals for their support on our project:

**Professor Noetscher**, for his continuous guide throughout the efforts on the project.

**Alexander Tang**, Associate Director of Advanced Energy at TRC companies, for his cooperation and knowledge on microgrids.

**Adam Eberwein**, Technical Lead at Earthspark International, for his cooperation and knowledge on remote microgrid deployment.

# Table of Authorship

<i>Section</i>	<i>Author</i>
<b>Abstract</b>	<b>Thomas</b>
<b>Introduction</b>	<b>Alexander</b>
<b>1.1) Microgrid Basics &amp; Standards</b>	<b>Alexander &amp; Thomas</b>
<b>1.1.1) Islanded v. Grid Connected</b>	<b>Thomas</b>
<b>1.1.2) IEEE Standards and Domains</b>	<b>Alexander</b>
<b>1.1.2.1) Generation</b>	<b>Thomas</b>
<b>1.1.2.2) Storage</b>	<b>Vincent</b>
<b>1.1.2.3) Distribution</b>	<b>Alexander &amp; Elie</b>
<b>1.1.2.4) Controls</b>	<b>Elie</b>
<b>1.1.2.5) Finances</b>	<b>Thomas</b>
<b>1.1.2.6) Load</b>	<b>Domenic</b>
<b>1.2) Microgrid Controllers</b>	<b>Elie</b>
<b>1.3) Resource Options</b>	<b>Thomas</b>
<b>1.3.1) Diesel</b>	<b>Domenic</b>
<b>1.3.2) PV Solar</b>	<b>Alexander &amp; Thomas</b>
<b>1.3.3) Solar Thermal</b>	<b>Alexander</b>
<b>1.3.4) Wind</b>	<b>Elie</b>
<b>1.3.5) Biomass</b>	<b>Thomas</b>
<b>1.3.6) Hydro</b>	<b>Thomas &amp; Vincent</b>
<b>1.3.7) Geothermal</b>	<b>Thomas</b>
<b>1.4) Storage</b>	<b>Vincent</b>
<b>1.4.1) Lithium-ion Batteries</b>	<b>Vincent</b>
<b>1.4.2) Pumped Hydro</b>	<b>Alexander</b>
<b>1.4.3) Fuel Cells</b>	<b>Alexander</b>

<b>1.4.4) Compressed Air</b>	<b>Vincent</b>
<b>1.5) Location Planning &amp; Selection</b>	<b>Thomas</b>
<b>1.5.1) South Sudan</b>	<b>Thomas &amp; Alexander</b>
<b>1.6) Carbon Footprint</b>	<b>Domenic</b>
<b>2.1) Microgrid Simulations</b>	<b>Thomas &amp; Domenic</b>
<b>2.2) High-Level-Simulations</b>	<b>Thomas &amp; Domenic</b>
<b>2.2.1) HOMER Pro</b>	<b>Thomas &amp; Alexander</b>
<b>2.2.2) Sandia's MDT</b>	<b>Elie</b>
<b>2.2.3) Xendee</b>	<b>Vincent</b>
<b>2.3) Low-Level Simulation</b>	<b>Thomas &amp; Domenic</b>
<b>2.3.1) MATLAB/Simulink Software</b>	<b>Thomas</b>
<b>2.3.2) Renewable Hybrid Optimized Energy (RHOME) Model</b>	<b>Thomas</b>
<b>2.3.3) RHOME Subsystems</b>	<b>ALL</b>
<b>2.4) Visual Interactive Component/GUI</b>	<b>Thomas &amp; Elie</b>
<b>2.4.1) Weather Data Analysis &amp; Condition Classification</b>	<b>Thomas</b>
<b>2.4.2) Interactive Dashboard</b>	<b>Thomas</b>
<b>2.4.3) Power Generation Suitability Conditions</b>	<b>Thomas</b>
<b>2.4.4) User Input</b>	<b>Thomas</b>
<b>2.5) Additional Simulation Features</b>	<b>Thomas</b>
<b>2.5.1) Energy Calculations</b>	<b>Thomas</b>
<b>2.5.2) Economical &amp; Environmental Metrics</b>	<b>Thomas</b>
<b>3.1) PV Solar</b>	<b>Alexander &amp; Thomas</b>
<b>3.2) Wind</b>	<b>Alexander</b>
<b>3.3) Battery</b>	<b>Alexander</b>
<b>3.4) Diesel Generator</b>	<b>Alexander</b>
<b>3.5) General System</b>	<b>Alexander</b>

<b>3.6) Cost Analysis</b>	<b>Alexander</b>
<b>4.1) High-level Results</b>	<b>Alexander &amp; Thomas</b>
<b>4.2) Low-level Results</b>	<b>Thomas</b>
<b>4.2.1) Excellent Conditions</b>	<b>Thomas</b>
<b>4.2.2) Typical Conditions</b>	<b>Alexander</b>
<b>4.2.3) Worst Conditions</b>	<b>Elie</b>
<b>4.2.4) User-input</b>	<b>Vincent</b>
<b>5.1) Economics</b>	<b>Alexander</b>
<b>5.2) Electrical</b>	<b>Elie</b>
<b>5.2.1) Solar</b>	<b>Elie</b>
<b>5.2.2) Wind</b>	<b>Elie</b>
<b>5.2.3) Battery</b>	<b>Elie</b>
<b>5.2.4) Diesel Generator</b>	<b>Elie</b>
<b>5.2.5) Renewable Penetration</b>	<b>Elie</b>
<b>5.2.6) Carbon Emission</b>	<b>Elie</b>
<b>5.2.7) Overall Resource Comparison</b>	<b>Elie</b>
<b>5.3) Reliability</b>	<b>Thomas</b>
<b>5.4) Feasibility</b>	<b>Thomas</b>
<b>5.5) Potential Enhancements</b>	<b>Vincent</b>
<b>5.6) Consideration of Public Health &amp; Other Factors</b>	<b>Thomas &amp; Domenic</b>
<b>5.7) Recognizing Ethical and Professional Responsibilities</b>	<b>Domenic</b>
<b>Conclusion</b>	<b>Thomas</b>
<b>References</b>	<b>Domenic</b>

## List of Abbreviations

---

Abbreviation	Definition
\$	United States Dollar
AC	Alternating Current
ADMS	Advanced Distribution Management System
AVR	Automatic Voltage Regulator
BESS	Battery Energy Storage System
BMS	Battery Management System
BOS	Balance-of-system
CAPEX	Capital Expenditure
CF	Capacity Factor
CHP	Combined Heat and Power
CPN	Customer Premises Network
CT-IAP	Communication Technology Interoperability Architectural Perspective
CRF	Capital Recovery Factor
DC	Direct Current
DER	Distributed Energy Resources
DERMS	Distributed Energy Resources Management Systems
DNP	Distributed Network Protocol
DOE	Department of Energy
DR	Distributed Resource
EMS	Energy Management Systems
ESI	Energy Services Interfaces
ESS	Energy Storage System
FAN	Field Area Network
FCR	Fixed Charge Rate
HMI	Human-machine Interface
HOMER	Hybrid Optimization Model for Multiple Energy Resources
HVAC	Heating Ventilation Air Conditioning
IEA	International Energy Agency
IEEE	Institute of Electrical and Electronic Engineers
IMG	Islanded Microgrid
IT-IAP	Information Technology Interoperability Architectural Perspective
KPI	Key Performance Indicator
LCOE	Levelized Cost of Energy
LF	Levelizing Factor
MCG	Cummins PowerCommand MG Control

---

<b>Abbreviation</b>	<b>Definition</b>
MCP	Market Clearing Pricing
MDT	Microgrid Design Toolkit
MG	Microgrid
MTU	Master Terminal Units
NPC	Net Present Cost
NREL	National Renewable Energy Lab
NTD	Nile Trading and Development
O&M	Operation & Maintenance
PCS	Power Conversion System
PEV	Plug-In Electric Vehicle
PLC	Programmable Logic Controllers
PMS	Power Management System
POC	Protection of Civilians
POWER	Prediction Of Worldwide Energy Resources
PS-IAP	Power Systems Interoperability Architectural Perspective
PV	Photovoltaic
RHOME	Renewable Hybrid Optimized Microgrid Energy
ROI	Return on Investment
RTU	Remote Terminal Units
SCADA	Supervisory Control and Data Acquisition
SEL	Schweitzer Engineering Laboratories
SOC	State of Charge
SoH	State of Health
UNMISS	United Nations Mission in South Sudan
WAN	Wide Area Network

---

# Table of Contents

<b>Abstract.....</b>	<b>2</b>
<b>Acknowledgments.....</b>	<b>3</b>
<b>Table of Authorship.....</b>	<b>4</b>
<b>List of Abbreviations.....</b>	<b>7</b>
<b>Table of Contents.....</b>	<b>9</b>
<b>Introduction.....</b>	<b>11</b>
<b>Background.....</b>	<b>12</b>
1.1) Microgrid basics and standards.....	12
1.1.1) Islanded vs grid-connected.....	12
1.1.2) IEEE Standards and Domains.....	12
1.1.2.1) Generation.....	14
1.1.2.2) Storage.....	16
1.1.2.3) Distribution.....	17
1.1.2.4) Controls.....	20
1.1.3.5) Finances.....	22
1.1.3.6) Load.....	23
1.2) Microgrid Controllers.....	25
1.3) Resource options.....	26
1.3.1) Diesel.....	26
1.3.2) PV Solar.....	27
1.3.3) Solar Thermal.....	29
1.3.4) Wind.....	30
1.3.5) Biomass.....	32
1.3.6) Hydro.....	33
1.3.7) Geothermal.....	33
1.4) Storage.....	34
1.4.1) Lithium-ion Battery.....	34
1.4.2) Pumped Hydro.....	35
1.4.3) Fuel Cells.....	35
1.4.4) Compressed Air.....	35
1.5) Location Planning and Selection.....	36
1.5.1) South Sudan.....	36
1.5.1.1) Juba.....	37
1.5.1.2) Bentiu.....	38
1.5.1.3) Wau.....	38
1.6) Carbon Footprint.....	39

<b>High-Level Simulation Layers in Microgrid Design.....</b>	<b>41</b>
2.1) General Information about Microgrid Simulations.....	41
2.2) High-Level Simulations.....	41
2.2.1) HOMER Pro.....	42
2.2.2) Sandia's MDT.....	44
2.2.3) Xendee.....	45
<b>Low-Level Simulation Layers in Microgrid Design.....</b>	<b>49</b>
3.1) MATLAB/Simulink Software.....	49
3.2) Renewable Hybrid Optimized MG Energy (RHOME) Model.....	50
3.3.1) RHOME Subsystems.....	52
3.3.3.1) Solar PV.....	52
3.3.3.2) Wind.....	58
3.3.3.3) Diesel Generator.....	61
3.3.3.4) Battery.....	65
3.3.3.5) Total Variable Load.....	68
3.3.3.6) Inverter Controllers.....	70
3.3.3.7) Power Management System.....	72
3.4) Visual Interactive Component / GUI.....	74
3.4.1) Weather data Analysis and Condition Classification.....	74
3.4.2) Interactive Dashboard.....	75
3.4.3) Power Generation Suitability Conditions.....	76
3.4.4) User input.....	77
3.5) Additional Simulation Features.....	78
3.5.1) Energy Calculations.....	78
3.5.2) Economical and Environmental Metrics.....	79
<b>Economical Optimization.....</b>	<b>82</b>
4.1) PV Solar.....	82
4.2) Wind.....	83
4.3) Battery.....	84
4.4) Diesel Generator.....	84
4.5) General System.....	84
4.6) Cost Analysis.....	88
<b>Results.....</b>	<b>91</b>
5.1) High-level Results.....	91
5.2) Low-Level RHOME Results.....	95
5.2.1) Excellent Conditions.....	95
5.2.2) Typical Conditions.....	100
5.2.3) Worst Conditions.....	104
5.2.4) User-input.....	109

<b>Analysis &amp; Discussion.....</b>	<b>114</b>
6.1) Economics.....	114
6.2) Electrical.....	115
6.2.1) Solar.....	115
6.2.2) Wind.....	116
6.2.3) Battery.....	116
6.2.4) Diesel Generator.....	116
6.2.5) Renewable Penetration.....	117
6.2.6) Carbon Emission.....	117
6.2.7) Overall Resource Comparison.....	118
6.3) Reliability.....	118
6.4) Feasibility.....	119
6.5) Potential Enhancements.....	120
6.6) Consideration of Public Health and Other Factors.....	122
6.7) Recognizing Ethical and Professional Responsibilities.....	123
<b>Conclusion.....</b>	<b>124</b>
<b>References.....</b>	<b>125</b>

# Introduction

South Sudan is among the least electrified countries in the world. According to the World Bank, only 8.4% of South Sudan has access to electricity [i]. Decentralized energy systems have emerged as viable solutions to these problems. According to the U.S. Department of Energy, a microgrid (MG) is a group of interconnected loads and distributed energy resources (DER) within clearly defined electrical boundaries that act as a single controllable entity with respect to the grid [ii]. Duke energy defines 3 types of MG that are transforming the industry: remote MG, grid-connected MG, and networked MG [iii]. Particularly, remote MG, also known as islanded microgrids (IMG), are physically isolated from the utility grid and operate in island mode at all times due to the lack of available and affordable transmission or distribution infrastructure nearby. If these MG are implemented, they have the potential to provide electricity to those in need.

The goal of our project is to create a comprehensive and interactive simulation in Simulink to inform a potential project in Juba, South Sudan. To achieve this goal, we utilized high-level MG simulations to approximate solutions in order to sustain the energy needs of a remote location. Based on these results, we designed a low-level simulation in Simulink MATLAB to determine which elements are the highest predictors of desired outcomes. Then, we optimized the highest predictors of desired outcomes via technical modifications and algorithms. Finally, we enhanced the low-level simulation to become visually interactive and illustrate varying MG scenarios by simplified adjustable parameters.

To achieve these goals, HOMER Pro, a high level MG simulation software, was used to estimate basic parameters of a MG needed to guide the creation of a low level simulation in Simulink. The low level simulation contained the power generation sources, energy management system (EMS), grid controller, as well as the estimated load. Once the basic simulation was completed, it became technically, economically, and environmentally optimized. The interactive component of the simulation incorporates various visual metrics and adjustable components for specific scenario customization.

This paper provides background on various renewable energy resources, standards, MG components, and considered locations in South Sudan for the MG to be accustomed to. The bulk of this report provides a detailed explanation of the functionality of HOMER Pro, how it was used, and primarily the functionality and breakdown of the low level version of the MG in Simulink. Along with the simulation, this report breaks down real world components of the MG and how they inform the economic metrics. Finally, the results of simulations inform the feasibility of the IMG system and potential for improving the design.

# Background

## 1.1) Microgrid basics and standards

The Department of Energy (DOE) defines a MG as an electrical system that “acts as a single controllable entity”, and utilizes distributed DERs and energy storage to power a small specific area. MGs can operate independently of the main electrical grid. They are often powered by renewable technologies like wind, solar, biomass, hydro, and geothermal. MGs also integrate information and communication technology to optimize cost and performance of electrical distribution [1]. Four important considerations need to be addressed before starting MG design: system characterization, the identification of policy and regulatory constraints, definition of design basis threats, and identification of critical loads. The system is characterized by the needs of those who will use the grid, which will influence the size, capacity, location, possible power generation and energy storage methods, and cost of the MG. Identification of policy and regulation constraints will determine the regulatory boundaries imposed on the system. Defining design-based threats will outline the potential risks to the MG in terms of weather, conflict, natural disasters, and other potential threats. The identification of critical loads allows the system to be designed to prioritize power to certain loads in the event of a power outage or drop in power output [2]. Based on interviews with Alex Tang, Associate Director of Advanced Energy at TRC Companies, and Adam Eberwein, Technical Lead at EarthSpark International, it was determined that cost is the most important factor in determining the feasibility of constructing a MG. Although MGs are technically feasible, they are only realistic if they are cost-effective.

[Alexander Tang, September 12, 2024] [Adam Eberwein, September 19, 2024]

### 1.1.1) Islanded vs grid-connected

The National Renewable Energy Lab (NREL) acknowledges that MGs exhibit the unique ability to seamlessly transition between grid-connected operation and islanded mode. In grid-connected mode, MGs integrate with the main power infrastructure, but during islanded mode, they function as autonomous energy systems. This dual-mode capability enables power reliability for consumers and enhances the overall energy network's resilience against potential disturbances [3]. MGs show great promise in providing reliable and environmentally friendly power to remote areas and systems not connected to the main grid. However, managing MGs requires coordinating various local energy sources and changing power needs effectively. The challenge lies in keeping the system efficient, stable, dependable, and self-sufficient, while also preparing it for unexpected issues. Consequently, analyzing different EMS and identifying aspects for optimization is crucial for providing more impactful energy access solutions [4].

### 1.1.2) IEEE Standards and Domains

IMGs are the main focus of this project, with the intention of providing power to remote populations lacking access to centralized infrastructure. This project aligns with the Institute of Electrical and Electronic Engineers (IEEE) Guide for Distributed Energy Resources Management Systems (DERMS) Functional Specification [45]. The design of the MG is based on the framework outlined in this Standard. The IEEE Guide for DERMS Functional Specification outlines 7 domains of an MG: DER generation, transmission, intelligent distribution, end-user use (load), market, control operations, and service provider. The service provider is excluded because it involves the connection to a main grid, which is not a feature of the IMG proposed in this design. Each domain is analyzed across three interoperability axioms:

1. Power systems interoperability architectural perspective (PS-IAP)
2. Information technology interoperability architectural perspective (IT-IAP)
3. Communication technology interoperability architectural perspective (CT-IAP)

Interoperability is the capability of multiple networks, systems, devices, applications, or components to exchange and use information securely and effectively [5]. The PS-IAP defines an MG in terms of how components related to power systems use and exchange information. The IT-IAP describes the MG “in terms of information flows, entities, and protocols used to exchange information... with an emphasis on information technology perspective [as] the control of processes and data management”. The CT-IAP describes the communication between systems, devices, and applications across the domain mentioned earlier [6].

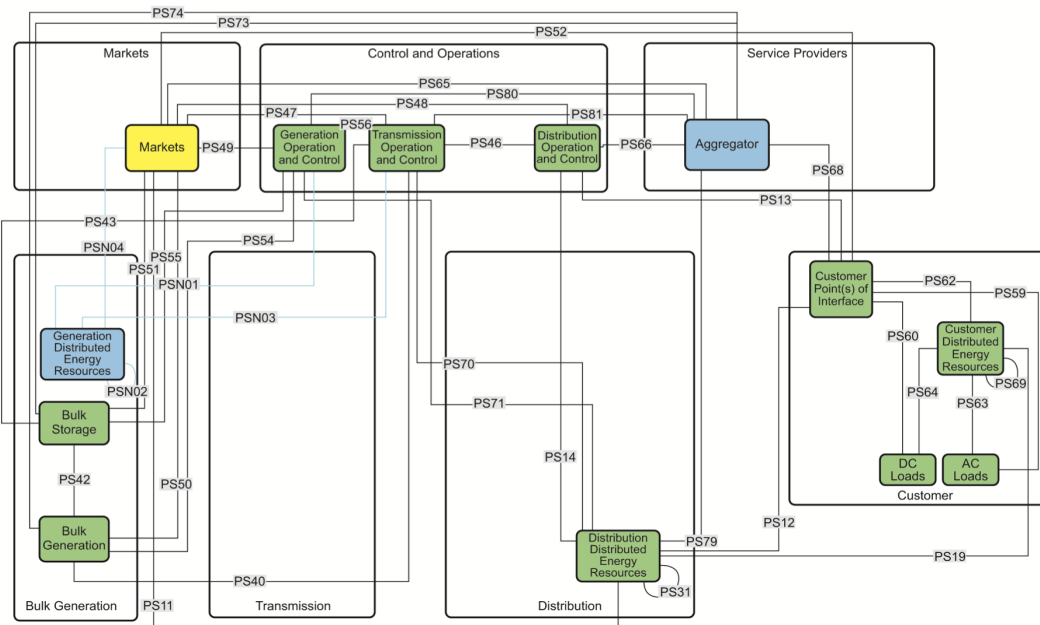


Figure 1: DERMS interoperability within the PS-IAP [45].

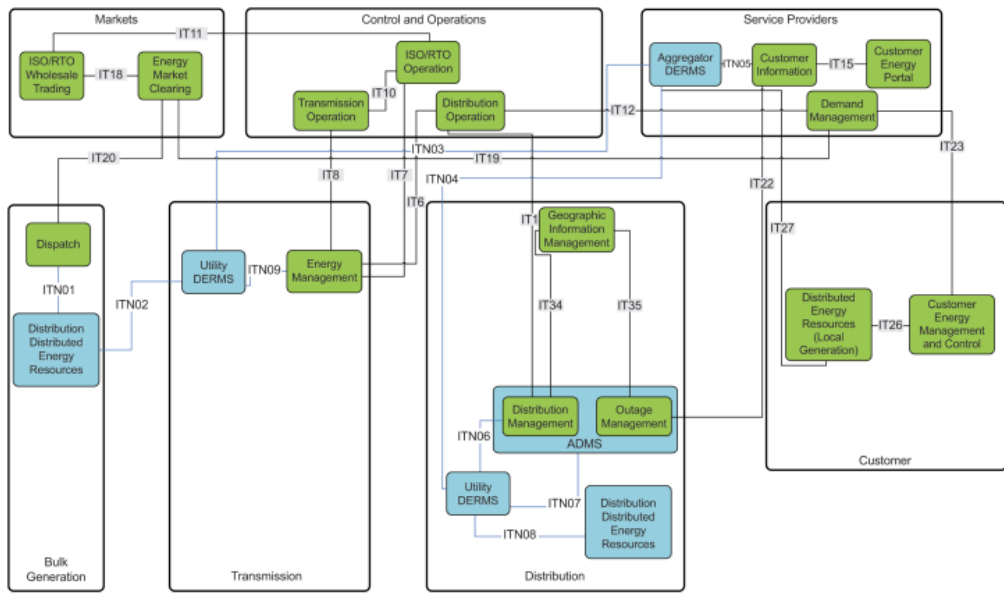


Figure 2: DERMS interoperability within the IT-IAP [45].

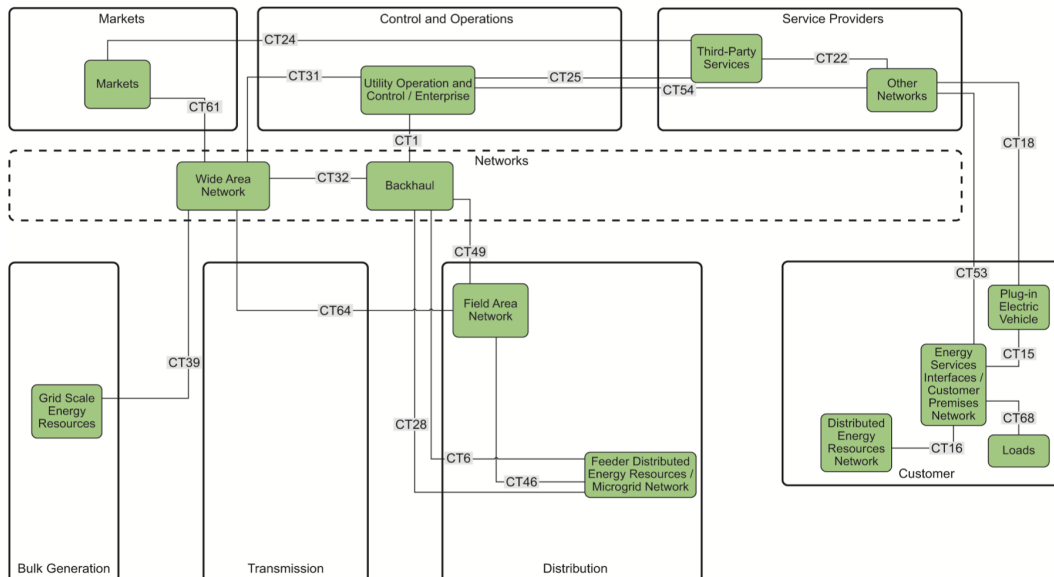


Figure 3: DERMS interoperability within the CT-IAP [45].

#### 1.1.2.1) Generation

The generation domain in a MG is a critical component that involves the production of electricity from various DERs. These resources include technologies such as solar panels, wind turbines, biomass, and other renewable and non-renewable sources that provide electric power capacity. In contrast with traditional centralized power plants, DERs are usually smaller and can

be strategically placed to meet specific local demands. This decentralized approach not only enhances energy resilience but also reduces dependency on fossil fuels, contributing to lower emissions and a more sustainable energy system [7]. It is crucial to manage this domain effectively through DERMS to ensure reliable and efficient operation when involving IMGs. This requires sophisticated control systems and interoperability across the three main perspectives to optimize energy production and integration into the MG infrastructure [8].

It is important to analyze and understand the role that generation plays in the context of the three main perspectives being referenced from IEEE standards (PS-IAP, IT-IAP, and CT-IAP). The PS-IAP focuses on how physical components interact to manage energy flow. Some of the main entities in this category, as seen in Figure 1, include Generation DERs like solar photovoltaic (PV) systems, wind turbines, bulk storage systems such as lithium-ion batteries, and larger bulk generation units like gas turbines. Some of the relevant interfaces under this perspective include:

- **PSN04 Interface:** Connects market operations with bulk storage. In real life, this involves software platforms like *Autogrid* analyzing market prices to optimize storage operations.
- **PS55 Interface:** Links generation operations with bulk storage through supervisory control and data acquisition (SCADA) systems, which monitor and control energy flow. SCADA systems ensure that energy is efficiently stored and dispatched, and often use the Distributed Network Protocol 3 (DNP3) for communication.
  - Some components on this interface include smart inverters such as the ones developed by *SMA* or *Solar Edge*, which convert Direct Current (DC) from solar panels into Alternating Current (AC) for grid use [9], [10]. Smart inverters support protocols like IEEE 1547 and UL 1741 for grid interconnection, providing voltage support and reactive power control [11]. Also, Schneider Electric's telemetry and SCADA systems monitor and control field operations across a widely dispersed infrastructure [12].
- **PS42 Interface:** Manages interactions between storage systems and generation units.
  - An example of these components is the Tesla Powerwall, used for storing excess energy. It interacts with generation units through the PS42 Interface, units using protocols like DNP3 or IEC 61850 [13], [14].

The IT-IAP on the other hand, emphasizes data management and operational control. Figure 2 showcases the main entities here as the bulk generation units connected to dispatch systems. The Interfaces observed within this perspective include:

- **ITN01 Interface:** Provides operational instructions to DERs using EMS that optimize dispatch schedules based on real-time data analytics.
  - EMS solutions integrate market data with operational controls. *Siemens Spectrum Power* is the global leader in power grid management software systems [15].
- **IT20 Interface:** Connects dispatch systems with energy market clearing platforms, facilitating the integration of market data with operational controls.

The CT-IAP focuses more on communication networks that connect various components, emphasizing Grid-scale energy resources as the main entity. Figure 3 shows that the most prominent interface described here is the CT39 Interface. This interface connects grid-scale resources to wide-area networks using fiber-optic or wireless communication protocols.

- Communication Gateways, like *Digi ConnectPort X2* or *Laird Sentrius RG1xx*, are devices that facilitate data exchange between DERs and central control systems using protocols like Modbus or IEC 61850 [\[16\]](#), [\[17\]](#), [\[18\]](#).

#### 1.1.2.2) Storage

A battery energy storage system (BESS) can match peak power demand, and improve grid stability, power quality, and balancing. BESSs are required to have a battery management system (BMS) to monitor and maintain safe and optimal operation for each battery pack [\[19\]](#). A BMS protects the battery from damage by ensuring that the batteries operate within their operating parameters. These parameters include the state of charge (SoC), state of health (SoH), voltage, current, and temperature to balance the system. BESS requires power conversion systems (PCS) which convert power bi-directionally. A PCS allows for DC power to be converted from the battery to AC power for the grid and load, while also being able to convert AC power to DC power to charge the battery. The controller monitors, protects, communicates, and schedules the BESS's components. It also communicates with external devices outside the BESS, such as transformers and electricity meters, to ensure the BESS is operating optimally.

The controller is also integrated with management systems such as SCADA and EMS for complete data acquisition and energy management [\[20\]](#). SCADA communicates with and controls devices throughout the solar PV system. It is the center of operation which allows operators to monitor operations in the system and send commands. SCADA communicates with the BMS to monitor battery readings such as SoC, current, voltage, and temperature. A SCADA system can also take the role of the EMS [\[21\]](#). An EMS is responsible for deciding when and how energy will be dispatched from the BESS by communicating with the PCS and BMS. By knowing the limitations of the BMS and PCS and recognizing when the BESS can be used most effectively, the EMS can optimize the performance of the BESS. The EMS is also a collection point for the performance data of the system, which allows it to gather, transmit, and analyze the data of the BESS to maintain the system and address any problems with the system [\[22\]](#). A heating, ventilation, and air conditioning (HVAC) system regulates the environment of a BESS by moving air between the inside and outside the system. The system will be able to maintain an optimal operating temperature, which will help prolong the life cycle of the BESS. Without HVAC the batteries are prone to overheating which will increase degradation, potential for thermal runaway, and damage. In addition, a fire suppression system adds another form of protection. If the temperatures of the BESS are outside the parameters then the BMS will shut down the system but in the case of thermal runaway, a fire suppression system will suppress the fire by providing a cooling effect and absorbing the heat. [\[20\]](#)

### 1.1.2.3) Distribution

The distribution domain refers to the distribution system of the MG where power is delivered from the source to the end load, via power lines, transformers, switches, and other components. At this stage, voltage is reduced to “safe customer-usable levels” [23], [1]. A MG has numerous components in its distribution system, outlined in Table 1.

<b>Electrical Cables</b>	used to facilitate power flow [24].
<b>Relays</b>	to monitor current, voltage, and frequency, and inform control of any abnormalities [24].
<b>Reclosers</b>	which are electrical devices, for household electric lines, that cut off power automatically in the event of power flow irregularities [25].
<b>Circuit breakers</b>	are also electrical switches, utilized in transmission lines, that cease current flow in the event of a fault or other oddity [26].
<b>Transformers</b>	are devices that step up and down current and voltage. They are used to change the voltage going to a load to a safer level than what the voltage would be had it come from the power sources directly.
<b>Inverter</b>	converts DC power to AC power
<b>Rectifier</b>	converts AC power to DC power.
<b>Converter</b>	can change the operation frequency, modify the voltage or current waveform, and step up or down the voltage. They are used to keep power quality in check [27].
<b>Switchgear</b>	is a series of components that facilitate switching, interrupting devices, controls, and regulation. The components within switchgear include breakers, disconnect switches, main bus conductors, interconnecting wiring,

	support structures with insulators, and enclosures [28].
<b>Outcoming feeders</b>	are conductors that carry electricity to distribution transformers [28].
<b>Bushbars</b>	are large uninsulated metallic conductors used to efficiently distribute current with a substation [28].
<b>Capacitor bank</b>	stores electrical energy in the form of charge. It is a source of reactive power that can help to decrease the phase difference between current and voltage [29].
<b>Lightning Arrestor</b>	is a component of a substation that protects equipment from the negative effects of lightning strikes.

Table 1: A table of the definitions of components within a distribution system in a MG.

The distribution system of a MG can be outlined in terms of power systems, as shown in Figure 1. The Distribution DERs entity represents typically inverter-based renewable energy resources connected to the electrical grid at distribution-level voltages (2.3kV to 39kV) [6]. The Generation Operation and Control entity represents the control systems for power generation sources. The Distribution Operation and Control entity represents the control interface for the power distribution system. One of the MG controllers that are currently available is the Cummins PowerCommand MG Control (MCG). The MCG300 and the MCG900 offer adjustable features such as a color touchscreen with various MG components, information tabs, and system menus [30]. This microcontroller can be used for Generation, Distribution Operation, and Control, as well as, controls for Customer Point(s) of Interface. Some of the relevant interfaces under this perspective include:

- **PS71 Interface:** connects the Generation Operation and Control entity in the control and operations domain to the Distribution DERs entity in the distribution domain.
- **PS14 Interface:** connects the Distribution Operation and Control entity in the controls and operations domain to the Distribution DER entity in the distribution domain.
- **PS11 Interface:** connects the market entity in the market domain to the Distribution DERs entity in the distribution domain.
- **PS12 Interface:** connects the Distribution DERs entity in the distribution domain to the Customer Point(s) of Interface in the Customer domain.
- **PS19 Interface:** connects the Distribution DERs entity in the distribution domain

The distribution system of a MG can be outlined in terms of information technology, as shown in Figure 2. An advanced distribution management system (ADMS) manages both distribution and system functionality during a power outage. Devices in the ADMS are sensors for measuring various parameters, actuators for receiving signals to perform operations, remote terminal units (RTU) that collect and transmit data to a central SCADA system, programmable logic controllers (PLC) that “process input signals from field devices and transmit appropriate output signals to control actuators,” master terminal units (MTU) that aggregate and analyze received data and human-machine interface (HMI), which all operators use to monitor the SCADA system [31]. Geographic Information Management allows for forecasting electricity demand and the development of spatial models for distribution systems [32], [33]. The Interfaces observed within this perspective include:

- **IT01 Interface:** connects the Distribution Operation entity in the controls and operations domain to the ADMS.
- **IT34/IT35 Interfaces:** connect the ADMS to the Geographic Information Management entity within the distribution domain.
- **ITN07 Interface:** connects the Utility DERMS entity to the ADMS entity for real-time awareness and control of the DER.
- **TN08 Interface:** connects the Utility DERMS entity to the Distribution DERs to monitor and control DER.

The distribution system of a MG can be outlined in terms of communication technology, as shown in Figure 3. A Field Area Network (FAN) is “a communication infrastructure that connects devices in the field to a network, allowing them to communicate with each other and with a central control center” [34]. A Feeder DERs/MG Network is a network of DERs. A Backhaul is an intermediate link in a telecommunication network between a “core network” and a “subnetwork” [35]. A core network “is a central conduit designed to transfer network traffic at high speeds” [36]. A subnetwork is a network within another network, they are primarily used for data transfer efficiency [37]. A Wide Area Network (WAN) connects networks over large distances [38]. The Cisco 1000 Series Connected Grid Routers provide a communication infrastructure [39], [40]. The four interfaces under this perspective are:

- **CT64 Interface:** connects the FAN entity in the distribution domain to the WAN in the network domain allowing networks of devices to be connected to other networks of devices of long distances.
- **CT49 Interface:** connects the Backhaul entity in the network domain to the FAN entity in the distribution domain where the Backhaul acts as a link between the WAN and FAN.

- **CT46 Interface:** connects the Field Area entity in the distribution domain to the Feeder DERs/MG Network also in the distribution domain. This links the device network to the DER.
- **CT28 Interface:** connects the Backhaul entity in the network domain to the Feeder DERs/MG Network in the distribution domain. This has the backhaul acting as a link to the WAN.

#### 1.1.2.4) Controls

A DERMS manages the system between the DERs and the demand from the load or distributed resource (DR). A DERMS must be able to receive and process any service requested from a DER or DR as well as contain detailed information about every resource and load in the system. It must be able to translate all of the information given by each resource into an upper-level program for processing. DRs trigger the DERMS to shift their resource allocation to meet the demand. A spike in demand could cause the DERMS to alert the user for a possible load not served or increase the capacity/input of the DERs. If any spike from the load is anticipated to cause damage to the DERs, the DERMS must shed the correct load and adjust internal systems to protect all of the assets. In addition to DERs as a whole, the DERMS must be able to prevent cyber attacks and protect against hardware failures. This can be done entirely by the main system but is usually handled with local microcontrollers sending request signals to the lower level of the main management system. The DERMS handles all allocation of resources and storage and can be programmed to prioritize renewable energy over nonrenewable resources. A DERMS does not have to be on a single controller and often is split up into different sections for easier overall control [6].

A centralized control system consists of a single controller holding all of the information for every resource and performing all functions [41]. This main controller handles all minor and major adjustments for every component in the system including storage units and loads. It is also responsible for the processing of all information and optimization of resources. However, as a result of all of the tasks that this single controller must complete, there is typically a large time delay in the information especially if the MG is larger in size. Since MG signals may need to be sent in millisecond intervals, a high quality communication system is needed for a centralized control strategy. In the case of a malfunction in the main controller, the entire system would likely shut down because there is no other support system which is a major disadvantage of this control strategy. Nevertheless, with every piece of information in one place, it facilitates the smooth operation and control of the system and lowers the complexity of the system. The diagram for a centralized control system for a grid-connected renewable MG can be seen in Figure 4.

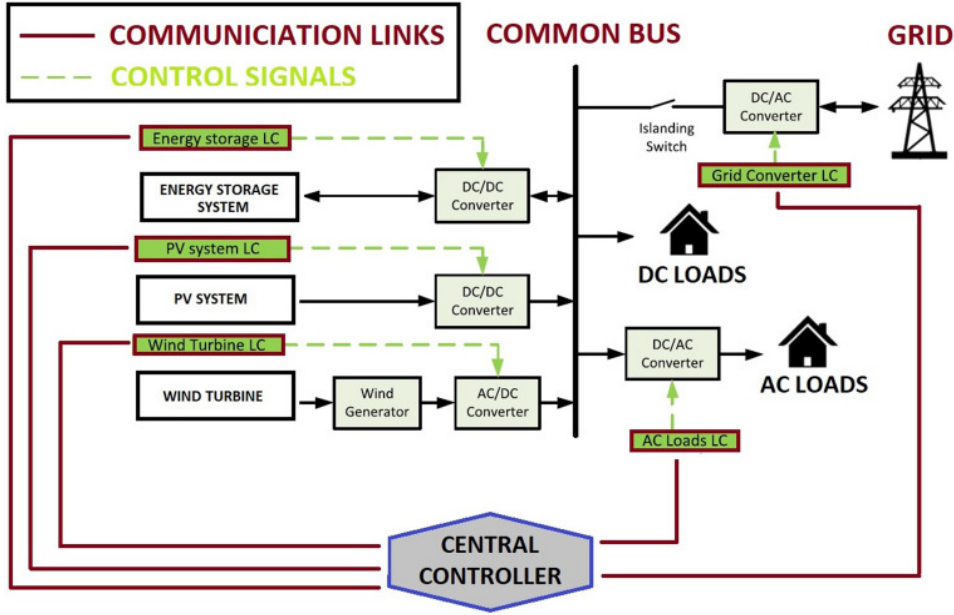


Figure 4: Centralized control system for a grid-connected MG [41].

A decentralized control system utilizes minimal communication and local controllers at every MG component such that each local controller holds all information and handles all tasks for that component [41]. In this strategy, each unit works independently of one another, only sending signals to the other controllers when necessary. This makes it very easy to add or take away components and takes away the single point of failure disadvantage that centralized control had. However, a higher level of communication is needed to make the transfer of information quicker and more efficient, especially in a MG focused on constant optimization.

A distributed control system is similar to decentralized control in the sense that there is no main controller but it does implement some communication methods [41]. Each unit has a local controller that holds all the information and performs tasks for that component. However, the local controllers do not work individually, as they all are connected through digital communication links. Every local controller is only connected to its neighboring , and they pass along information until the data or command has reached its destination. The diagram for a distributed control system for a grid-connected renewable MG can be seen in Figure 5.

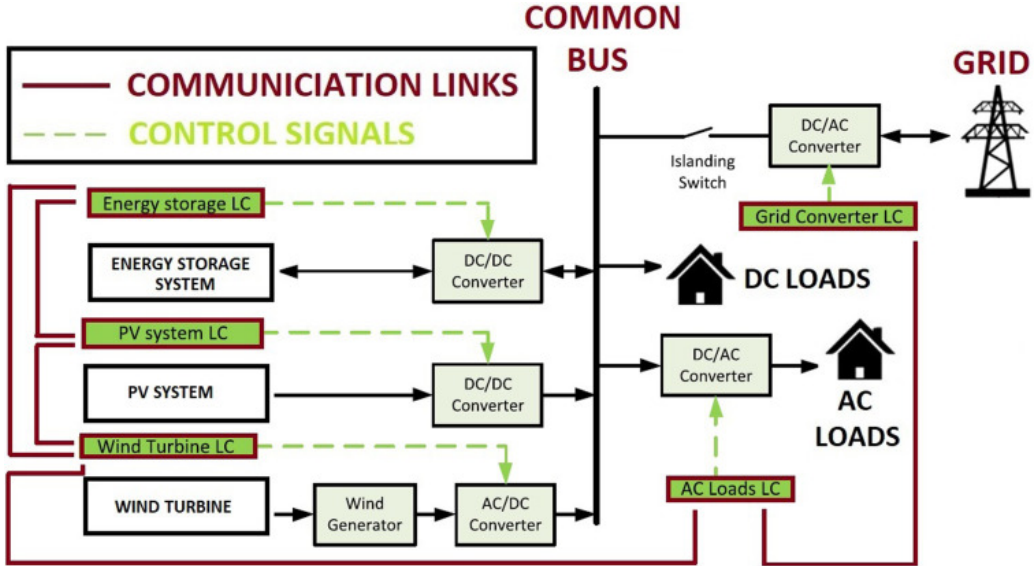


Figure 5: Distributed control system for a grid-connected MG [41].

We will be using a sort of distributed control that incorporates a centralized controller. Each component will have a local controller that manages the power output and internal systems of that element. When anything happens in a certain element that will affect other elements, it relays a message to the central controller. From there, it performs any processing or calculations and relays the necessary information to the correct component.

#### 1.1.3.5) Finances

In IMGs, the IEEE standards referenced before need to be modified, as external market interactions are minimal or nonexistent, and therefore the financial domain focuses mainly on internal economic mechanisms. These systems, unlike traditional grid-tied systems, manage energy transactions within the MG itself, relying on internal pricing models for the particular remote location and local market simulations to ensure economic efficiency and sustainability [42].

Internal financial management is critical for these scenarios, as the MG must balance local generation, consumption, and storage to ensure reliable power and economic viability. Financial models prioritize cost recovery and demand-side management, optimizing energy generation and distribution.

The PS-IAP perspective for this approach focuses on the physical interactions between MG assets such as energy storage systems (ESS), DERs, and generation units. These interactions ensure that the MG operates efficiently, with energy dispatch optimized through internal Market Clearing Pricing (MCP) mechanisms. Guerrero et al. developed an artificial neural network combined with a Markov chain (ANN-MC) approach to predict non dispatchable power generation and load demand considering uncertainties [43]. Interfaces in IMGs such as PS48, PS49, PS0 ,PS51, and PS52 adapt to rely on internal signals. For instance:

- **PS51 Interface:** Connects market operations with bulk storage, adjusting charge-discharge cycles based on local demand rather than external pricing [44].
- **PS50 Interface:** Guides local generation units through internal market signals reflecting local consumption patterns, optimizing resource dispatch [44].
- **PS49 Interface:** Links finances to generation operations through billing systems integrated with SCADA, particularly crucial for maintaining 7-day autonomy targets.
- **PS48/PS52 Interfaces:** Connect finances to distribution operations and customer interfaces, respectively, with engineering and design costs estimated at 12.5% of construction equipment costs [43].

The IT-IAP perspective includes data management and operational control, with a focus on software that simulates market behavior. In IMGs, traditional interfaces like IT11, IT18, or IT20 are adapted to handle internal market operations. This ensures that energy dispatch and financial simulations align with operational strategies.

The CT-IAP in this case targets secure communication within the MG more prominently. In islanded setups, interfaces such as CT24, CT39, CT61 are critical for ensuring that local market operations and financial transactions are secure and reliable, utilizing protocols like IEC 61850. These adapted perspectives ensure that IMGs operate efficiently through internal economic models and secure data exchanges [44].

#### 1.1.3.6) Load

The customer domain refers to the output load for the three perspectives of the electric power system. This domain often links back to outside domains to allow for monitoring and control of information regarding customer loads. The information regarding energy generation and storage is important across other domains since it determines how management needs to react when the outputs are altered.

For the PS-IAP, four entities make up the customer domain. The Customer Point(s) of Interface entity is where all the entities connect inside the customer domain and how communication can occur between entities outside this domain [45]. There may be multiple points of interface that the customer has, which could be a physical interface box, meter, EMS, generator controller, controllable load devices, or directly connected. The Customer DER entity involves the customer's electrical system and the demand response, generation, and energy storage relating to it. The last two entities, DC Loads and AC Loads, refer to the type of electric power used for the loads at the customer site.

The customer domain for the PS-IAP contains six internal interfaces (PS59, PS60, PS62, PS63, PS64, PS69) that connect across the entities, but it also contains five external interfaces (PS12, PS13, PS19, PS52, PS68) that allow for connections to entities of other domains [45]. The Customer Point(s) of Interface has three internal interface connections (PS59, PS60, PS62) and four external interface connections (PS12, PS13, PS52, PS68) that branch out from it. The Customer DER has four separate interfaces (PS63, PS64, PS69, PS19) aside from PS62 that split from the entity.

- **PS59 Interface:** Connects the AC load to the Customer Point(s) of Interface.
- **PS60 Interface:** Connects the DC load to the Customer Point(s) of Interface.
- **PS62 Interface:** Connects the Customer DER to the Customer Point(s) of Interface.
  - All three of these interfaces allow for the exchange of information and control of the internal entities by other outside entities of the customer domain.
- **PS12 Interface:** Connects the Customer Point(s) of Interface to the Distribution DER entity to collect together information from the customer domain and provide a way to locally balance energy generation and loads.
- **PS13 Interface:** Connects the Customer Point(s) of Interface to the Distribution Operation and Control entity and gives access to the information and control of the customer domain to this entity.
- **PS52 Interface:** Connects the Customer Point(s) of Interface to the Market entity which allows for more control over the customer domain.
- **PS68 Interface:** Connects the Customer Point(s) of Interface to the Electric Service Provider entity which also gives control of the customer domain.
- **PS63/PS64 Interfaces:** Connects the AC and DC load to the Customer DER, respectively, allowing for information exchange and internal control of these loads.
- **PS69 Interface:** Connects the Customer DER back into itself for when there are multiple Customer DER entities for information sharing among them.
- **PS19 Interface:** Connects the Customer DER externally to the Distribution DER entity so there is better coordination of the DER entities.

For the CT-IAP, four entities make up the customer domain. The Energy Services Interfaces (ESI)/Customer Premises Network (CPN) entity combines ESI and CPN together, which both have their own functions. The ESI is specifically responsible for the connection between internal customer energy resources to external systems [46]. Its role as a communication gateway allows for two-way customer energy services where it works as both a service consumer and provider. The CPN is a general term that encompasses home area networks (HANs), business area networks (BANs), and industrial area networks (IANs). The DER network entity is where the services involving the customer's generation, storage, and management of energy are connected through wired or wireless networks. The Plug-In Electric Vehicle (PEV) entity involves keeping a balanced energy supply by giving power to the grid through acting as both a load and source or storage. The Loads entity refers to load management and load communication by local networks to allow for better functionality and information exchange. "Loads" is a general term that encompasses physical electrical systems such as HVAC or home appliances, but also industrial facilities or homes. The customer domain for the CT-IAP includes five interfaces (CT15, CT16, CT53, CT68, CT18) that connect the different entities:

- **CT15/CT-16 Interfaces:** CT15 connects the PEV and ESI/CPN entities, whereas CT16 connects the DER network and ESI/CPN entities. They both provide a connection that gives support to functions such as charging, billing, load shedding, and storage.
- **CT68 Interface:** Connects between the ESI/CPN and Loads entities also allows for the support of functions, however, these functions include energy management, lighting control, solar protection, HVAC control, security/access control, and control of audio/video services.
- **CT53 Interface:** Connects the ESI/CPN with the Other Networks entity to have wide-area connectivity into the CPN from different areas.
- **CT18 Interface:** Connects the Other Networks with PEV, so that other networks can also have access to the PEV for the support of functions.

For the IT-IAP, only two entities make up the customer domain, which includes the DER (Local Generation) and Customer Energy Management and Control entities. The DER (Local Generation) entity simply refers to the DERs where the customer is located [45]. The Customer Energy Management and Control entity covers home, business, and industrial EMS (HEMS, BEMS, IEMS). It refers to the energy being handled depending on the customer's needs. The customer domain under the IT-IAP only has three interfaces (IT26, IT27, IT23).

- **IT26 Interface:** Connects the two entities within the domain, which allows for general access of the DERs by the EMS for control and monitoring.
- **IT27 Interface:** Connects externally to the Distribution Management entity from the DER (Local Generation) entity. This is intended for monitoring the power system of the customer's energy generation.
- **IT23 Interface:** Connects the Customer Energy Management and Control entity to the Demand Management entity for information on response signaling, price signals, and detailed load usage.

## 1.2) Microgrid Controllers

MG controllers produced by companies execute all the functions needed for a highly performing MG and can be customizable based on the size or resources of the MG. These MGs all include islanded and grid-connected modes, DER reallocation and protecting all assets from hardware faults and cyberattacks. The controllers all have priority load shedding capabilities in order to ensure that the critical loads are always being met under any circumstance. The main difference between the MG controllers is the optimization programs and software that runs on each one.

Every company has their own optimizing software that they market, such as Tesla with Opticaster, Schweitzer Engineering Laboratories (SEL) with SEL<sub>POWER</sub>MAX, and ComAp with IntelliSys. Tesla's MG controller offers machine learning algorithms to manage load and generation forecasting as well as dispatch optimization and load management [47].

SEL attempts to aim for a slightly different market by offering less advanced algorithms at a much lower price than the competition. They focus more on the flexibility and reliability of the system using real-time automation to update external data (market prices, etc.) and internal system data to optimize prices [48]. ComAp has many different options of MG controllers but prioritizes the resiliency and security of their system. They highlight the fault prevention features as well as using encryption to protect system information. Additionally, ComAp highlights the amount of support available and flexibility of their products with many types of MG systems [49].

### 1.3) Resource options

MGs can integrate different DERs to create reliable and efficient power systems. Diesel generators have traditionally dominated MG installations, but renewable energy sources are becoming increasingly more popular. Different dispatchable and non-dispatchable generations can make up a MG generation system [50]. There are several dispatchable generation options, including combined heat and power (CHP), biogas, and natural gas generators. Renewable energy sources like PV solar, wind, hydro, biofuels, etc. are examples of non-dispatchable generation. Based on field experience from implemented projects, solar PV systems have emerged as the most widely deployed and dependable power source for remote IMGs [Adam Eberwein, September 19, 2024]. Additional resource options include geothermal, biomass, and solar thermal.

Each resource has unique properties that affect its suitability. Geographical location, resource availability, load requirements, environmental considerations, infrastructure requirements, and economic viability are some of the factors that influence the choice of suitable resources.

#### 1.3.1) Diesel

Diesel generators are widely utilized in remote areas due to these areas having no access to a main grid, but also due to their predictability and independence from climatic change [51]. However, diesel generators have several drawbacks that prompt people to seek alternative options. Diesel generators tend to be expensive, inefficient, and responsible for copious emissions of greenhouse gasses [52]. While the overall purchase cost of a diesel generator is relatively inexpensive, the delivery of fuel to these areas for operation and maintenance (O&M) is what leads to a large price elevation. Fuel itself fluctuates frequently in cost which contributes to the overall cost as well. When being dependent on fuel deliveries, if fuel is unavailable due to weather or other circumstances, widespread power outages are likely to occur too. Diesel generators are simply not cost-effective when compared to other energy sources like PVs and wind turbines [52].

Aside from high costs, diesel generators are also proven to have technical problems and lead to the production of noise and carbon pollution. Diesel generators tend to operate at low loads due to the inconsistent renewable energy sources and constant changes in the load profile.

When these generators are working at low loads, combustion residue builds up on the interior walls causing friction which reduces the efficiency and increases fuel consumption. This can be avoided by operating the engine at a higher speed but that leads to more problems like icing and wet stacking [52]. While diesel generators have their share of problems, it's important to recognize that they are the most convenient form of energy generation for most people.

### 1.3.2) PV Solar

PV Solar is one of the most important energy sources for supplying the growing global energy demand and accelerating the transition to a future mostly powered by renewable energy sources. It is plentiful, clean, safe for the environment, and, with more research, getting cheaper and more effective. As a result, solar panel installations have significantly increased globally [53]. For instance, at the end of 2023, global renewable power capacity amounted to 3870 GW. Solar accounted for the largest share of the global total, with a capacity of 1419 GW [54].

PV Solar systems convert solar radiation directly into electrical energy through specialized semiconductor devices. These fundamental units, called PV cells, utilize the photoelectric effect to generate DC electricity when exposed to sunlight. Multiple cells are electrically connected and encapsulated to form modules or panels, which can then be combined into larger arrays to achieve desired power output levels [55].

#### Units to measure potential

Data on solar irradiance and weather are crucial for PV system simulation and design. Due to their similar measurements and wording, solar irradiance and solar irradiation are frequently confused. Solar irradiance is a real-time measurement of solar power over a certain area ( $\text{W/m}^2$ ) [56]. However, solar irradiation is a measurement of its intensity over time. While solar irradiation values are shown in  $\text{kWh/m}^2$  when examining monthly data, commonly used meteorological data with hourly granularity have solar irradiance data in  $\text{W/m}^2$  [57]. A good benchmark for solar energy production is around  $1000 \text{ W/m}^2$  at peak conditions. For daily averages, an excellent potential would be  $> 6 \text{ kWh/m}^2/\text{day}$ , good potential:  $4\text{-}6 \text{ kWh/m}^2/\text{day}$ , moderate potential:  $3\text{-}4 \text{ kWh/m}^2/\text{day}$ , and low potential:  $< 3 \text{ kWh/m}^2/\text{day}$  [58].

#### Components and operation

The module (panel) is the central component of a PV system. The vast majority of global PV module shipments (96% in 2020) employ crystalline silicon (c-Si) technology. In addition to PV modules, a PV system may require a battery charge controller, an ESS, an inverter or power control unit (for AC loads), safety AC/DC disconnects and fuses, combiner boxes, grounding circuits, wiring, and transformers. Figure 6 shows and generalizes these connections. Inverters, which convert DC electricity from modules to AC, are the most important and costly balance-of-system (BOS) components. Other components include wiring, meters, junction boxes, AC and DC disconnects, combiner boxes, transformers, electrical panels, and mounting structures [59].

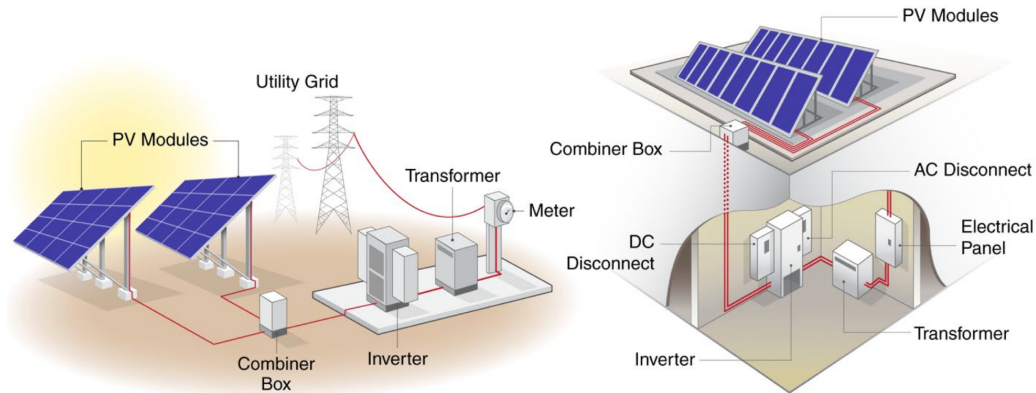


Figure 6. Illustrations of a utility scale PV system (left) and a commercial rooftop system (right) [60].

The system components and designs vary depending on the type of installation. For example, the mounting structures used for residential rooftop PV systems differ significantly from commercial rooftop systems, and the mounting structures used for both types of rooftop systems differ significantly from ground-based systems. Batteries are increasingly being used in PV systems, relying on the addition or substitution of components such as battery-based inverters and charge controllers.

### Efficiency

The conversion efficiency of a PV cell is the percentage of the solar energy shining on a PV device that is converted into usable electricity [61]. The average panel conversion efficiency has increased from 15% to over 23% due to advances in PV technology [62]. The efficiency depends on the amount of light reflected away from the cell's surface, the intensity of the sun, the amount of cloud cover, and heat build-up, which affects the conductivity of the semiconductors in the PV cells. A 23% efficient solar cell exposed to 1000W of sunlight per m<sup>2</sup> will produce 230W of electricity per m<sup>2</sup>. This means that out of every 1000W of sunlight that hits the solar cell, 230W is converted into usable electricity.

### Energy density

Energy density is the amount of energy stored in a given system or region of space per unit volume. For solar power, the energy density is relatively low compared to other energy sources. For instance, solar energy has a density of 1.5J/m<sup>3</sup> which is over twenty quadrillion times less than oil, and human energy density is approximately 1000 J/m<sup>3</sup> [63].

### Cost

The cost of power generation technologies such as PV Solar is important when designing a MG. Cost analysis allows investors to determine if a project merits pursuing. A cost analysis can include capital cost, operation, and maintenance cost, LCOE, and other cost considerations.

The typical capital cost per MW for a PV Solar array is approximately \$800,000 to \$1,300,000 [64], [65], [66]. In South Sudan, based on a 150.2 million USD total (cost Juba) Solar Power Plant Project, the capital cost per megawatt vastly exceeds that of the U.S. at 30.04 million USD [67]. The typical operational and maintenance costs for a commercial-scale solar array, 5-1 MW or less, are around \$17.21 per kWh/yr. These costs come from operations administration, insurance, asset management, security, property tax, land lease, inverter replacement, module replacement, parts replacement, system inspection and monitoring, and module cleaning and/or vegetation and pest management [64], [68], [69]. The Austrian Government's Department of Climate Change, Energy, the Environment and Water recommends that qualified individuals service solar panels about every two years. In the U.S., the levelized cost of energy of utility-scale PV Solar ranges from about \$0.024/kWh to \$0.096/kWh [70], [71].

For unsubsidized and subsidized community-scale PV Solar, the LCOE is between 0.049/kWh to 0.185/kWh and \$0.039/kWh to \$0.155/kWh, respectively [72]. Although there is limited information on the LCOE of PV Solar in South Sudan specifically, based on the Juba Solar Plant Project, considering the \$150.2 million using Equation #1, the LCOE is \$0.17145/kWh.

$$\text{Equation \#1: } LCOE = [\text{Total Project Cost} / (\text{Project Lifetime} * \text{Annual Energy Output})]$$

Using the \$3.96 million to \$5 million approximation of the project and the same equation, the LCOE is \$0.00452/kWh and \$0.00571/kWh, respectively.

$$\text{Equation \#2: } \text{Annual Energy Output} = \text{Day in a Year} * \text{Power Plant Capacity} * \text{Hours in a Day}$$

#### Land Use

Other considerations for the viability of a PV solar panel energy resource within a MG include land use, supporting infrastructure requirements, potential inhabitant complaints, and local system management. Commercial-scale fixed-tilt (ground-mounted) PV solar panels require about 5.5 acres or 22,258 m<sup>2</sup>/MW [73]. However, before construction begins on the selected land, there needs to be a site evaluation for stormwater assessment and vegetation management capabilities, roads and transmission infrastructure access, permitting, and regulatory compliance [74], [75]. It can then take approximately 3 to 5 years to complete project permitting and to select the correct size for a solar panel array; following that, construction typically lasts 4 to 14 months [76], [77], [78], [79], [80]. The solar panel construction involves advanced electrical wiring, piping, heat transfer, pumps and power distribution [81].

### 1.3.3) Solar Thermal

A Parabolic Trough System is a concentrated solar power source. Concentrated Solar Power is an energy generation method that focuses sunlight on a single point to heat a medium. In a Parabolic Trough System, sunlight from a mirror is focused on tubes equal to the length of the mirror. The medium material inside those tubes is a flowing liquid utilized to heat water until it becomes steam, which can then be used for heating, water desalination, or turning a turbine to generate electricity [82], [83]. A parabolic trough system converts about 32.85% of the energy from the sun into electrical energy [84], [85], [86], [87]. The thermal efficiency, the amount of sunlight that is turned to heat over to the theoretical total energy of the sunlight, of a parabolic trough system is around 73% at 350°C (662°F); steam turbines have an isentropic efficiency of around 20% to 70%. The power density of sunlight is 1.36-1.37 kW/m<sup>2</sup>, thus, after accounting for thermal efficiency and isentropic efficiency, the power density of the power electricity generated by the parabolic trough system is about 0.447 to 0.45 kW/m<sup>2</sup>. This means that for every square meter, there is 1.36-1.37 kW of power from the sun, but a parabolic trough system utilizes only about 0.447 to 0.45 kW of power [88].

Cost, scalability, infrastructure, and operability are other important considerations for incorporating energy generation technology into a MG. As of 2021, the capital expenditure (CAPEX) for a parabolic trough system is approximately \$7,254,000/MW and is expected to drop to \$5,078,000/MW by 2030 and \$4,352,000/MW by 2050 [89]. In 2015, O&M cost was projected to be around \$69/kW by 2021. Despite the cost, it has a life-time of around 30 years [89]. A parabolic trough system becomes commercially viable at sizes ranging from 14 to 80 MW thereby exceeding the capacity required for small remote populations. Because more troughs can be added to the system it is easily scalable [90], [91]. However, a drawback to parabolic trough systems is that there is less energy collected when it's not properly aligned with the sun. This is because the mirrors must be able to constantly track the sun, which adds complexity to the system [92], [93]. A parabolic trough system requires general infrastructure such as access to roads and electrical systems as well as more specific elements such as cooling systems, control systems, and thermal energy storage [90], [94], [89]. Local populations would need training specific to the parabolic trough system, and while there are multiple PV solar training programs, there are no parabolic trough system training programs. These courses, which vary in length, include the residential and commercial Photovoltaic Systems Certificate, Solar Energy Technician Training Program, and PVOL350 Solar Training [95], [96].

### 1.3.4) Wind

Wind energy is another common renewable resource used in MGs and general energy grids. It produces no carbon emissions and has grown significantly over the last 10 years. The United States' wind capacity has more than doubled since 2014, increasing the utility scale wind capacity by 83 GW [97]. Globally, wind capacity is also growing by 12% annually in the last decade, reaching 1,021 GW in 2023 [98].

## Components and Operation

Wind turbines consist of blades attached to a rotor and shaft. The shaft is connected to a set of gears, leading into a generator, converting the mechanical energy from the blades spinning into electrical energy. As wind passes, the blades and shaft begin to spin. As the wind speed and direction change, the turbine head spins to face the wind to get more power output using a yaw drive and motor. These changes in wind speed and direction are measured using an anemometer and a wind vane, respectively. A diagram of the components of a traditional wind turbine can be found in Figure 7.

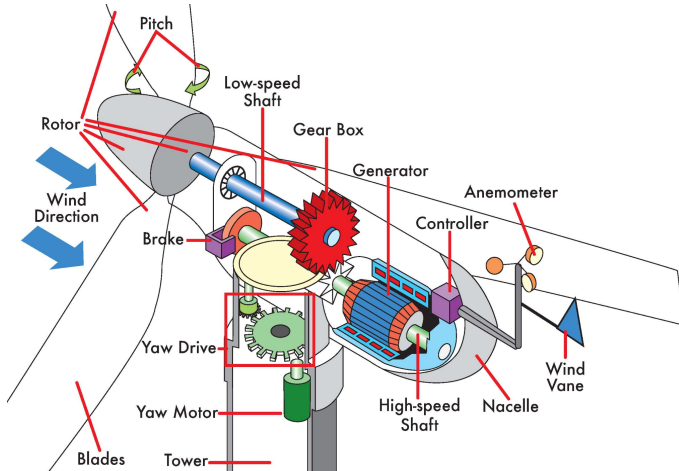


Figure 7: A visual representation of the machinery components in a wind turbine [99].

## Efficiency

The efficiency of a turbine is determined by dividing the amount of energy produced from the turbine by the total kinetic energy available in the wind. Turbines vary greatly in terms of physical size and capacity, allowing for a large variety of wind speeds in each area depending on the height of the turbine. Therefore, wind turbine efficiency has a wide range from 20% to 40% with larger turbines being more efficient than smaller ones [100].

## Cost

The general cost of a wind turbine in the United States is around \$1,300,000/MW with most commercial turbines being 2 to 4 MW in size [101]. Using fewer, larger wind turbines increases the cost per turbine but lowers the complexity of the system with fewer moving parts. It lowers the overall cost per kW because the larger turbines reach higher wind speeds than smaller ones. The annual operating and maintenance cost of a turbine in the United States is between \$25-\$40 per kW per year [101], [102]. Typical turbines have a lifespan of 15-20 years and need a general maintenance check every 4-6 months [100]. The maintenance cost varies greatly between different turbines and is highly dependent on how often the components of the turbine wear down or break. Often, engineers can choose stronger, more flexible material that is less prone to breaking. However, there is also a large factor of risk in uncontrollable scenarios such as natural weather events.

## Land Use

Turbines come in many different sizes and capacities and therefore many different heights. The amount of space needed between each turbine and any other structure is at least the height of the turbine plus the length of the blade. This way if it tips over, nothing can be broken around it. Usually, engineers build the turbines with a bit of leeway (about 10% of height) in case some pieces of the turbine become disconnected while falling.

### 1.3.5) Biomass

Biomass is a unique renewable energy source that provides the only renewable source of fixed carbon, which is required to meet a variety of fuel and energy requirements [103]. Unlike intermittent renewable sources such as solar and wind, biomass can generate dispatchable power when properly managed, making it especially useful for MGs applications.

#### Types and Characteristics

Biomass resources include a diverse range of organic materials such as woody biomass from forestry operations, agricultural residues, organic waste streams, and purpose-grown energy crops. A sustainable woody biomass crop typically yields 10-15 dry tons per hectare annually in northern regions, with the potential to reach 20 dry tons per hectare in more favorable climates [103]. This relatively low-density means biomass is a diffuse resource requiring significant land area for meaningful power generation. Approximately 100 hectares of the planted area can sustainably produce enough biomass for 150-300 kWh of power output depending on conversion efficiency [104].

#### Collection and Processing Requirements

The diffuse nature of biomass resources presents unique logistical challenges for MG applications. Biomass materials must be collected over large areas and often require significant preprocessing before conversion. Most biomass resources also exhibit strong seasonality, which means forestry and coppiced crops can typically only be harvested during winter months, while agricultural residues follow crop-specific harvest schedules [105]. This leads to a more careful planning of storage infrastructure and inventory management.

#### Conversion Technologies

Three primary thermal conversion pathways exist for biomass resources in MGs:

1. Direct combustion for heat and power generation
2. Gasification to produce combustible gasses
3. Pyrolysis to generate bio-oils and chars

For MG applications, thermochemical conversion typically offers higher efficiencies (20-35%) and greater flexibility in feedstock handling compared to biochemical processes [104]. The choice of conversion technology depends on factors including available biomass types and quantities, desired energy products, scale of operation, and local infrastructure.

### 1.3.6) Hydro

Hydropower is one of humanity's oldest and most reliable renewable energy sources, using the energy of flowing water to generate electricity. Micro-hydro systems that can generate up to 100 kW are especially useful in MG applications because they can provide consistent base load power. In contrast to intermittent renewable sources such as solar and wind, properly sited hydropower can provide continuous power generation, which is critical for MG stability and reliability.

Micro-hydro systems can generate useful power using as little as 2 gallons/minute or head heights of only 2 feet under the right conditions [106]. These systems convert the potential and kinetic energy of flowing water into run-of-river installations that use natural stream flow and storage systems that use small dams or diversions. The power output is primarily determined by the vertical distance the water falls (head) and the flow rate. Overall system efficiencies typically range from 60 to 80 percent [107]. Micro-hydro systems offer several significant advantages for MG applications, including frequency regulation, black start functionality, and the ability to operate in both grid-connected and islanded modes. The technology is especially cost-effective in remote communities near suitable water resources, with leveled energy costs ranging from \$0.03 to \$0.12 per kWh, depending on site conditions and system size.

### 1.3.7) Geothermal

Geothermal energy can offer unique advantages for MG applications through its ability to provide both consistent base load power and thermal energy. This technology harnesses underground heat through either direct use for heating/cooling or electricity generation via binary cycle or steam turbine systems [108]. Small-scale geothermal systems typically range from 100 kW to 5 MW of electrical output. The technology also has an exceptionally high capacity factor (typically 90-95%) and dispatchability, which is an advantage because it makes it an ideal complement to intermittent renewable sources in hybrid MGs [109]. Modern geothermal systems can achieve overall system efficiencies of 45-65% for CHP applications. Heat storage capabilities provide additional flexibility for load management. Recent advances in Enhanced Geothermal Systems (EGS) have expanded the potential application range beyond traditional high-temperature geothermal regions. Small-scale binary cycle systems can now effectively utilize moderate temperature resources (80-150°C) for both power generation and direct-use applications in MGs [108]. The technology offers competitive leveled costs of energy ranging from \$0.04 to \$0.14/kWh for electricity generation, with significantly lower costs for direct-use applications.

## 1.4) Storage

### 1.4.1) Lithium-ion Battery

Lithium-ion batteries are made up of an anode, cathode, separator, electrolyte, and two current collectors. The lithium is stored in the anode and cathode. The electrolyte carries positively charged lithium ions from the anode to the cathode and vice versa through the separator. This movement creates free electrons in the anode that creates a charge at the positive current collector. The electrical current then flows from the current collector through a device that is being powered to the negative current collector. The separator blocks the flow of electrons inside the battery. When the battery is discharging the anode releases lithium ions to the cathode. When the battery is charging the opposite happens and the lithium ions are released from the cathode and received by the anode [110].

Lithium-ion batteries are considered to have a high energy density at 200-300 watt-hours per kilogram (Wh/kg) [111], [112]. A higher energy density means it can store a significant amount of energy, so it can provide energy for longer periods between charges. With the ability to store larger amounts of energy the size and weight of the battery can be reduced. Lithium-ion batteries are also considered to have a higher power density at approximately 250-340W/kg [113]. A higher power density indicates that the battery delivers energy quickly while also being about to recharge quickly.

With proper maintenance higher-end lithium-ion batteries can last several years. They can go through more than 1000 charge and discharge cycles while retaining a significant portion of their capacity. The typical lifespan of lithium-ion batteries is around 2-3 years or 300-500 charge cycles [114], [112]. This is assisted by their low self-discharge rate which allows them to retain their charge for longer periods when they are not in use. However, if the batteries are stored within the right temperature they lose less than 2-3% of their charge per month depending on their SOC [112]. If the battery has a SOC of 100% then the battery could lose 5-10% of its charge over a month, but if the SOC is between 30%-80%, then the self discharging rate is around .5% under the right conditions [115]. Therefore, when charging and discharging a battery, the SOC should be charged to 80% SOC and discharged to 20% SOC. The batteries that are approaching their lifetime need to be monitored since they are ready to be replaced once the run time drops below 80% [116], [117].

Lithium-ion has the highest coulombic efficiency in rechargeable batteries as it exceeds 99% when it is maintained in the right temperature [118]. Coulombic efficiency is the charge efficiency in which electrons are transferred in batteries. The ratio of coulombic efficiency is the ratio of total charge extracted from the battery to the total charge put into the battery over a full cycle.

While lithium-ion batteries are the most commonly used, they tend to be expensive and more sensitive to temperatures. The price of lithium-ion batteries varies based on the device that they're used for, voltage, and amp hours. Over the years, the price has dropped to an average price of \$151/kWh [119]. Lithium-ion batteries need to be maintained within a specific

temperature range to work optimally since they are sensitive to extreme temperatures, both high and low. Extreme temperatures increase the degradation of the battery and can lead to fires or explosions. These batteries can also encounter thermal runaway if the temperature is too high, which is another way for them to overheat and explode [112]. Lastly, even though lithium-ion batteries have a long life cycle, over time their capacity decreases and they can degrade by about 20% after 500 charge and discharge cycles.

#### 1.4.2) Pumped Hydro

Pumped hydro can be utilized as an energy storage method. It involves pumping water from a low reservoir into a water tower while there is excess energy. When there is less power output from the other power generation sources, the potential energy stored in the water tower is released. The water spins a turbine, generating electricity for the MG. The round-trip efficiency, the ratio of energy put into storage to the amount released from storage, ranges from 70% to 87% [120]. Pumped hydro storage, via a water tower, was considered an energy storage method for this project; however, because the idea has minimal practical implications, conventional storage energy methods were taken more seriously.

#### 1.4.3) Fuel Cells

In hydrogen fuel cells, excess electricity generated is used to split hydrogen and oxygen atoms for a MG system. When there is energy demand, the hydrogen atoms enter into an anode where they are stripped of their electrons, they then pass through a membrane to the cathode. While this occurs the electrons pass through a circuit and generate electricity, when they enter the cathode they recombine with the hydrogen atoms, and oxygen atoms are also released into the cathode for water [121]. The MG in this project will not feature hydrogen fuel cells due to their 3 fold lower efficiency when compared to lithium-ion batteries [122]. This decision also comes as a result of recommendations by Adam Eberwein, on not implementing technologies that are not part of a financially capable system [Adam Eberwein, September 19, 2024].

#### 1.4.4) Compressed Air

Compressed air energy storage involves using excess energy from renewable energy sources in order to pump, cool, and compress air into a cavern or storage container in order to use the air later when energy is needed. By storing air and heat they can later go through expanders and heat exchangers in order to then go through air turbines and electric generators to generate energy. The MG in the project will not have any compressed air energy storage because the efficiency of the compressed air energy storage ranges from 40%-70% depending on the size of the system. The efficiency is 40%-70% because air and heat can be lost in the system when stored for long periods of time. The system also uses energy from other renewable energy sources in order to extract and discharge the air and heat [123].

## 1.5) Location Planning and Selection

The challenge of electricity access remains a critical global issue, with approximately 733 million people living without electricity access as of 2022 according to the International Energy Agency (IEA) [\[124\]](#). Sub-Saharan Africa faces the most severe electricity access challenges, where nearly half of the population lacks basic electricity services. Given South Sudan's significant renewable energy potential and evident need for electrification, this project sought to identify the best locations within this country for MG implementation. The selection process prioritized areas with an established humanitarian presence, primarily involving the UN Mission in South Sudan (UNMISS), with a focus on Protection of Civilians (POC) camps. Juba, Bentiu, and Wau are locations in South Sudan that were chosen due to their high population density, existing infrastructure, and potential for humanitarian funding and impact. They were each evaluated on solar and wind potential based on NASA POWER data, population demographics from UN reports, geographical characteristics, existing infrastructure, and security concerns.

### 1.5.1) South Sudan

South Sudan stands out as the least electrified nation globally, with only 7.2% of its population having access to electricity [\[125\]](#). The country's electricity infrastructure faces multiple challenges, with a total installed power capacity of approximately 103 MW against an estimated demand of 800 MW in 2020. Despite being oil-producing, South Sudan has no domestic refining capacity. All electricity generation relies on imported diesel fuel, requiring hard currency that drains the government's limited cash reserves [\[126\]](#). To reach end users, the distribution of diesel fuel must pass through dozens of checkpoints manned by various armed groups across the country. This adds costs for security and access, making the reliance on diesel fuel a core component of the country's fossil-fuel dependency and struggling economy [\[125\]](#).

Making matters worse, the recent civil war destroyed most of the existing limited electricity infrastructure, including projects developed in the immediate pre- and post-independence periods. However, South Sudan still possesses significant untapped renewable energy potential.

The country receives exceptional solar radiation, with more than 10 hours of daily sunshine and approximately 5.5-6.0 kWh/m<sup>2</sup>/day year-round, according to data from NASA's Prediction Of Worldwide Energy Resources (POWER), which is an excellent condition to produce solar power according to relevant research [\[127\]](#), [\[128\]](#). The White Nile flowing through South Sudan presents substantial hydroelectric potential, with five identified high-potential sites capable of generating up to 2,105 MW. Additionally, eighteen potential locations for mini-hydro have been identified, anticipated to generate up to 40 MW electricity. The country possesses over 70 million hectares of forest and woody biomass resources, currently utilized primarily by 70% of the population for traditional cooking and heating needs [\[129\]](#).

### 1.5.1.1) Juba

Juba, the capital and largest city of South Sudan with a population of almost 480,000, serves as the country's primary economic and administrative center. It hosts two significant IDP camps that transitioned from UN POC sites: POC1 with 7,679 individuals (2,124 households) and POC3 with 25,034 individuals (7,090 households), totaling 32,713 individuals in these camps alone [130]. Infrastructure-wise, Juba has relatively better access than other parts of the country, with an international airport and road connections to Uganda. The city's status as the capital provides better access to technical expertise, though overall capacity remains limited. Since the area is relatively flat, detailed site assessments would be needed to evaluate flood risks, especially with recent climate-related flooding events in the region.

The city possesses multiple renewable energy resources beyond solar. The White Nile is located approximately 7 km away, and a water stream near POC3 offers potential for small-scale hydropower development. The city generates household waste at 0.42 kg/person/day, providing potential biomass material for energy generation [125]. Recent successful solar implementations in Juba's health facilities have demonstrated the viability of hybrid systems, with Aptech Africa installing systems at facilities like Kator Primary Health Care Center and Juba Teaching Hospital. The presence of UN facilities, ongoing renewable energy projects, and the city's status as the administrative and economic center of South Sudan demonstrates its potential for successful MG implementation.

The area has an “All Sky Surface Shortwave Downward Irradiance” (total solar radiation reaching the surface under all sky conditions) consistently higher than 5.41 kWh/m<sup>2</sup>/day, indicating excellent solar potential [127]. Despite the location's solar potential, wind resources are limited, with annual average wind speeds ranging from 2.57 m/s to 2.81 m/s. This makes it less suitable for wind power generation as it falls below EIA standards of 4.0 m/s for small wind turbines [131]. Aside from solar and wind, hydro and biomass systems could also be considered. The White Nile is located approximately 7km away, and a water stream near POC3 offers potential for small-scale hydropower development. The city generates household waste at 0.42 kg/person/day, providing potential biomass material for energy generation [125]. Recent successful solar implementations in Juba's health facilities have demonstrated the viability of hybrid systems, with Aptech Africa installing systems at facilities like Kator Primary Health Care Center and Juba Teaching Hospital.

For energy demand calculations in the IDP camps, considering tier 1 access for the combined 9,214 households with 22 kWh/household/year, the annual energy demand is 202,708 kWh/year, resulting in approximately 555.36 kWh/day [132]. This calculation assumes basic electricity access for lighting and basics which aligns with humanitarian standards for emergency settings. Juba's current energy infrastructure, while the most developed in South Sudan, remains severely limited. The city has an off-grid installed generation capacity of 28.93 MW, almost equal to the installed grid capacity, with 99% generated from diesel generators causing toxic emissions and noise.

Two 20 MW utility-scale solar projects are under construction: the Ezra hybridization IPP and the government-owned Nesitu project (which includes a 10 MW/35MWh BESS), with a third 20 MW Juba solar IPP (GWG) in planning stages [126].

#### 1.5.1.2) Bentiu

Bentiu, South Sudan was also a location considered for MG implementation. As of August 2024, the city has an IDP population of approximately 106,000 people [133], [134]. Located at a latitude of 9.27 and a longitude of 29.79, according to data from the last 11 years gathered from NASA Power, the area has an “All Sky Surface Shortwave Downward Irradiance” of 5.7 kWh/m<sup>2</sup>/day, which indicates good solar potential [58]. The Bentiu area has a wind speed at 50 meters of 4.74 m/s, a wind direction at 50 meters ranging from 31.62 to 62.81 degrees, a wind speed at 10 Meters of 3.154 m/s, and a wind direction at 10 Meters at 36.94 to 64.06 degrees. This indicates that overall the location is not suitable for wind power, but wind speeds in the winter months (December-March) exceed EIA standards of 4.0 [m/s] at a height of 10 meters and 5.8m/s at a height of 50 meters [131]. Considering tier 1 access, the annual energy demand from 16,093 households with 22 kWh/household/year is equal to 354,046 kWh/year. The daily energy demand therefore is approximately 970 kWh/day [135]. Creating a system to support this amount of households would require the ability to produce around 2000 kWh/day to account for variation in load.

Important aspects of Bentiu also include geographic features, political stability, demographics, and infrastructure. In terms of geography and infrastructure, Bentiu is susceptible to flooding because it has a relatively flat geography [136], [137], [138]. This means the area only has access to roads for part of the year, making transportation of people and equipment challenging [139]. Other geographical features such as forests could be used for biomass energy are also taken away by these floods [140]. When conflict broke out in 2013, local generators were damaged and looted with no plans for repair implemented. Now only areas considered affluent had access to electricity [125]. Thus there is limited energy infrastructure.

In terms of available labor about a quarter of the working-age individuals are enrolled in education and unemployed, thus some of this population, that is undergoing education, could be hired to construct or maintain the MG [141]. Although Bentiu has promising solar potential, severe and frequent flooding, infrastructure, and safety are large concerns for the potential implementation of a MG.

### 1.5.1.3) Wau

Wau, South Sudan was another location considered for MG implementation. It has a population of 10,000 civilians [142]. At a latitude and longitude of: 7.7144 and 27.9641 respectively, according to data from 2012 through 2022 gathered from NASA Power, the area has an “All Sky Surface Shortwave Downward Irradiance” of 5.741kWh/m<sup>2</sup>/day, which indicates good solar potential [58]. In terms of wind power availability, the average speed throughout the year wind at 50 meters is 3.97 m/s, the wind direction at 50 meters ranges from 31.06 to 342.44 degrees, the average wind speed throughout the year at 10 meters is 2.904 m/s, and the wind direction at 10 Meters 34.56 to 347.75 degrees. This indicates that overall the location is not suitable for wind power, but wind speeds in the winter months (December-March) exceed EIA standards of 4.0 m/s at a height of 10 meters and 5.8 m/s at a height of 50 meters [131]. To estimate the number of households for civilians seeking safety in Wau, the Bentiu population of 106,000 people was divided by its number of households of 16093 households to obtain 6.5867 people/household. Dividing the 10000 people in Wau by 6.587 people/household returns 1,518 households. Considering tier 1 access the annual energy demand from 1,518 households with 22 kWh/household/year is equal to 33,396 kWh/year. The daily energy demand therefore is approximately 91.5 kWh/day [135].

Other important aspects of Wau are its political stability and infrastructure. There is overall limited information on the state of Wau’s road infrastructure, and parts there is information on, such as a “single-track railroad between Babonosa (Sudan) and Wau”, do not indicate solid infrastructure [143], [144]. The electrical grid is in part not operational, although there are efforts by Trinity Energy to rehabilitate the grid [125]. There are also feasibility studies being conducted by Egypt and South Sudan for a Wau Dam project, which could generate 64 GWh of energy [145]. Because 65% of households rely on subsistence farming, all the food grown is primarily for consumption and therefore is unlikely to contribute as a significant enough source of biomass material for energy generation [144]. Along with more projects and positive government attention “Wau exhibits relatively low levels of political fragility” [146]. Because plans for large energy infrastructure are already underway, meaning the area could potentially become electrified shortly, Wau may not be a suitable location for a MG.

## 1.6) Carbon Footprint

Since many IMGs are primarily using diesel generators as their main source of power generation, it is important to address the carbon footprint left by them. The carbon footprint normally only refers to carbon dioxide ( $\text{CO}_2$ ) due to monitoring issues of greenhouse gasses [147]. However, diesel generators are also responsible for the release of many other hazardous greenhouse gasses aside from  $\text{CO}_2$ , such as diesel soot, aerosols, carbon monoxide, and oxides of nitrogen. While  $\text{CO}_2$  is the primary gas being considered, it does not undermine the effects of the other gasses. All the greenhouse gasses that are released into the atmosphere by diesel generators not only result in air pollution, but they have long term negative effects on the Earth. Greenhouse gasses lead to warming of the Earth's surface which causes retreating glaciers, rising sea levels, and climate change [148]. The introduction of renewable power sources, such as solar panels and wind turbines, would make the carbon footprint nonexistent. Since they do not release any gasses into the atmosphere, it would alleviate the negative effects of greenhouse gasses. While greenhouse gasses will always exist, gradually replacing these diesel generators with renewable systems will have lasting effects on the Earth.

$\text{CO}_2$  emissions are linked with the amount of fuel that is consumed by the diesel generator [147]. Fuel consumption can be calculated using this formula [149]:

$$\text{Equation \#3: } F = 0.246 * P_{\text{out}} + 0.08415 * P_r$$

Where,  $F$  is the fuel consumption rate (L/hr),  $P_{\text{out}}$  is the actual operating output power (kW), and  $P_r$  is rated power of diesel generator (kW). If the fuel consumption is divided by the energy per hour (kWh/h), it provides how much fuel is consumed with the change of energy (L/kWh). The carbon footprint can then be achieved by multiplying the average carbon emission factor of 3.0kg- $\text{CO}_2$ /L by the fuel consumption over energy (kg- $\text{CO}_2$ /kWh).

# High-Level Simulation Layers in Microgrid Design

## 2.1) General Information about Microgrid Simulations

To obtain any meaningful results in scientific endeavors a systematic approach is imperative, including thorough background research, data gathering and interpretation, hypothesis formulation, and rigorous analysis and simulation to test the hypothesis before comparing results with real-world experimentation. At this stage, the project focuses on exploring the part of the process where several simulations and analyses are performed to prove the claim that MGs and renewable energy could be the answer to power remote locations like South Sudan that rely so heavily on fossil fuels and ultimately also contribute to the enhancement and development of a new global integrated grid that can support the process of harnessing cleaner, robust, and reliable energy anywhere. Particularly, this project uses both high-level and low-level simulations to best understand how MGs could work in environments with different parameters and characteristics. High-level simulations are more effective in understanding the big picture and seeing whether a project with a particular configuration of equipment is economically and physically viable. These simulations typically involve techno-economic analyses and optimization of system components.

On the other hand, Low-Level simulations are crucial because they present a robust representation of how the specific components of the MG would work separately and interact with each other making a highly complex and holistic organism. This approach allows for a more rigorous and precise power flow analysis and simulation that ideally would be highly representative of what's expected to happen in real life; therefore, the use of reliable data and suitable equipment and algorithms is imperative. Following the conclusions from the previous section, these simulations will be centered on the location detailed around Juba, South Sudan. This approach will help assess the potential of MGs as a long-term energy solution for remote areas, taking into account local resources, energy demands, and environmental conditions.

## 2.2) High-Level Simulations

The conduction of high-level simulations was completed before moving into low-level simulations. The software that was chosen is considered high-level simulations, as they aim to unveil macro levels of the complexities of putting MGs together. We explored HOMER Pro, Sandia National Laboratories' Microgrid Design Toolkit (MDT), and Xendee due to their direct focus on MGs, ability to integrate several relevant complex economic and geographical variables as well as accessibility. For example, these inputs could narrow down a location on a map or allow for a value of power output of wind turbines and solar panels. From the provided inputs, these simulations would project and estimate a variety of different outputs, such as expected costs, power consumption, and fuel usage.

HOMER Pro (Hybrid Optimization Model for Multiple Energy Resources) is a very useful software intended to obtain simulations and optimize MG systems. It enables you to

evaluate different system designs and links different energy solutions with technical and economic parameters [150]. At the planning stage of an MG, tools like HOMER Pro are often used to perform adequacy planning (“sizing”) and preliminary economic optimization and feasibility studies [151].

Some of the main features of the software include being able to conduct sensitivity studies on selected variables, integrate varying renewable and non-renewable energy systems, model numerous system arrangements, and analyze system layout optimization based on selected cost and performance criteria. The ability of HOMER Pro to integrate site-specific information and to adjust simulations to the specific local circumstances makes it possible to be very useful in MG simulations in isolated regions like South Sudan. HOMER Pro has the advantage of being able to perform thousands of simulations in a few seconds due to its simplified, non-derivative optimization [152].

Some of the important factors that are often included in these simulations are site-specific solar and wind resources imported directly from NASA Power, rural community load profiles in the area, and regional component cost and specification. The software analyzes several KPIs (Key Performance Indicators) that are critical for determining the feasibility and efficiency of the MG systems. Particularly for this project and in general, some of the more robust and suitable economical and technical KPIs calculated by HOMER Pro to contrast different MGs are:

#### Economical

- Net Present Cost (NPC): HOMER Pro defines the net present cost (or life-cycle cost) of a component as the present value of all the costs of installing and operating the component over the project lifetime, minus the present value of all the revenues that it earns over the project lifetime. HOMER calculates the NPC of each component in the system, and of the system as a whole [153].
- Levelized Cost of Energy (LCOE): LCOE measures the lifetime costs of a project divided by energy production. It calculates the present value of the total cost of building and operating a power system over an assumed lifetime and it allows the comparison of different technologies (e.g., wind, solar, natural gas) of unequal life spans, project size, different capital cost, risk, return, and capacities. LCOE is the most popular and critical indicator for making informed decisions to proceed with the development of a facility, community, or commercial-scale project [154]. In HOMER Pro, LCOE is calculated by dividing the annualized cost of producing electricity by the total electrical load served, which includes primary AC and DC loads, deferrable loads, and energy sold to the grid. [155]. Hybrid micro-grid configurations incorporating solar PV, batteries and diesel in Sub-saharan Africa are considered affordable and viable if their LCOE is on the order of \$US 0.70/kWh [156].
- Return on Investment (ROI): ROI is a critical metric for energy projects because it provides a clear measure of the financial viability of the investment. It puts into perspective how integrating the new technologies can decrease certain costs in the future,

making it an important factor in deciding which projects to pursue and prioritize based on their expected profitability over time [157]. HOMER Pro calculates the ROI by comparing the annual cost savings of a new energy system to the initial investment required by it. For instance, if the new system saves \$10,000 a year and costs an extra \$50,000 to install, the ROI would be 20% per year, meaning one would recover their investment in 5 years [158].

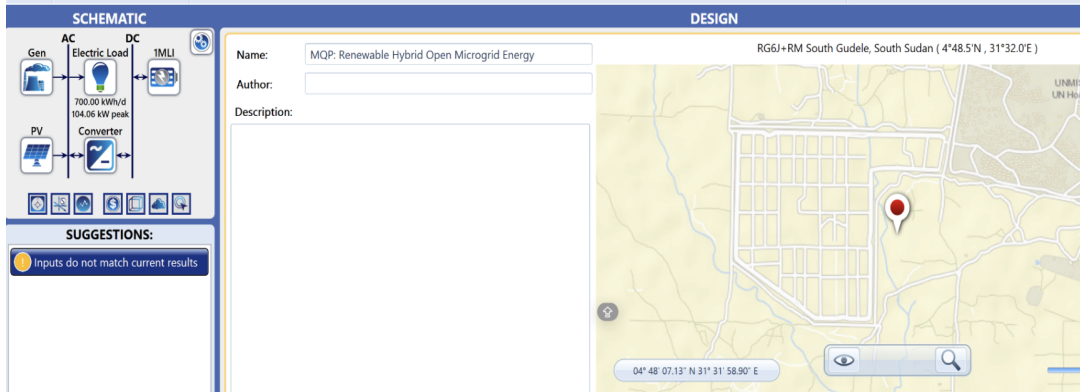


Figure 8: HOMER Pro Layout Example.

## Technical

- Renewable penetration
  - This metric is used to indicate how much of a grid's load is powered by renewable energy sources. The percentage of renewable energy that serves a load, is calculated by dividing the total load served by the amount of renewable energy produced by the system [159]. Suppose a MG produced 75 kWh of energy from solar and wind for a load of 100 kWh, the renewable penetration would be 75%.
- System reliability (Unmet load fraction)
  - The unmet load fraction is a measure of how much of an electrical grid's demand is not met. This is calculated by dividing the total load by the load that was met by the energy sources. This parameter identifies weaknesses in the system and specific times when demand is unmet. If there is a time when a system can not meet demand, then the system is considered unfeasible.
- Excess Electricity
  - There is excess electricity when the power sources produce more power than is needed. A MG typically uses an ESS to capture this excess energy, so that it can be used at a time when demand is not met by the power sources. Otherwise, excess electricity can be converted to thermal energy via a Thermal Load Controller or dissipated through a dump load.

## 2.2.2) Sandia's MDT

Sandia National Laboratories' MDT is a software for MG designers meant for the early stages of the development process. The MDT can compare thousands of configurations of different MG components and score them based on user-defined metrics such as performance, cost, and percentage of energy supplied by renewables. It allows the user to choose from many preset component configurations or input completely new components. The user sets each component to a baseline specification but is allowed to add more variable specifications, which the simulation will cycle through until it finds the best configuration of all components. The user can input site-specific information like solar, wind, and hydro resource availability as well as design basis threats that could affect a single component or the entire MG. This software allows designers to quickly and efficiently compare many different component types and specifications, all while allowing the user to control how the software scores each MG.

Market Information		Monthly Usage Charges		Carbon Emission Rates	
Monthly Connection Fees		Contract Demand Charge (\$/kW-month)	0	Electricity Carbon Emission Rate (kg/carbon/kWh)	0
Monthly Electricity Connection Fee (\$/month) :	<input type="text" value="0"/>	Standby Charge (\$/kW-month) :	<input type="text" value="0"/>	Natural Gas Carbon Emission Rate (kg/carbon/kWh) :	<input type="text" value="0"/>
Monthly Natural Gas Connection Fee (\$/month) :	<input type="text" value="0"/>	Carbon Tax (\$/kg-carbon) :	<input type="text" value="0"/>		

Usage Charge Rates							
Electricity	Others						
<b>Electricity Rates</b>							
Name	Start Month	End Month	Start Hour	End Hour	Period Type	Electricity Rate (\$/kWh)	Notes
* 1	double-click or type to add new						

Peak Demand Rate							
Name	Start Month	End Month	Start Hour	End Hour	Peak Demand Type	Daily Peak Demand Rate (\$/kW)	Monthly F
* 1	double-click or type to add new						

Figure 9: Sandia's MDT Layout Interface.

For our simulations, we used solar, wind, and diesel generators along with a battery and one variable load section that mimicked the average load use per day. A diagram of the system in the MDT can be found in Figure 10.

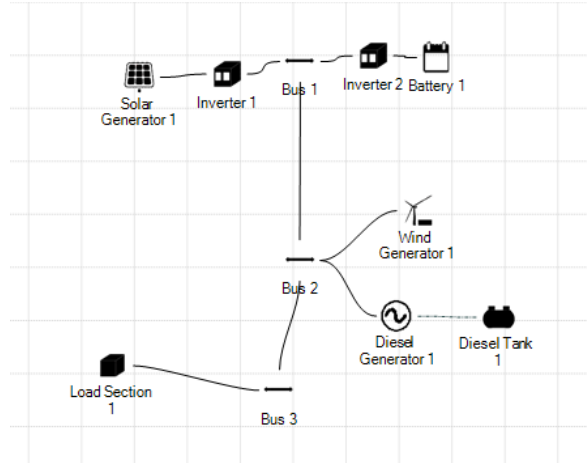


Figure 10: Sandia's MDT Layout Results.

### 2.2.3) Xendee

Xendee's design software allows for the modeling of power and energy flow in MGs and EV charging networks with constraints to create an optimal energy system with improved cost efficiencies, reduced carbon emissions, resiliency support, and automatic cable and transformer sizes.

When starting a design in Xendee you can choose several different options for the different kinds of technologies that your system may need. For DERs, there is solar PV, BESS, EV charging, wind turbine, run of the river hydro, generator, gas turbine, heat pump, etc. Once you choose the technologies for your system you will start with 3 blocks load, island connection, and controller. You are then able to place your chosen technologies from the start into your system which will all be connected to the island connection block.



Figure 11: Xendee Layout.

For all blocks except load, you will be able to set parameters such as install cost, maintenance cost, and lifetime of the technology. For the load, you can import your load data for an entire year and Xendee will produce a graph of the average load of a day for every month of the year. If you do not have a load, Xendee can generate a potential load for your system based on the type of building, the age of the building, the climate of the location, and the different kinds of technologies that might be used such as electricity, heating, cooling, etc. Xendee has included for the DERs a catalog where you can choose different kinds of that specific DER in case you don't know the specification of a DER. For generators, you can set the kind of fuel your generator will be using while also setting the cost of the fuel, the annual limit, the monthly access fee, and the emissions factor. You are also able to set the rated size and efficiency of the generator. For the wind turbine, you may choose the model of the wind turbine you would want to use along with its rated size and hub height. You are also able to upload the wind data or Xendee can generate wind data based on the previous parameters that were mentioned. This wind data will be shown as the average wind potential per kW capacity for a day for each month.

For solar PV and BESS, you can put in the cost and lifetime of an inverter. Specifically for solar PV, you can draw out the space where the solar panels could be and Xendee can

determine the area of that space. Then the parameters you can set for solar PV are unit spacing, panel rating, panel efficiency, inverter efficiency, DC to AC ratio, and the kind of array your solar panels may have. The different kinds of arrays you can choose are roof-mounted, open rack, axis tracking, and axis backtracking with the option to set the array's tilt angle and the direction the array is pointing. With these parameters for solar PV, you can generate solar data for your system or upload your data over a year. The data will be shown as the average kWac/kWdc for one day for each month. For the BESS, you can set the charging efficiency, discharging efficiency, min and maximum SoC, charging rate, and min and max annual cycles, etc. The DERs also have an option for optimization where Xendee during the analysis can consider using the DERs that will be the best which might not include one if it is the best option. There is also an option to include existing technologies which allows you to set the existing kWh and Xendee will perform its optimization with that in mind. Xendee also has an option to force the optimization to use a certain amount of kWh for a DER.

On the financial parameters, you can set a discount rate, project length, the kind of service you are looking for the system to be, a loan interest rate, etc., in order to see what kind of money you can make with the system. After setting the parameters of your system Xendee can optimize your system by reducing the cost, CO<sub>2</sub>, and any redundancy of electric and thermal energy. Xendee also allows you to choose a minimum amount of renewable energy that needs to be used in the system. Your optimization can also be compared to your previous optimizations, system from Xendee, or baseline cost and emissions.

Result	Value
Generation-Based Levelized Cost of Electricity (\$ / kWh) ⓘ	\$5.0762 / kWh
Load-Served Levelized Cost of Electricity (\$ / kWh) ⓘ	\$5.1996 / kWh
Starting EaaS Rate (\$ / kWh) ⓘ	\$5.2323 / kWh
Break-Even Year ⓘ	10 years
Payback Year ⓘ	9 years
IRR at End of Project (%) ⓘ	10.00%
NPC at End of Project (dollars in thousands) ⓘ	\$1,047k
Customer Metrics	
Result	Value
Total Cost (dollars in thousands) ⓘ	\$13,448k
Total Annual CO <sub>2</sub> Emissions (metric tons) ⓘ	312 mt

Figure 12: Xendee Financial Parameters example.

After Xendee has optimized the system they show the total new capacity and the initial equipment cost of the DERs that are the best for meeting the load demands and meeting your minimum required amount of renewable energy generation. Xendee also shows the

generation-based leveled cost of electricity which is the average cost per kWh of electricity purchased and generated by the system over the project term. It also shows the load-served leveled cost of electricity which is the average cost per kWh of electricity supplied by the system over the project term. Both represent the price per kWh that the system would need to receive to break even over its lifetime. Xendee shows the financial costs that you would spend a year for the total length of the project on things such as fuel, maintenance, equipment replacement, and the NPC.

There are also graphs for the return on interest and the cash accrued over the length of the project. For the DERs, you can see the distribution of energy between all DERs to see the amount of electricity being consumed and curtailed each month over a year. Lastly, Xendee has a detailed graph of all components of the system over a day for each month. This graph shows when each of the components is being used for energy, when the solar PV and wind turbine are being used for curtailment, when the BESS is being supplied energy, the SoC of the BESS, and the load.

The most important results are the total new capacity for each of the DERs which is the best combination that Xendee could come up with to meet the amount of renewable energy generation and the amount of energy needed for the load. The distribution of energy being generated by each DER shows which DER is generating the most energy while also showing the amount of electricity being curtailed. This also shows data on the amount of fuel being used each month from the diesel generator and the cost. Lastly, the graph of how all the components of the MG would work for each hour of a day for each month of the year is the most important. This graph puts into perspective why some components would be used more during specific hours or months while also seeing the load. From the graph, it is clear that during early mornings and night time, the wind turbine generates the most electricity while solar is generating more energy during the middle of the day. You can also see how when excess energy is being generated the battery is being charged and when the battery has hit max SOC it discharges and all the other DERs don't need to generate as much electricity because of the battery. During months where the solar PV and wind turbines generate less energy, you can see how much the diesel generator makes to compensate for them. The graph truly puts into perspective how the system would work with the parameters that were set.

# Low-Level Simulation Layers in Microgrid Design

After grasping a better understanding of the foundational concepts about MGs, the specific technical, environmental and economical restrictions and opportunities related to remote locations, and performing a high-level simulation informed by HOMER Pro in an extreme case like South Sudan, the next logical step is to design a more granular and informed low-level simulation that can accurately model dynamic interactions between power electronics, control systems, and transient events.

## 3.1) MATLAB/Simulink Software

Recent research has validated MATLAB/Simulink as a robust platform for low-level simulation purposes, offering the advantages of high-fidelity component modeling and multi-domain integration. In particular, Simulink includes a dedicated power system-specific toolbox within Simscape Electrical that allows for detailed modeling of components such as solar PV arrays, wind turbines, battery storage systems, inverters, etc [160]. These pre-built blocks allow users to customize parameters such as battery SOC dynamics, solar irradiance inputs, and inverter switching frequencies. This allows for precise replication of real-world conditions, corroborated on multiple studies, including a simulation in a conference paper that achieved 24-hour autonomy under transient loads [161]. This fidelity is critical for MGs where component failures can cascade rapidly.

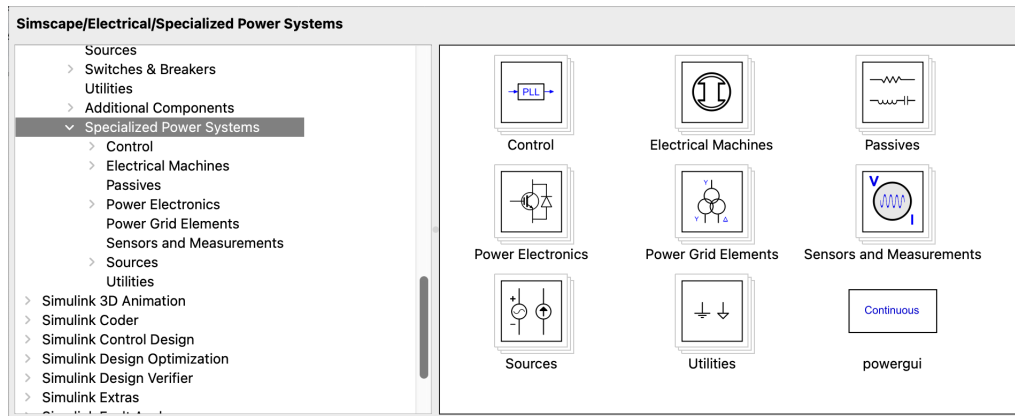


Figure 13: Layout of Specialized Power Systems Library in Simulink.

Furthermore, Simulink allows for the simulation of discrete, continuous, and transient dynamics at the same time, which is essential for modeling complex MG interactions. For example, a hybrid MG case study published by IEEE combined AC/DC subsystems with different solver configurations like continuous power flow and discrete control logic.

This versatility allows for the simulation of both small power electronics devices like droop-controlled inverters and large-scale grid dynamics including fault recovery or switching between grid-connected or islanded modes [162]. By being able to design the MG with any parameters for each component, it allowed for the optimization of the MG design. Once the design was completed, the higher variable predictors for MG's desired outcomes were identified. With an optimized MG, the results of different inputs could be inspected and analyzed.

### Subsystems

The Simulink subsystems are independent functional blocks, modeling specific components and their interaction. Each subsystem is given in the form of a masked block presenting the detailed component models and control logic [163]. In this case, the MG's subsystems are interconnected components that work together to provide consistent power delivery and optimal system performance. Each subsystem has a specific function while communicating and coordinating with the others and has a very easy to set up interface for related inputs and outputs. The main subsystems in this low-level simulation which will be explored in detail shortly, include power generation, power conversion, energy storage, distribution, and control systems.

### 3.2) Renewable Hybrid Optimized MG Energy (RHOME) Model

The energy transition is a reality that's being heavily shifted in multiple directions that aim to incorporate renewable energy sources into the grid effectively, as well as modernize the current system and infrastructure that allows for energy transmission and distribution worldwide. The Soviet astronomer Kardashev proposed a scale in 1964 that was later on refined by Carl Sagan, that intended to measure the level of technological development of civilizations based on the amount of energy that they are able to utilize [164]. According to them, a Type I civilization would be able to consume all energy that reaches its home planet from its parent star. According to Sagan's extended model, modern-day humanity is described as a Type 0.73 civilization as of 2020 [165]. Attaining this status would allow humans to have cleaner and easily accessible energy systems, which will accelerate progress and improve the quality of life for everyone on Earth. Such an effort would require highly efficient energy management at a planetary scale, which is only possible if access to electricity is safe, reliable, and abundant everywhere on Earth, especially to those populations that need it the most and where potentially there is not even access to the grid.

As an attempt to further investigate and understand the challenges and opportunities of deploying IMGs in the most demanding possible conditions, the RHOME Simulink model (Figure 14) aims to showcase the details of how it would be practically feasible to deploy and run a completely remote MG on a location like South Sudan with the lowest energy access per capita in the world and showcase the most relevant details on a 24-hr basis. This simulation was informed by economic, technical, and environmental factors specific to the region.

Initially informed by HOMER Pro's analyses, the design includes a robust 1.4MW PV Solar system, a 100kW Wind Turbine, a 1MW Diesel Generator, a 6MWh Battery with its respective Management System, an inverter controller, approximated variable load, real irradiance and wind speed values from different conditions, and several other power electronics components and algorithms that further enhance the simulation making it as realistic as possible.

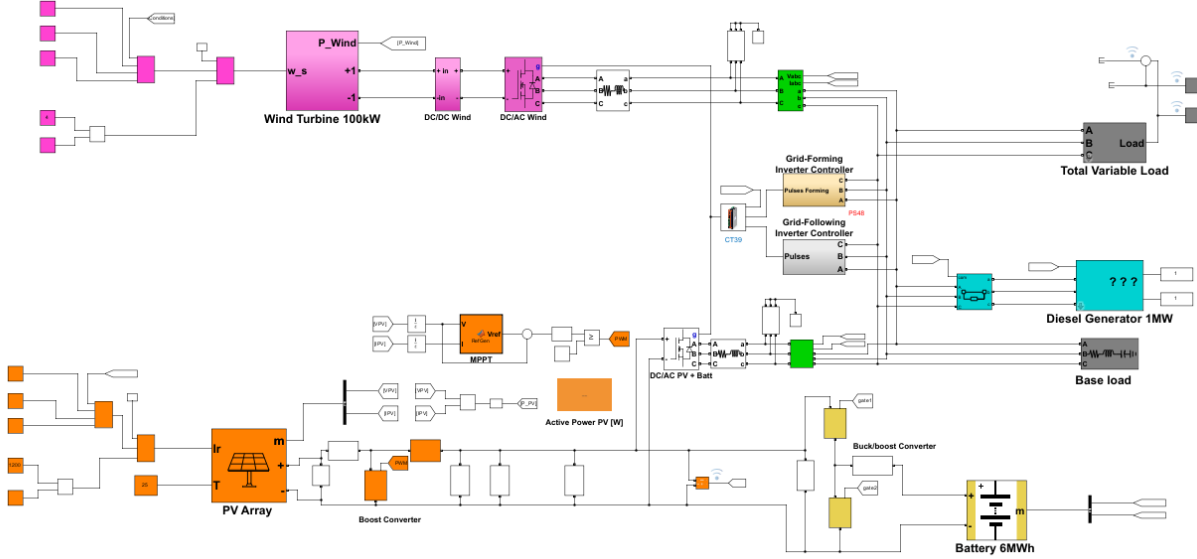


Figure 14: RHOME System

Figure 15 shows the IEEE standards adapted for the RHOME simulation. Incorporated into the RHOME system are the IEEE Std 2030-2011 power systems, information technology, and communication technology axioms. The battery system falls within the storage domain. The storage domain connects to the generation domain via the PS42 Interface, which manages interactions between storage systems and generation units. These domains are also connected to the distribution domain via the PS42 Interface. This connection is shown in the BMS of the RHOME simulation, shown in Figure 27. The distribution, storage, and generation domain all communicate via the CT39 Interface, in the simulation, as shown in Figure 31. This CT39 interface connects grid-scale resources to wide-area networks using fiber-optic or wireless communication protocols. For the purposes of this simulation, it only allows coordination between the storage, generation, and distribution domains.

The battery storage system also connects to the financial domain via PS51 Interface, which connects the storage domain to the market operations domain, shown in Figure 40. The battery storage domain is connected to the controls and operations domain via the PS55 Interface. This interface connects the generation operations with bulk storage through SCADA systems, which monitor and control energy flow, in the simulation, shown in Figure 33.

Interfaces PS48 and PS49 connect the financial domain to the controls and operation domain. PS48 links to the energy distribution system, while PS49 links to the energy generation system within the operations and controls domain.

These connections are referenced in Figures 31 and 33 in the RHOME simulation. The financial domain in the simulation is shown in Figure 42. The generation domain consists of the diesel generator, PV array, and wind turbine. The generation domain connects to the financial domain via the IT20 Interface, which connects the generation domain to the financial domain, in the simulation, as shown in Figure 42. Interface ITN01, in the simulation, shown in Figure 33, informs the conditions under which the power generation source operates.

This simulation incorporates several IEEE Std. 2030-2011 standards, but not all of them were applicable to the RHOME simulation. The RHOME simulation primarily focused on the power system aspects of an IMG. The IEEE standards served primarily as guidelines, as opposed to blueprints.

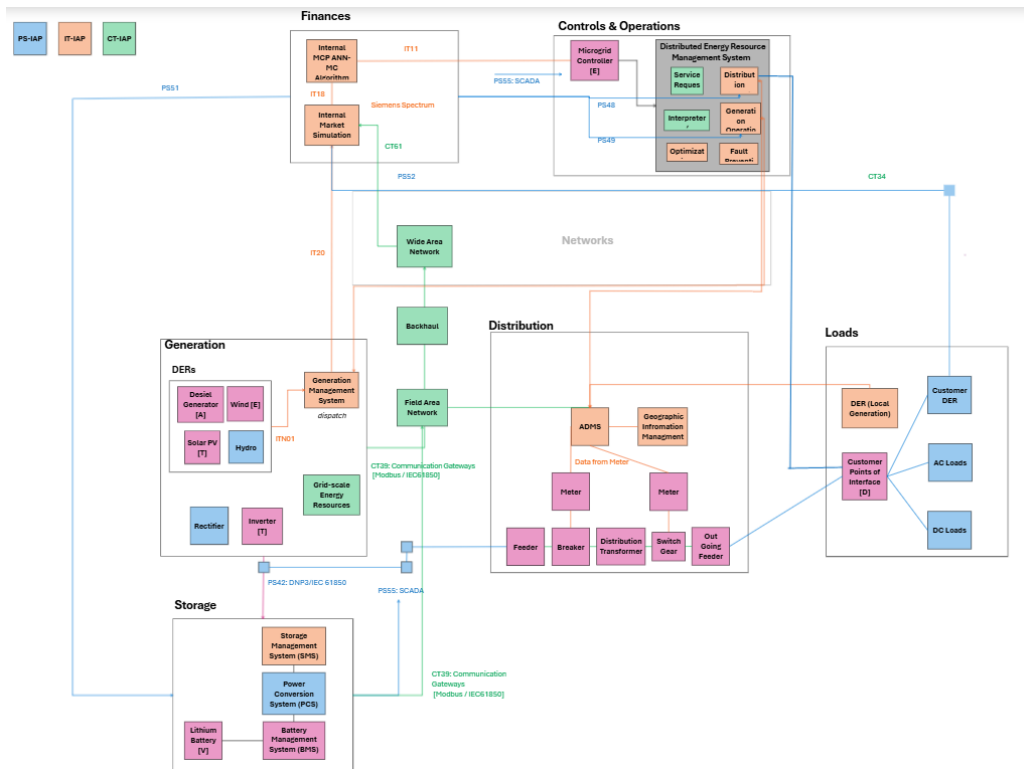


Figure 15: IEEE and MG model synthesis

### 3.3.1) RHOME Subsystems

#### 3.3.3.1) Solar PV

The 1.4MW rated Solar PV subsystem aims to simulate a real solar array designed to account for different energy production standards under varying environmental conditions of irradiance and temperature. The system consists of three main components including the PV array itself, a Maximum Power Point Tracking (MPPT) controller, and a DC/DC boost converter, in addition to other filters, controls, and measurements.

The PV array is the main energy generation unit in the system as geographically South Sudan has excellent potential for solar energy and taking advantage of that is imperative. The array is modeled using Soltech 1STH-215-P modules, configured with 660 parallel strings and 10 modules per string, resulting in a total rated capacity of 1.4 MW under standard test conditions, although it is always possible to arrange different configurations of panels and strings to achieve the same DC rating. Solar irradiance and temperature are dynamically varied in the simulation to replicate real-world conditions but incorporate real data from NASA Power from the location in Juba described in detail in previous sections. Higher irradiance increases current output, while higher temperatures reduce open-circuit voltage, slightly lowering efficiency. The PV array outputs voltage VPV and current IPV, which are then passed to the MPPT controller for optimization.

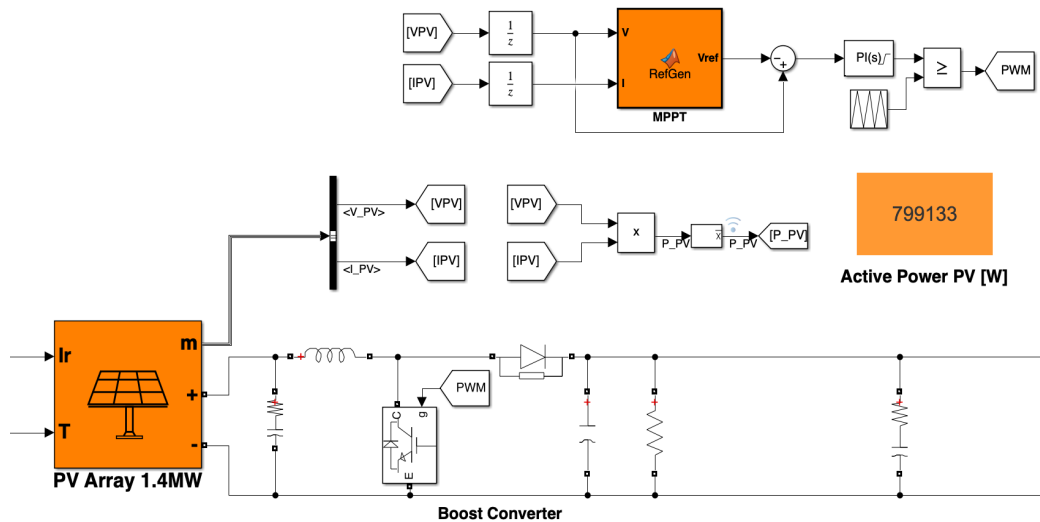


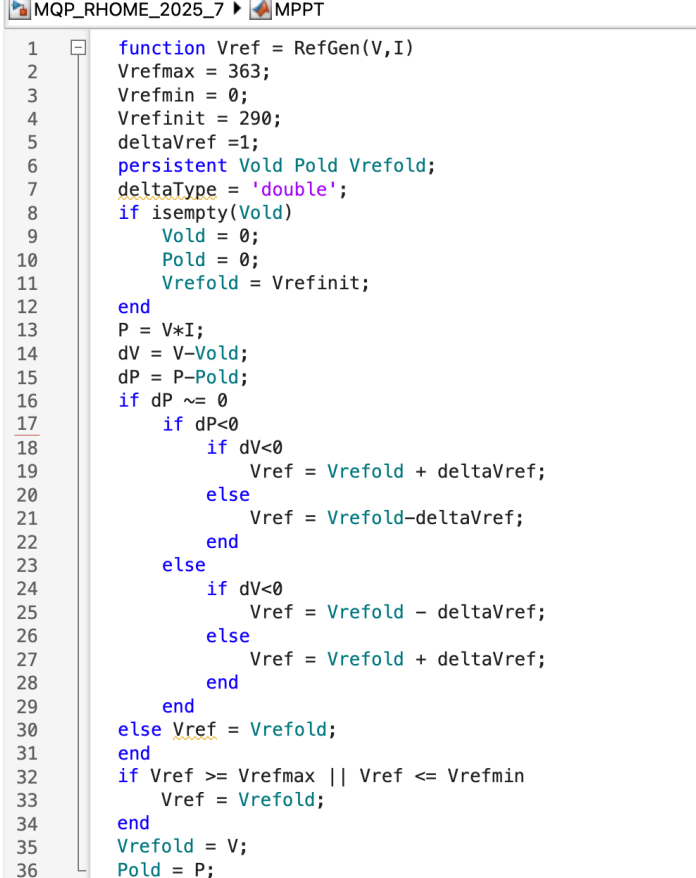
Figure 16: PV Solar Subsystem.

Moreover, an RC input filter was placed between the PV array and the boost converter to stabilize the voltage and reduce the noise in the system. The resistor has a value of  $1 \text{ m}\Omega$  which aims to minimize power losses while providing enough damping without causing a huge voltage drop. The cap has a value of  $1000 \mu\text{F}$  so that it can handle high power ratings and provide suitable energy storage for smoothing out voltage ripples. This basically would make sure that the boost converter receives a stable input voltage and improves its efficiency and performance.

#### Maximum Power Point Tracking

The MPPT controller ensures that the PV array is always operational at its maximum power point, providing maximum power output for the environmental conditions existing at the time. The Perturb and Observe algorithm adjusts Vref in small increments in order to optimize power output. The controller measures VPV and IPV continuously to calculate power.  $P_{\text{PV}} = VPV \times IPV$ . The perturbation of Vref is made smaller and smaller until enough changes occur in the power. If the power output increases, Vref continues in the current direction; if not, the process is reversed (process explained in Figure 17).

Basically, the system is allowing for the dynamic adaptation to the variable irradiance and (if needed) temperature conditions. The MPPT generates the error signal through comparison of Vref and VPV to a PI controller. The output of the controller is a PWM signal that controls the DC-DC boost converter operation.



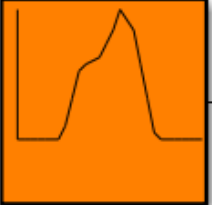
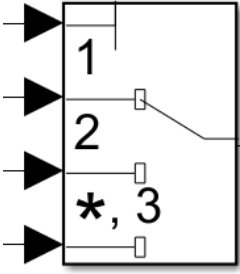
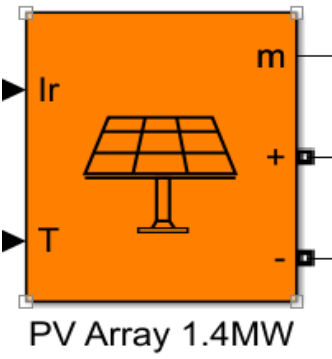
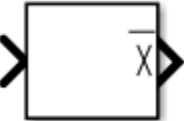
```

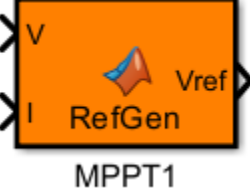
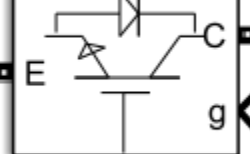
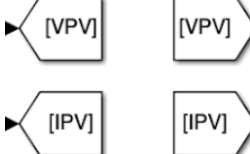
1  function Vref = RefGen(V,I)
2      Vrefmax = 363;
3      Vrefmin = 0;
4      Vrefinit = 290;
5      deltaVref =1;
6      persistent Vold Vrefold;
7      deltaType = 'double';
8      if isempty(Vold)
9          Vold = 0;
10         Pold = 0;
11         Vrefold = Vrefinit;
12     end
13     P = V*I;
14     dV = V-Vold;
15     dP = P-Pold;
16     if dP ~= 0
17         if dP<0
18             if dV<0
19                 Vref = Vrefold + deltaVref;
20             else
21                 Vref = Vrefold-deltaVref;
22             end
23         else
24             if dV<0
25                 Vref = Vrefold - deltaVref;
26             else
27                 Vref = Vrefold + deltaVref;
28             end
29         end
30     else Vref = Vrefold;
31     end
32     if Vref >= Vrefmax || Vref <= Vrefmin
33         Vref = Vrefold;
34     end
35     Vrefold = V;
36     Pold = P;

```

Figure 17: MPPT algorithm for PV Subsystem.

The boost converter steps up the variable DC voltage from the PV array to a stable DC bus voltage. It includes an inductor, diode, switch IGBT, and capacitor. The MPPT controlled PWM signal alters the duty cycle of the switch to control the output voltage. Whereas during this phase, energy is stored into the inductor, when the switch is opened, the stored energy is released through the diode to increase the output voltage. The output capacitor smooths out the ripples present in the boosted voltage. The boost converter is designed under the worst-case scenario, considering the minimum input voltage being 290 V and the maximum input voltage being 365 V, and output voltage is about 550 V. The switch control frequency is set at 10 kHz to run with a balance of efficiency and performance. Finally, key design parameters include an inductor of 4.15 mH and a capacitor of 0.053 F, which maintain current and voltage ripples as per industry standards (i.e. current ripple below 5% and voltage ripple below 1%) [223].

	<p><b>Repeated Sequence Interpolated:</b> This component outputs a discrete time sequence. The data within this component would then be inputted into another component, which in this case would be a multiport switch (useful for irradiance, temperature, and other values that vary sequentially).</p>
	<p><b>Multiport Switch:</b> This component receives input data and sends it out based on the control port, which is the first input port. The other ports are data ports for the switch. In this case, it helps to determine which irradiance to use depending on the Power Generation Suitability Condition set.</p>
	<p><b>PV Array:</b> This component replicates a PV array that has PV modules connected in parallel. It contains a variety of different parameters for proper modeling of an actual PV array.</p>
	<p><b>Terminator:</b> This component ends output signals, but can also be used to plug unconnected output ports to prevent warnings. It also helps to log in signals when there's no need to connect them anywhere else.</p>
	<p><b>Mean:</b> This component takes the mean of the signal being inputted using 50 Hz frequency.</p>

	<p><b>Bus Selector:</b> Output of measurement component signals for testing or verification</p>
 MPPT1	<p><b>Function block:</b> MPPT algorithm block that is able to take V and I from a PV system and then provide a Vref value that's then contrasted before a PWM is generated.</p>
	<p><b>IGBT/Diode:</b> This component replicates an ideal IGBT, GTO, or MOSFET and antiparallel diode.</p>
	<p><b>From/Go to signal blocks:</b> Useful to check/use signal values in multiple places in the simulation to avoid long/confusing wiring.</p>
	<p><b>Diode:</b> This component replicates an ideal diode that is in parallel with a series RC snubber circuit.</p>
	<p><b>Series RLC Branch:</b> This component replicates a series connection of RLC parts. Its appearance changes depending on the selection.</p>

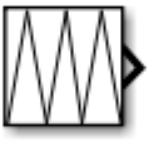
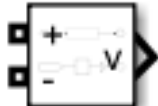
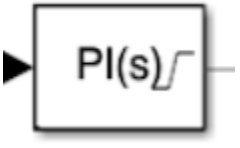
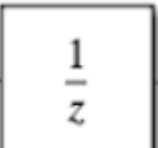
	<b>Relational Operator:</b> Compare 2 signals constantly with the specific operator set.
 Active Power PV [W]	<b>Display:</b> Displays the real-time value of an input signal in a user-defined format, aiding in monitoring and debugging.
	Repeated triangular sequence for comparison
	<b>Voltage Measurement:</b> This component takes the voltage where it is connected at.
	<b>PI controller:</b> A Proportional-Integral controller that minimizes error between a desired setpoint and actual output by adjusting system inputs dynamically.
	<b>Delay:</b> Introduces a discrete-time delay to prevent algebraic loops and simulate real-world signal propagation delays.

Table 2: The list of Components within the Solar System.

### 3.3.3.2) Wind

The wind turbine system is rated for 100kW and supplies the MG with energy throughout the day and into the night when solar power becomes ineffective. The entire turbine system is made up of three main parts. The first is the simulated wind turbine, the second is the DC/DC converter and the final part is the universal bridge. These three parts work together to transform the output signal from the wind turbine to match the voltage and frequency of the rest of the system.

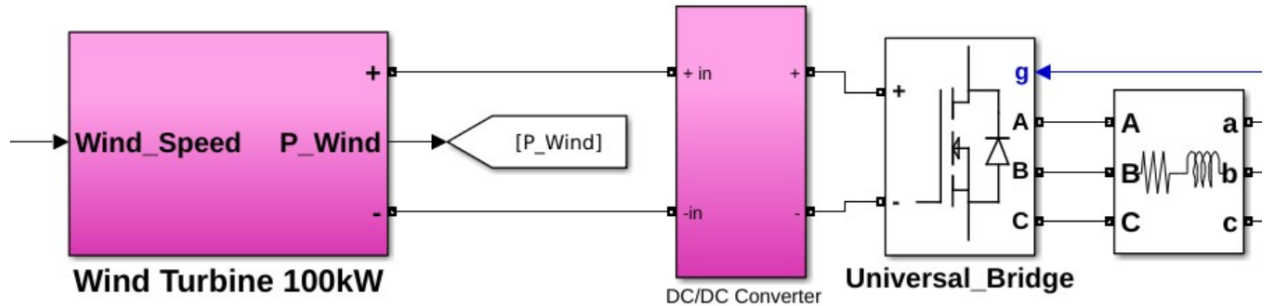


Figure 18: Wind Turbine related subsystems.

Inside the wind turbine subsystem, the wind turbine model used is rated for 100kW and takes inputs of wind speed, pitch angle and generator speed. In the simulation, the wind speed data used can be changed by the user between fabricating wind speeds relative to real-world data or by selecting actual data from NASA Power in Juba. The pitch angle controller takes the per unit rotational radians per second of the generator and calculates the pitch angle necessary for the highest amount of energy to be produced. Additionally, if wind speeds get too strong to the point where they would damage the wind turbine, the pitch angle controller changes the pitch angle so that the turbine blades are in line with the wind, stopping the blades from spinning.

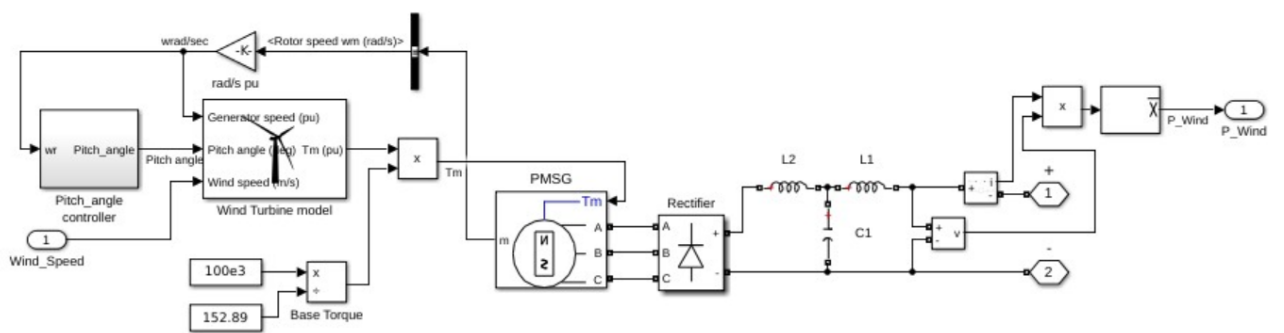


Figure 19: Wind turbine subsystem (internal).

The output of the wind turbine is the per-unit torque generated, which can be turned into the total torque by multiplying the output by a base torque value. This base torque value is determined by the torque produced at the rated power of the wind turbine, and is calculated by dividing the rated power by the rotational speed in radians per second at that rated power. The output torque from the wind turbine feeds into a permanent magnet synchronous machine which is the generator for the turbine system, producing three-phase power to the rest of the system. Next, the three-phase power is converted into DC power in order to filter the signal and prepare it for the next section of the turbine system, the DC to DC converter.

The second major section of the wind turbine system is the DC/DC converter that stabilizes the output from the turbine and bucks or boosts the voltage to a usable value for the rest of the system. This converter contains a chopper that bucks the voltage to the desired output. The desired voltage output is calculated by measuring the current output voltage, inputting it through a transfer function and determining the error between current and desired voltages. It then calculates a duty cycle based on how to achieve the desired voltage from the current one and feeds that duty cycle back into the chopper.

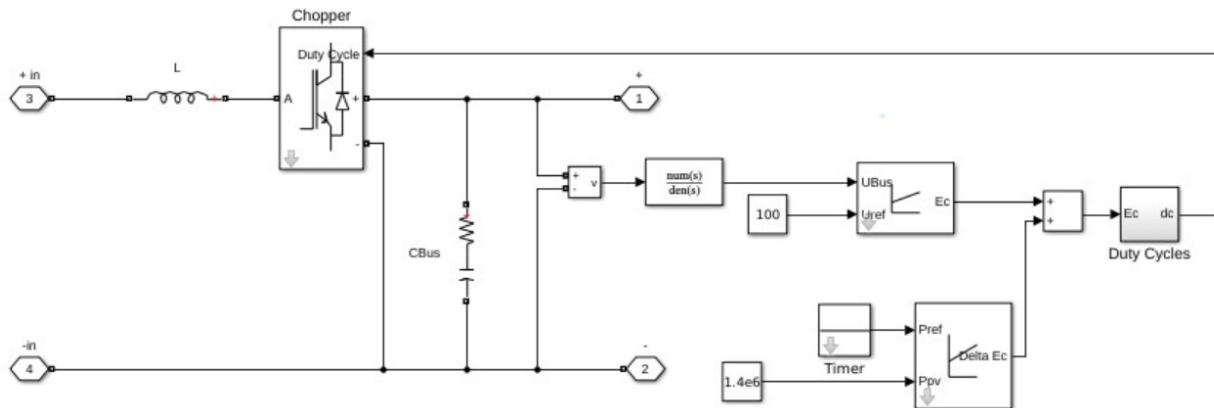
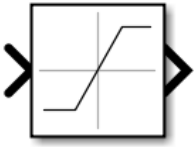
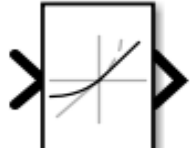
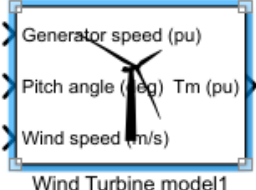
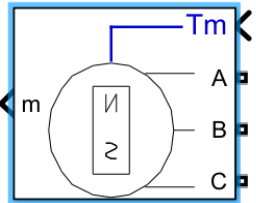
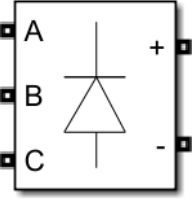
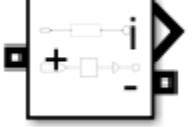


Figure 20: DC/DC Converter subsystem (internal).

The third important component in this turbine system is the universal bridge, used to get the desired voltage in an AC sine wave so that the main bus of the system has a standard and synchronized voltage. The pulse of this universal bridge is inputted from the inverter controller and is used to convert the output of the wind power to match the voltage of the MG.

	<p><b>Value Limiter:</b> This component limits the input signal to the values specified within the component and outputs the filtered signal.</p>
	<p><b>Rate Limiter:</b> This component limits the rate of a signal increasing or decreasing and outputs the filtered signal</p>
	<p><b>Wind Turbine Model:</b> This component resembles a wind turbine structure with many parameters the user can edit such as output power, efficiency, and rated power of the electric generator.</p>
	<p><b>Permanent Magnet Synchronous Machine:</b> This synchronous machine takes in the amount of torque applied to it and generates three-phase power in response.</p>
	<p><b>Rectifier:</b> This component transforms three-phase signals into a DC signal.</p>
	<p><b>Current measurement:</b> This component measures the current of the signal it is placed on.</p>

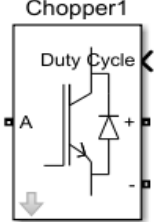
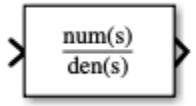
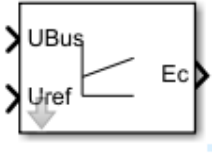
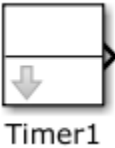
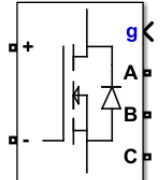
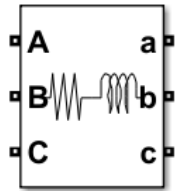
	<b>Chopper (DC/DC Converter):</b> This component resembles a buck converter with a duty cycle.
	<b>Transfer Function Block:</b> Represents a transfer function in the Laplace domain useful for filtering.
	<b>Error Calculation:</b> Computes the error signal by subtracting a reference voltage $U_{ref}$ from a measured bus voltage $U_{bus}$ . Essential to determine the deviation from the desired setpoint.
	<b>Timer block:</b> Simulates a timer module that increments a counter based on an external or internal clock source.
	<b>Universal Bridge:</b> This component transforms DC power into three phase AC by receiving a pulse signal and using a switching device to create the desired voltage output.
	<b>Three-Phase Series RLC branch:</b> This component replicates a three phase series connection of RLC parts. Its appearance changes depending on the selection.

Table 3: The list of Components within the Wind System.

### 3.3.3.3) Diesel Generator

The diesel generator (Figure 21) generates approximately 1 MW of power. The purpose of the diesel generator is to provide power when there is not enough solar power, wind power, or sufficient battery capacity to sustain the MG's load demand. The diesel generator is responsible for setting the frequency and voltage reference for the MG by operating in droop control mode, dynamically adjusting its output to stabilize both frequency and voltage when renewable sources and the battery are unable to meet the variable load demand. The diesel generator system in this model was adapted from an available for-download simulation [166]. The quantities and inputs were changed to match the needs and specifications of our system. The switch is operated depending on the power generation suitability conditions.

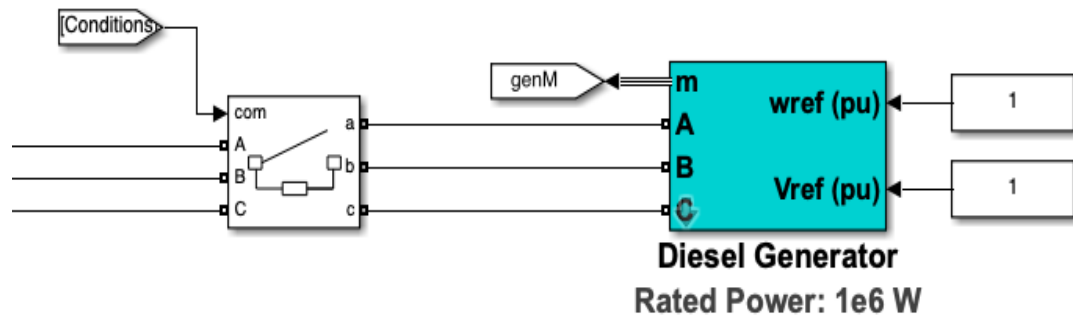
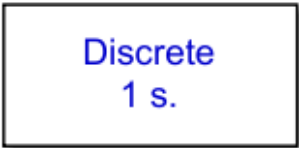
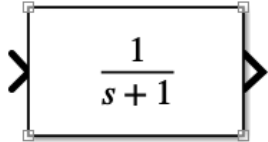
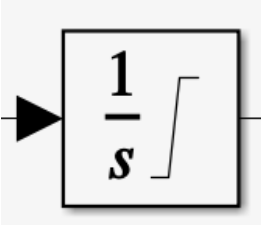
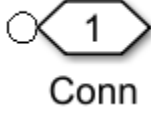
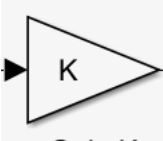
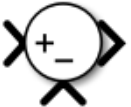
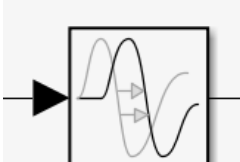


Figure 21: MG Diesel Generator with reference voltage and frequency as inputs.

	<b>Synchronous pu Machine Standard:</b> takes mechanical power and field voltage as inputs, models a three-phase salient-pole synchronous machine, and yields a measurement signal [167].
	<b>AC1A Excitation System:</b> models the excitation system of IEEE Standard 421 [168].

	<p><b>Powergui:</b> facilitates the method of circuit solution and “opens tools for steady-state and simulation results analysis and for advanced parameter design.” It is also required to simulate a system <a href="#">[169]</a>.</p>
	<p><b>Transfer Fcn:</b> depicts, in the frequency domain, the relationship between the input and output of the function <a href="#">[170]</a>.</p>
	<p><b>Integrator:</b> integrates a signal.</p>
	<p><b>Physical Modeling Connection Port block for subsystems:</b> “transfers a physical connection or signal across subsystem boundaries” <a href="#">[171]</a>.</p>
	<p><b>Gain:</b> magnifies the input value by some constant.</p>
	<p><b>Sum:</b> add or subtract inputs.</p>
	<p><b>Transport Delay:</b> delays the input signal by a specified amount of time <a href="#">[172]</a>.</p>

	<b>Import:</b> provides an input port for a subsystem.
	<b>Outputport:</b> provides an output port for a subsystem.
	<b>Fcn:</b> Represents a function
	<b>Constant:</b> outputs a specified constant.
	<b>Product:</b> Outputs the product of two inputs.

Table 4: The list of Components within the Diesel Generator System.

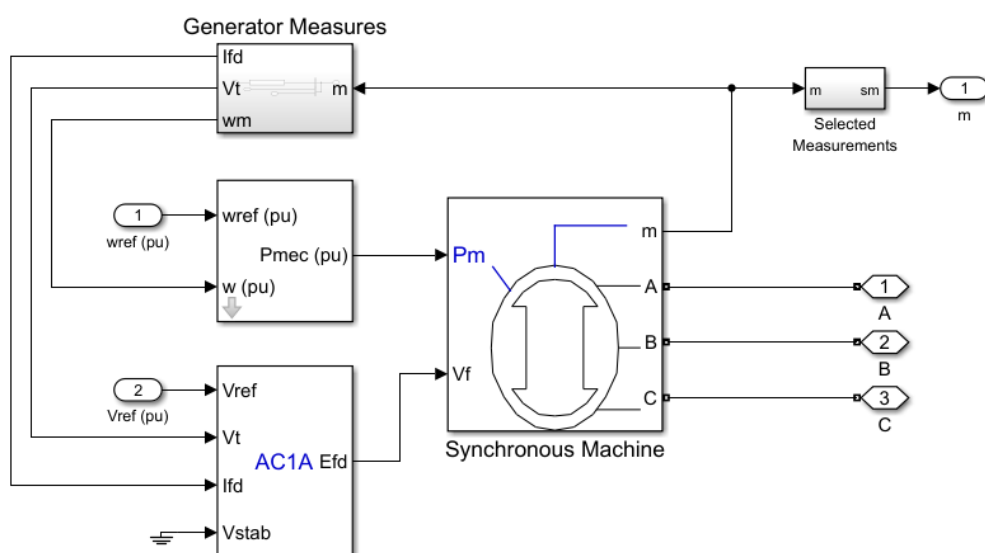


Figure 22: Internal Visualization of Diesel Generator.

The Synchronous pu Machine Standard block takes in mechanical power and field voltage as the inputs to output a three-phase voltage of 285V phase-to-ground to transmit power to the rest of the load. The Synchronous pu Machine Standard block also has a measurement port that measures the quantities shown in Figure 22. Relevant measurements are also fed back into the system, shown in Figure 22, to minimize errors, where they go into the Prime Mover and Governor, and Automatic Voltage Regulator (AVR) and Exciter. The mechanical power, fed into the  $P_m$  port on the Synchronous pu Machine Standard block, takes in the Prime Mover and Governor output, shown in Figure 22 as the block in the middle left. The field voltage, fed into the  $V_f$  port on the Synchronous pu Machine Standard block, takes in the output from the AVR and Exciter, shown in Figure 22 as the block on the bottom left.

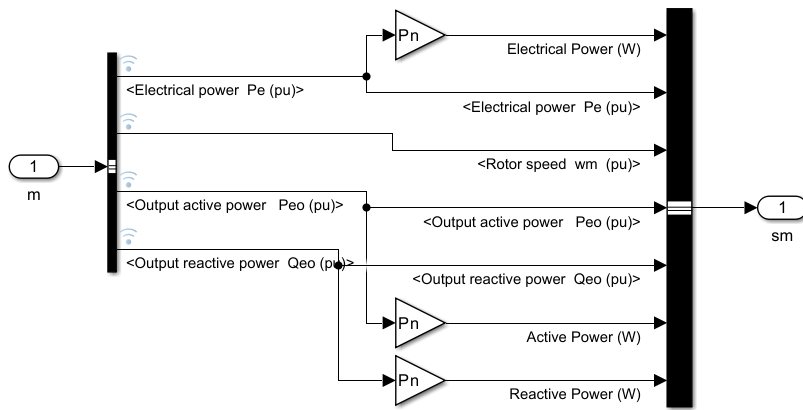


Figure 23: The measurements of the Diesel Generator.

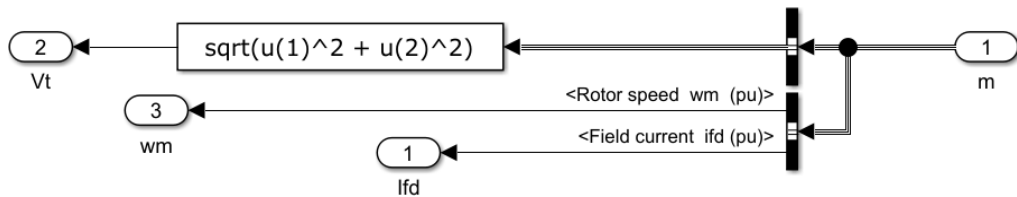


Figure 24: The rotor speed, field current, and terminal voltage from the Synchronous pu.

Machine Standard blocks are fed back into the corresponding components. The function, shown, calculates the magnitude of the terminal voltage from the stator voltage ( $v_d$ ) and stator voltage ( $v_q$ ). The AVR maintains a stable output voltage regardless of how the load changes by controlling the field voltage of the generator. It controls the generator's voltage by comparing a stable reference voltage and adjusting the field current to match [221]. The AVR compares the reference voltage with the actual generator voltage and generates an error signal; this error is then processed by a controller that adjusts the excitation voltage ( $E_{fd}$ ) applied to the field voltage winding of the synchronous machine.

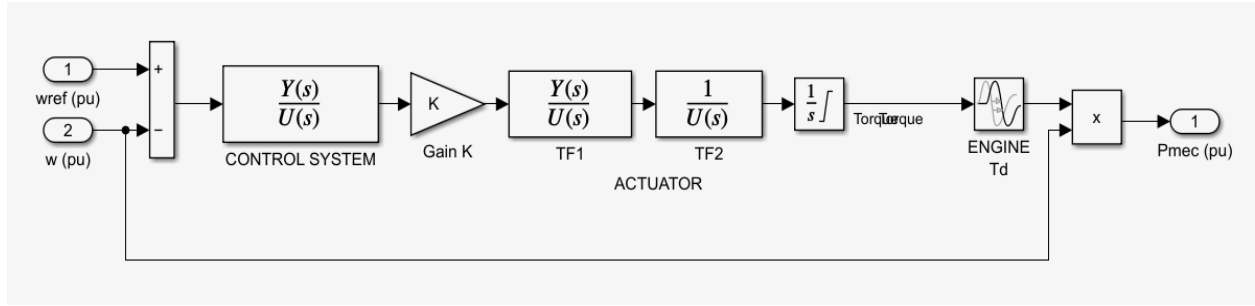


Figure 25: The internal view of the Prime Mover and Governor of the Diesel Generator.

The Prime Mover and Governor (Figure 25) of the system are responsible for the regulation of mechanical power that is imputed into the generator to control the rotor speed and thereby frequency. The governor compares a reference frequency with the actual rotor speed or frequency and generates an error signal. The system is represented via an actuator. In this model, the actuator is composed of transfer functions, a gain, an integrator, and a transport delay. Thus, the system can maintain a stable rotor speed and frequency despite changes in load or other disturbances so that electrical power output can remain within acceptable limits.

### 3.3.3.4) Battery

The BESS uses a 6MWh lithium-ion battery to store excess amounts of energy when solar PV can exceed the current load and the SOC is under a certain amount of charge. It is also able to discharge stored energy to the load when solar PV is unable to meet the load. The system consists of the simulated battery and the buck/boost converter. The simulated battery is set to be a lithium-ion battery with a nominal voltage of  $400/\sqrt{3}$  V and a rated capacity of 17000Ah. The voltage is set to  $400/\sqrt{3}$  V to match the voltage of our entire system (1 phase) and the rated capacity of 17000Ah represents the amount of current the battery can provide over an hour. To control when the battery is charging and discharging, data from both the battery and the solar PV are taken, which will make the buck/boost converter swap depending on the data. When the solar PV exceeds the amount of power needed for the load, the converter will operate in buck mode, which will decrease the voltage from the solar PV and charge the battery. When the solar PV is unable to meet the load, the converter will operate in boost mode, which increases the voltage from the battery and discharges energy to the load.

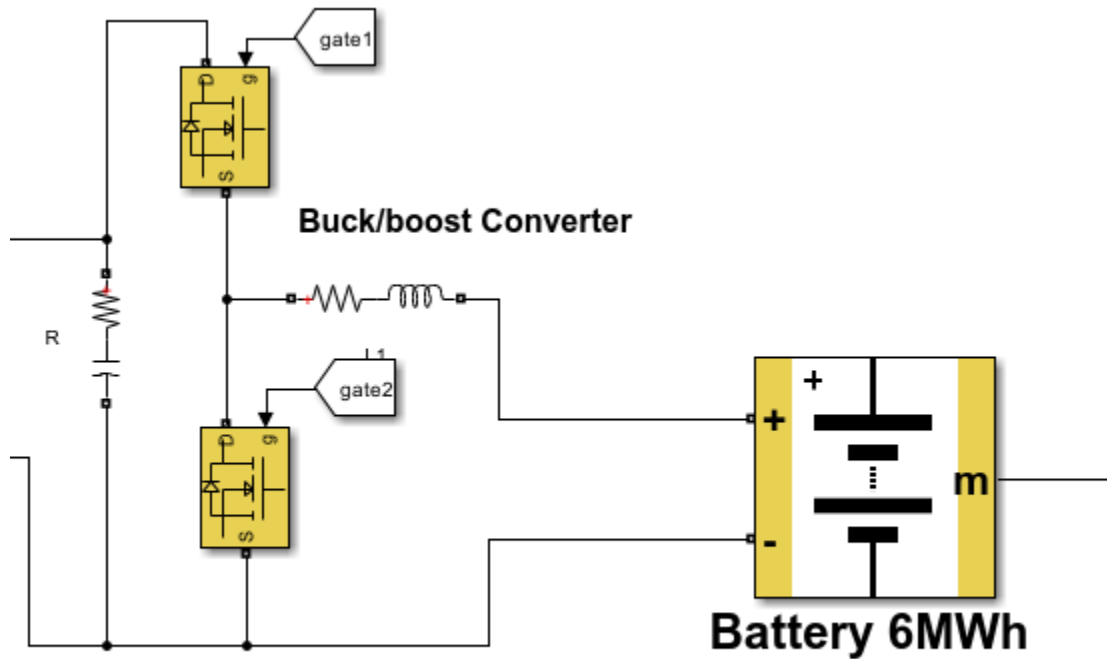


Figure 26: Battery system and buck/boost converter.

	<b>Battery:</b> This component replicates a single battery and contains various parameters in order to properly model an actual battery in an ESS.
	<b>Mosfet:</b> This component replicates a MOSFET and internal diode in parallel.
	<b>Series RLC Branch:</b> This component replicates a series connection of RLC parts. Its appearance changes depending on the selection
	<b>Voltage Measurement:</b> This component takes the voltage where it is connect at

Table 5: The list of Components within the Battery System.

## Battery Management System

The BMS in the RHOME model is a critical control system that was designed to regulate the operation of the battery in relation mainly to the PV. Its primary function is to make sure that the battery can charge and discharge accordingly when there's more or less power available from the PV subsystem, while also intending to reliably maintain the stability of the MG in terms of constant 400V AC voltage and 50 Hz frequency for South Sudan. The BMS helps make this happen by managing the charging and discharging processes, monitoring key battery parameters, and stabilizing the DC bus voltage.

The system continuously measures the actual DC bus voltage  $V_{bus}$  and compares it to a reference value set at 550 V (which is about 1.5 times greater according to industry standards). This reference represents the desired operating voltage for the MG. Any difference between these two values creates an error signal, which is then processed by the PI controller. The PI controller outputs a reference current,  $iB_{ref}$ , for the battery, which then determines how much current should flow into or out of the battery to correct deviations in the DC bus voltage. By adjusting  $iB_{ref}$  in this way, the BMS is making sure that when, for example, there are sudden changes in load demand or renewable energy generation, it doesn't destabilize the system abruptly.

In addition to stabilizing the DC bus, the BMS manages whether the battery is in a charging or discharging state, which is being controlled through a logic block that processes the duty cycle signal,  $duty_B$ . The duty cycle signal also tells the DC-DC converter how to operate and determines how energy flows between the battery and other components of the MG.

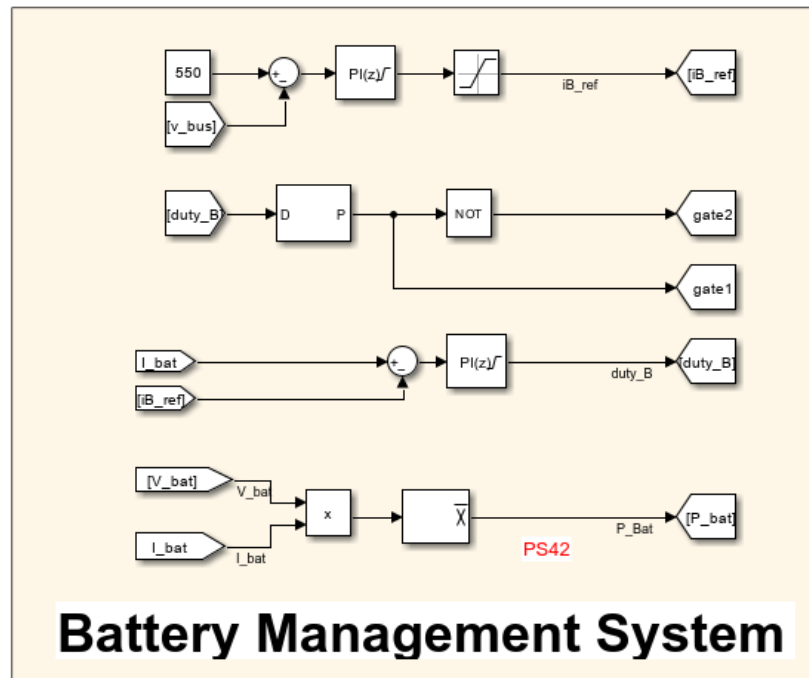


Figure 27: Battery Management System

The BMS also is continuously checking battery parameters such as  $V_{bat}$  and  $I_{bat}$ . These measurements are used to calculate real-time power output from the battery,  $P_{bat}$ , which is determined by multiplying  $V_{bat}$  and  $I_{bat}$ . Monitoring  $P_{bat}$  provides valuable insights into how much energy is being delivered to or drawn from the battery at any given moment, which helps to understand if the demand is being met in real-time or not. Additionally, another PI controller compares  $I_{bat}$  with  $iB_{ref}$  and adjusts  $duty_B$  accordingly, ensuring that the actual current flowing through the battery matches the real limit reference current as closely as possible.

### 3.3.3.5) Total Variable Load

The variable load (Figure 28) represents the daily power demand fluctuation of a population in South Sudan. This data, represented as the signal block in Figure 28, inputs 24 points at different magnitudes to represent energy demand fluctuation at various points in a 24-hour day. These values were approximated from a study of an off-grid energy system for a remote rural community and scaled up to 7000 kWh per day, based on the HOMER Pro calculation [173]. The goal of the MG system is to provide enough power to consistently meet the population's energy demands. The diesel generator system in this model was adapted from the same simulation as the diesel generator. The total load was split into a total variable load and a base load (250kW) because the diesel generator is the only power source in the model that can follow a variable load. The base load is to be satisfied by the other energy sources in the system.

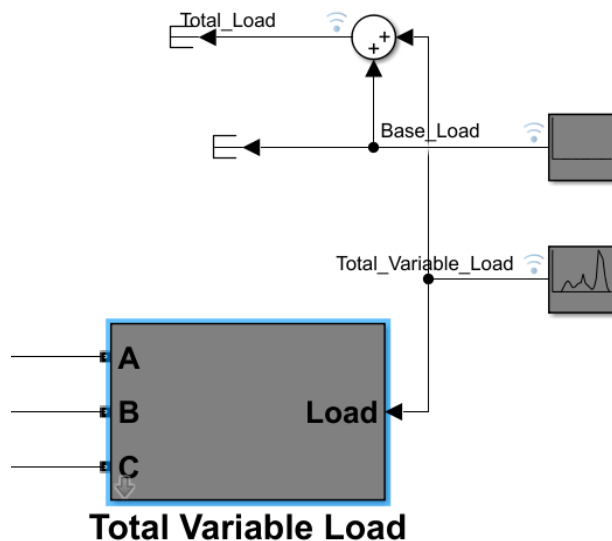


Figure 28: A top-level view of the variable load.

Figure 29 depicts an internal view of the variable load. Power feeds into the three-phase dynamic load block from the rest of the MG and outputs active and reactive power as measurements.

The dynamic load takes in the phase-to-phase voltage and the operation frequency of the rest of the grid. The PQ port takes in a custom active and reactive power via the dynamic load control block. The power factor is used to calculate what the real power needs to be multiplied by to output the correct reactive power based on the power factor of the system [166].

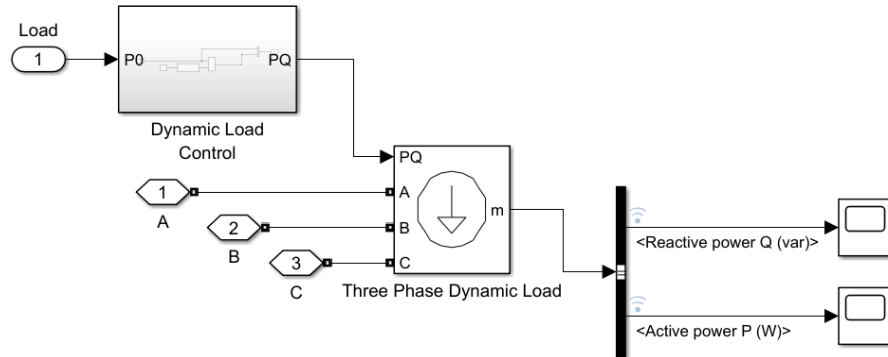


Figure 29: The internal view of the variable load.

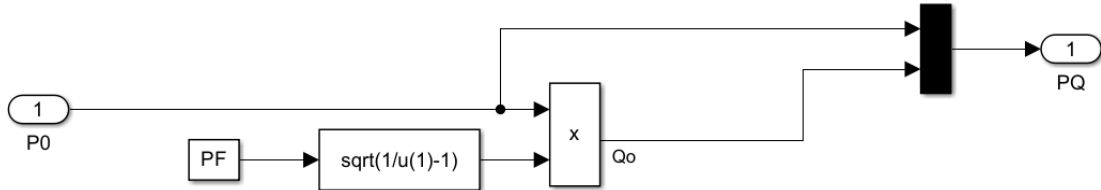


Figure 30: The internal view of the dynamic load control.

	<b>Three-Phase Dynamic Load:</b> The active and reactive power can change via a custom input or by the voltage [174].
	<b>Mux:</b> “Combines scalar or vector signals of the same data type” [175].

Table 6: The list of Components within the Load System.

### 3.3.3.6) Inverter Controllers

The control systems in the RHOME MG model handle the conversion of DC power into 400V AC power for the load while ensuring regulation of voltage and frequency. There are two types of controllers in the system. A Grid Following Inverter Controller that functions when the diesel generator is running and a Grid Forming Inverter Controller that takes over once the diesel generator is turned off. This setup with the controllers allows for adaptability under the different power generation suitability scenarios. The controllers constantly monitor output voltage phases to align PWM signals correctly, avoiding power quality issues or instability. They dynamically adjust their output to maintain a stable 400V AC supply under changing load or renewable generation conditions, ensuring reliable power delivery across all scenarios.

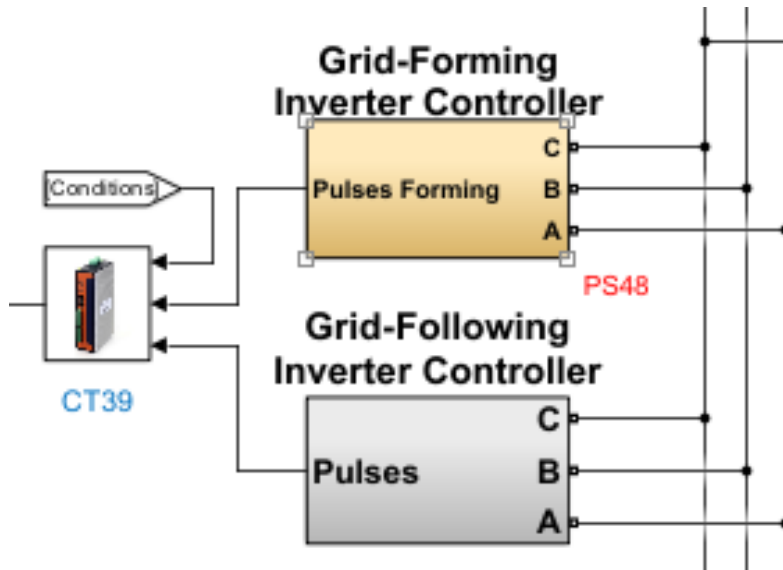


Figure 31: Inverter Controllers external.

The Grid Following Inverter Controller synchronizes its PWM signals to the PV/battery and wind subsystems, with the diesel generator's voltage and frequency reference in order to function as a source while keeping the system stable. In contrast, the Grid Forming Inverter Controller utilizes a Sine Wave Generator of the Phase Locked Loop (PLL) to produce fixed frequency and amplitude sinusoidal references. This allows the system to control voltage and frequency independently and serve as a voltage source when there is renewable energy available.

The two controllers analyze voltage measurements from three phases using a control module that generates signals to adjust the output wave, in the PWM Generator system. To prevent loops in Simulink and ensure operation with real world processing delays taken into consideration, a  $1/z$  delay is included in the setup for stability.

In specific predetermined situations controlled by the “Conditions” signal set by the initial panel, the system decides which controller to use according to the power generation suitability conditions to determine if the diesel generator is linked or not to the simulation.

If conditions are great, the diesel generator is switched off. The voltage and frequency are controlled by the grid forming controller. However, in poor conditions, the diesel generator runs and the grid following controller keeps it in sync with its power output. Conditions are described further in the following section.

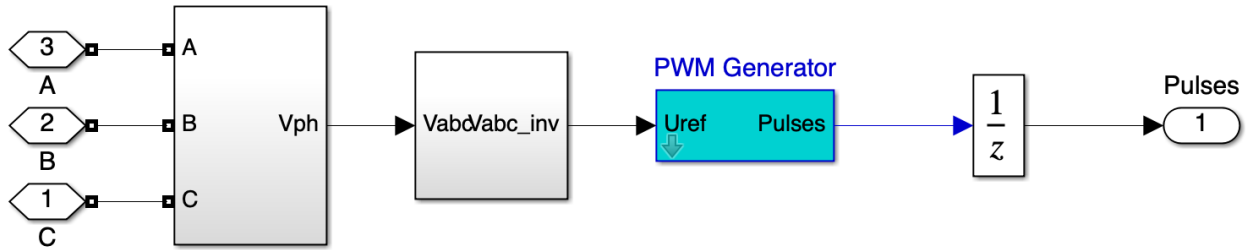


Figure 32: Inverter Controller internal subsystem.

### 3.3.3.7) Power Management System

The Power Management System (PMS) of the RHOME system for the DER is part of the technical optimization that dynamically manages the operation of the MG by tracking power generation and load status to optimize system operation. The system evaluates the total power output from each source (solar PV, wind, battery, and diesel generator) and calculates renewable penetration as a percentage of total generation. Based on these calculations, it determines whether the diesel generator will remain ON or OFF.

The "Conditions" signal plays a central role in the following logic because it takes into account the main representative/pre-defined scenarios for the user in the main panel (i.e., excellent, typical, or worst conditions) in the specific location in South Sudan. When there is very high or sufficient renewable generation (high solar and wind production), the system turns off the diesel generator and allows the grid-forming inverter controller to regulate voltage and frequency autonomously. Conversely, when renewable energy is insufficient, the diesel generator is activated, and the grid-following inverter controller ensures synchronization with the generator's output.

This management ensures that whenever possible, renewable energy is prioritized with limited diesel consumption but a constant 400V AC supply to the load. The system ensures maximum efficiency and reliability for the MG through dynamic controller switching and power flow control.

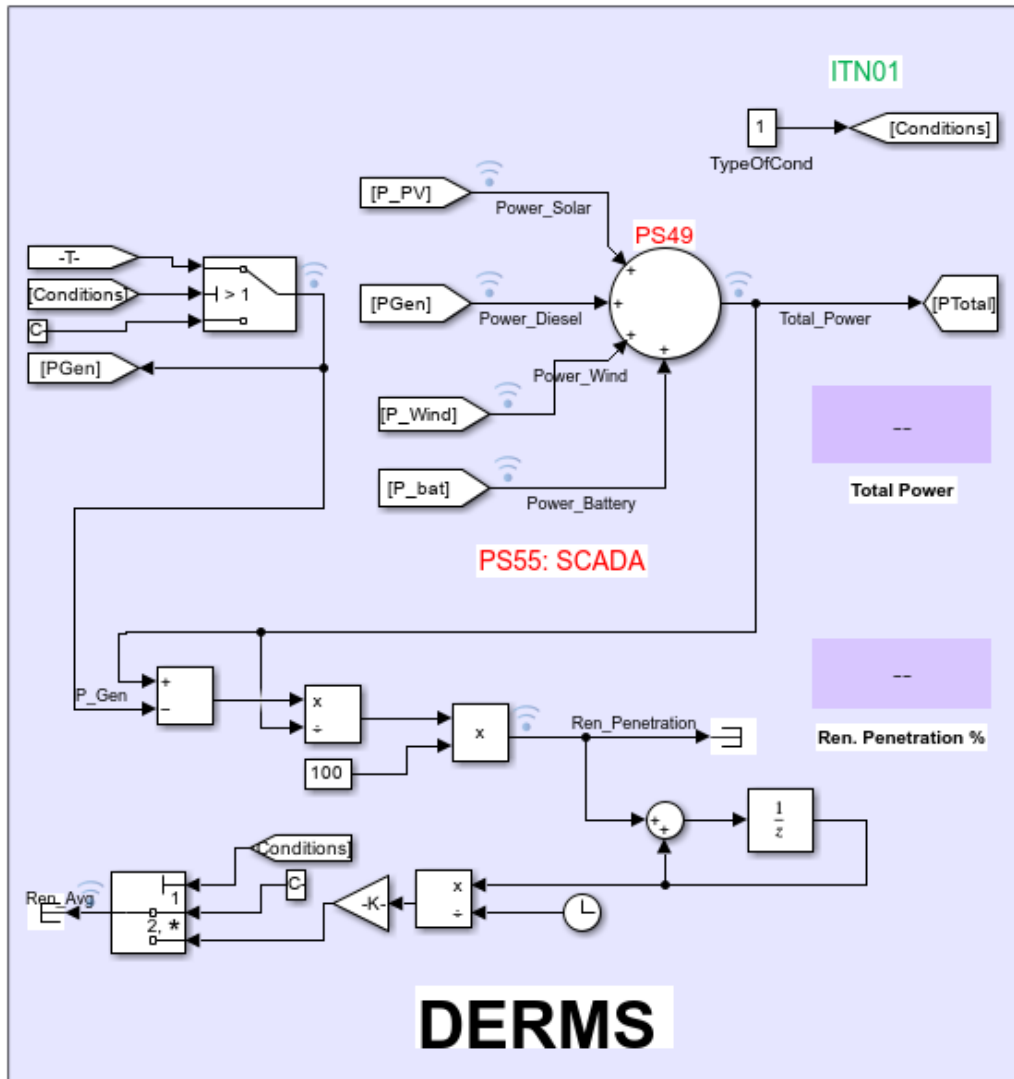


Figure 33: Power Management System.

Additionally, calculations regarding the instantaneous percentage of renewable energy present in the system (renewable penetration) and its daily average are performed and displayed in the bottom part of the subsystems. These calculations are extremely crucial as they provide an unbiased picture of how clean actually the energy system is under different conditions.

### 3.4) Visual Interactive Component / GUI

#### 3.4.1) Weather data Analysis and Condition Classification

The Virtual Interactive Component of the RHOME MG model was initiated with an elaborate analysis of environmental data concentrating mainly on solar irradiance, wind speeds, and temperature patterns in South Sudan. A suitability scoring system was established using Python data processing, categorized according to the power generation conditions of Excellent, Typical, and Worst-case days. This categorization considered a formula weighing solar and wind resources' contributions in relation to their capacities in the MG (1.4 MW solar and 100 kW wind). Due to solar having a larger contribution to total capacity, its weight was greater than that accorded to the other. Hourly weather data from a publicly accessible Google Sheets (with NASA Power data from Juba in 2023) file were analyzed through a Python script.

A day's suitability score was obtained through a mix of two factors: total solar irradiance, adjusted according to temperature impacts, and average wind speed, normalized per the maximum wind speed observed. Days when irradiance was high and temperatures were moderate received the highest suitability score, while the days when irradiance was low and temperatures extreme received the lowest. This formed the basis for analyzing the two best days, the two worst days, and the most typical day, based on proximity to the annual average score. This classification framework provides reasonable environmental inputs for simulations, showing a range of operating conditions.

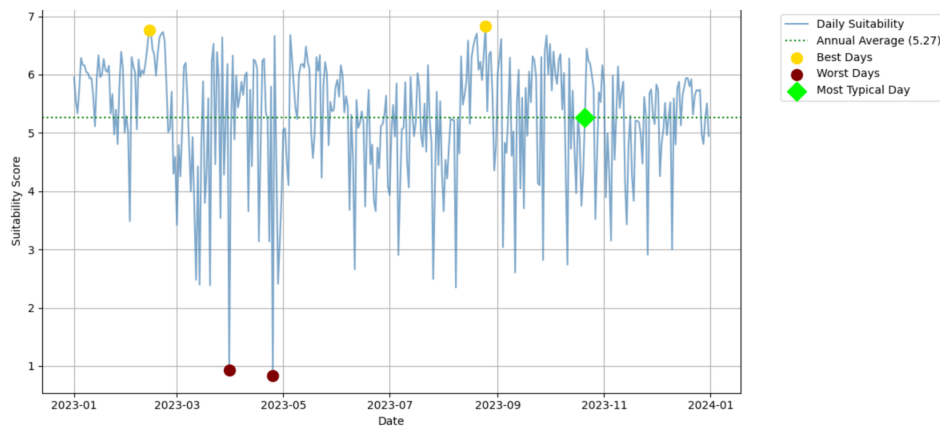


Figure 34: Power generation suitability analysis, South Sudan wind and solar from 2023.

From this analysis, August 25th and February 13th with scores of 6.83 and 6.77 emerged as the best days. On these days, solar irradiance was high, temperatures were moderate, and wind speed was above average. In contrast, the worst-performing days were April 25th and 31st March, which were rated 0.84 and 0.93 because of the low irradiance, excessive temperature losses, and little contribution from the wind. The average day was October 21st with a score of 5.26, which means moderate solar irradiance, average wind speeds, and representative temperature conditions. The mean yearly suitability score was found to be 5.27.

### 3.4.2) Interactive Dashboard

The research outcomes of the data analysis show an integration of the RHOME interactive component into a virtual interface for live monitoring and control of MG performance under varying environmental settings. This module allows for an interactive visual representation of KPIs in real-time and has the option to run different scenarios using current weather data or custom inputs. The dashboard provides users with a straightforward but comprehensive overview of how the system behaves. This allows for the indications of real-time power supply by each generation source (solar PV, wind turbine, diesel generator, and battery) alongside total power supply versus demand curves. Other parameters include the renewable penetration percentage (and daily average), frequency stability monitoring of the grid, total energy generated, LCOE, and kg-CO<sub>2</sub>/kWh emissions. By visualizing these data together, this facilitates analysis on how the different components cooperatively satisfy the load demand amidst changing conditions as well as providing a holistic picture of how the MG is affecting different aspects of the reality of the community where it is embedded.

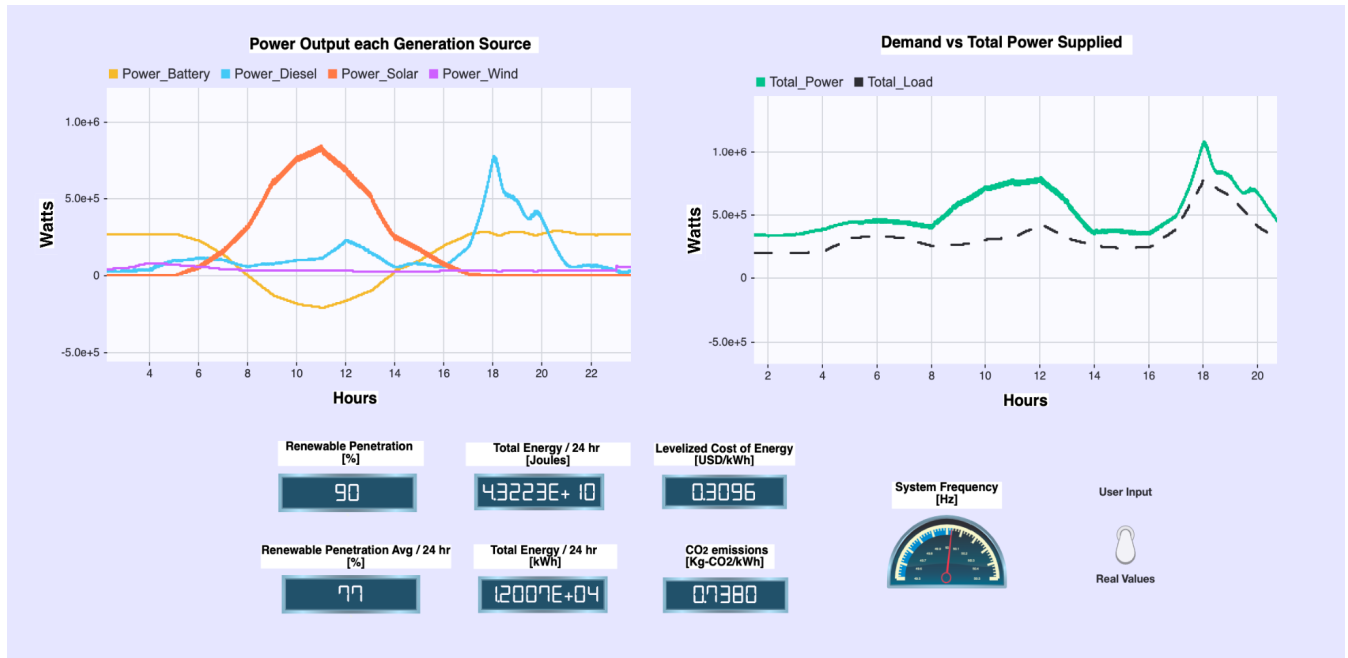


Figure 35: Interactive Dashboard Layout [Typical Conditions].

### 3.4.3) Power Generation Suitability Conditions

A critical feature of this simulation is in replicating various modes for power generation suitability: excellent, typical, and worst-case scenarios derived from classification according to historical data analysis. Each conditional preset automatically modifies environmental parameters, such as solar irradiance and wind speed, to correspond to actual data from aligned days in South Sudan. In the excellent mode, extraordinarily bright sunshine and moderate temperature conditions give the maximum output for PV while favorable wind speeds would add further to generation. Typical conditions denote the generally stable average daily variations in the spectrum of resource availability, to provide a reference for expected performance. The worst-case conditions represent the testing capacity by simulating tough conditions where low overall irradiance and low wind speed exist to study the resilience of the system. The presets give the operators the opportunity to check how well the MG performs under different operational conditions.

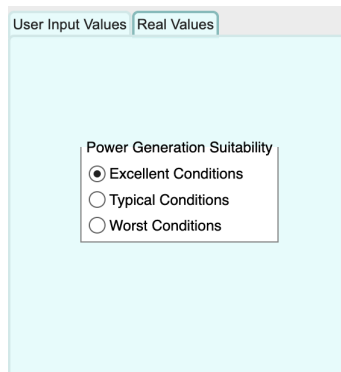


Figure 36: Power Generation Suitability Conditions.

For example, for the very good conditions of generation, renewable penetration peaks to about 94% of power generation, thereby reducing the use of diesel backup and reliance on battery storage. On the other hand, a worst-case scenario brings out the importance of battery storage in supporting the load balance during periods of low renewable generation.

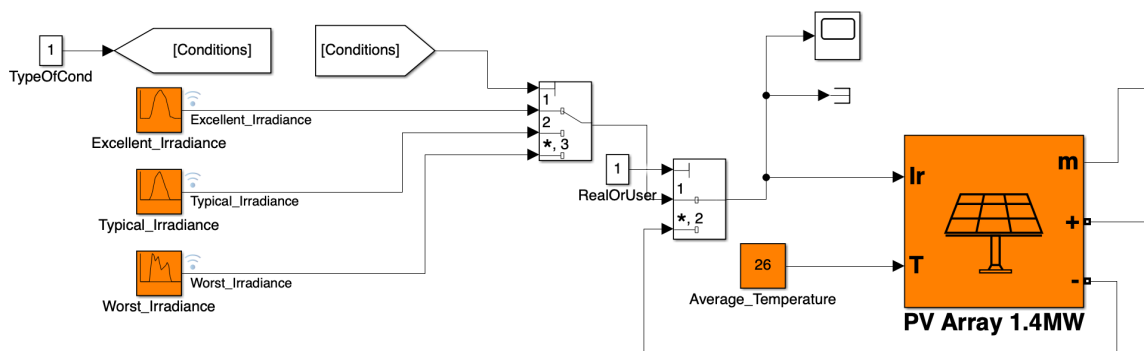


Figure 37: Example PV Solar different Inputs according to Power Gen Suitability

### 3.4.4) User input

Apart from preset scenarios, user input mode allows operators to also manually alter environmental parameters such as solar irradiance and wind speed. This feature may allow testing of highly customized scenarios that may not have historical precedent, for instance, for use in edge cases or extreme events, such as simulating maximum solar with minimum wind contribution, or simulating behavior under extreme events, like prolonged overcast skies or high temperatures. Base data is set from zero to one to reflect the average wind speed and irradiance distribution throughout an efficient day. The user can then set their maximum value for wind speed and irradiance and scale up the base data to the desired testing conditions.

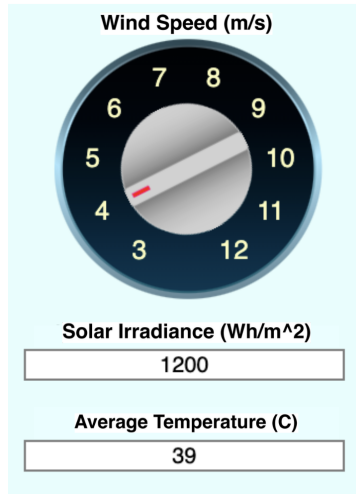


Figure 38: User input Values.

Changes update key performance metrics such as total supply vs total demand or percent renewables penetration on the dashboard in real-time. Such interactivity with the model provides useful insights into system operation across different scenarios, training operators towards improved control strategies for real-world implementation.

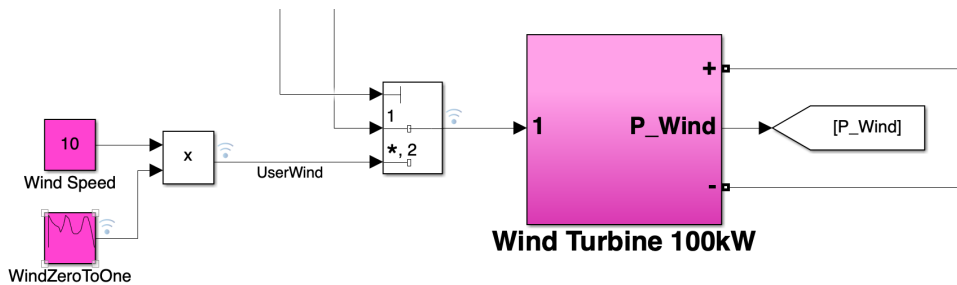


Figure 39: User input Wind Speed Values.

### 3.5) Additional Simulation Features

#### 3.5.1) Energy Calculations

This simulation has a MATLAB function that calculates the energy output of each power source, as shown in Figure 40. Shown in Figure 41, the function calculates cumulative energy contributions from different power sources using trapezoidal integration. It measures the power of every second of every hour of the day, by dividing each second in the simulation by 3600, and adds it together. There is a 0.25-second delay for the simulation, to account for a massive spike in power of the diesel generator. This is just a feature of the simulation, as a real diesel generator would not have a significant spike in power at the beginning relative to its normal rated power output.

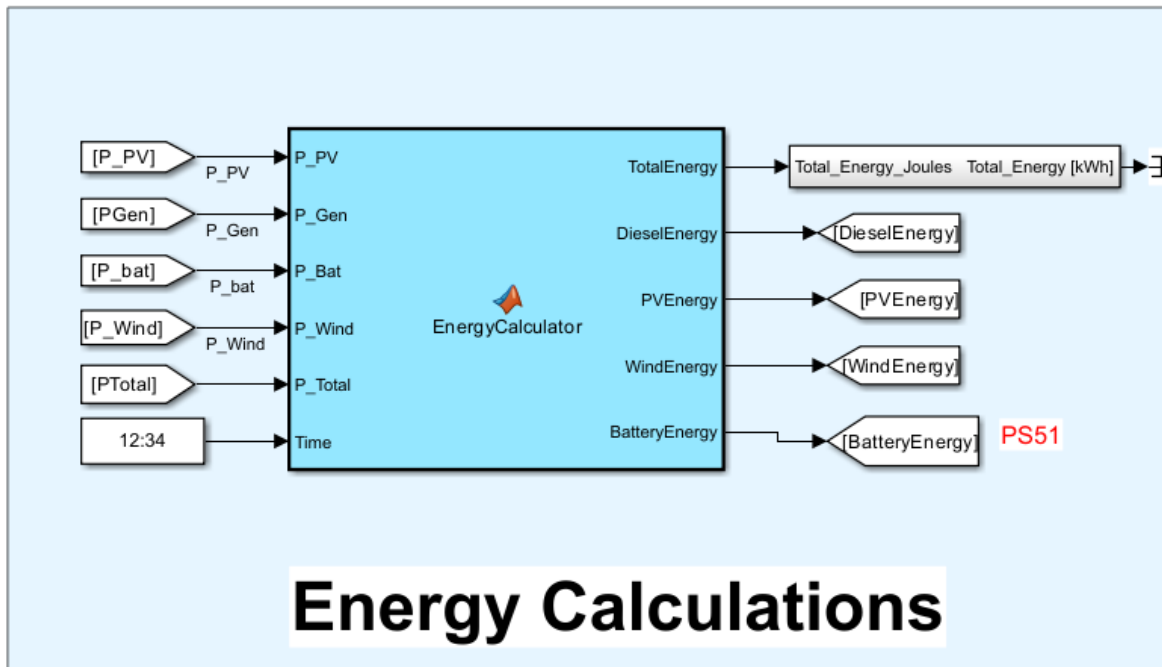


Figure 40: Energy Calculation Function with power values as inputs and energy

```

function [TotalEnergy, DieselEnergy, PVEnergy, WindEnergy, BatteryEnergy] = EnergyCalculator(P_PV, P_Gen, P_Bat, P_Wind, P_Total, Time)
    % Persistent variables for energy accumulation
    persistent total_energy diesel_energy pv_energy wind_energy battery_energy last_time;
    persistent last_P_Total last_P_Gen last_P_PV last_P_Wind last_P_Bat;

    % Initialize persistent variables
    if isempty(total_energy)
        total_energy = 0; diesel_energy = 0;
        pv_energy = 0; wind_energy = 0;
        battery_energy = 0; last_time = 0;
        last_P_Total = 0; last_P_Gen = 0;
        last_P_PV = 0; last_P_Wind = 0;
        last_P_Bat = 0;
    end

    if Time >= 0.25
        % Calculate time step in seconds
        dt = (Time - last_time) * 3600;

        %----- Trapezoidal Integration -----
        % PV Energy (only generation)
        pv_energy = pv_energy + 0.5 * (max(P_PV,0) + max(last_P_PV,0)) * dt;

        % Wind Energy (only generation)
        wind_energy = wind_energy + 0.5 * (max(P_Wind,0) + max(last_P_Wind,0)) * dt;

        % Diesel Energy (only generation)
        diesel_energy = diesel_energy + 0.5 * (max(P_Gen,0) + max(last_P_Gen,0)) * dt;

        % Battery Energy (net flow: + = discharge, - = charge)
        battery_energy = battery_energy + 0.5 * (P_Bat + last_P_Bat) * dt;

        % Total Energy (generation + battery discharge only)
        total_energy = total_energy + 0.5 * (... 
            max(P_Total,0) + max(last_P_Total,0) ...
            ) * dt;

        % Update previous power states
        last_P_Total = P_Total; last_P_Gen = P_Gen;
        last_P_PV = P_PV; last_P_Wind = P_Wind;
        last_P_Bat = P_Bat;
    end

    % Update time tracker
    last_time = Time;

    % Output energy values in JOULES (conversion handled externally)
    TotalEnergy = total_energy;
    DieselEnergy = diesel_energy;
    PVEnergy = pv_energy;
    WindEnergy = wind_energy;
    BatteryEnergy = battery_energy;
end

```

Figure 41: The code used to calculate the energy from the PV solar, wind, diesel, and battery power inputs.

### 3.5.2) Economical and Environmental Metrics

This simulation is able to calculate the LCOE and displays it after the simulation has finished running as shown in Figure 42. It also calculates and displays the amount of CO<sub>2</sub> produced in kilograms per kilo-watt-hour, also shown in Figure 42. The LCOE calculations, shown in Figures 43 and 44, are based on the equations 5-17, which are introduced in section 4 of this paper. The CO<sub>2</sub> calculation, shown in Figure 45, in the simulation was adapted based on equation 3, with the amount of diesel energy produced being a variable input. This allows the simulation to produce a value of CO<sub>2</sub>/kWh that varies with different simulation conditions (e.g. excellent conditions, typical conditions, worst conditions, and user inputs).

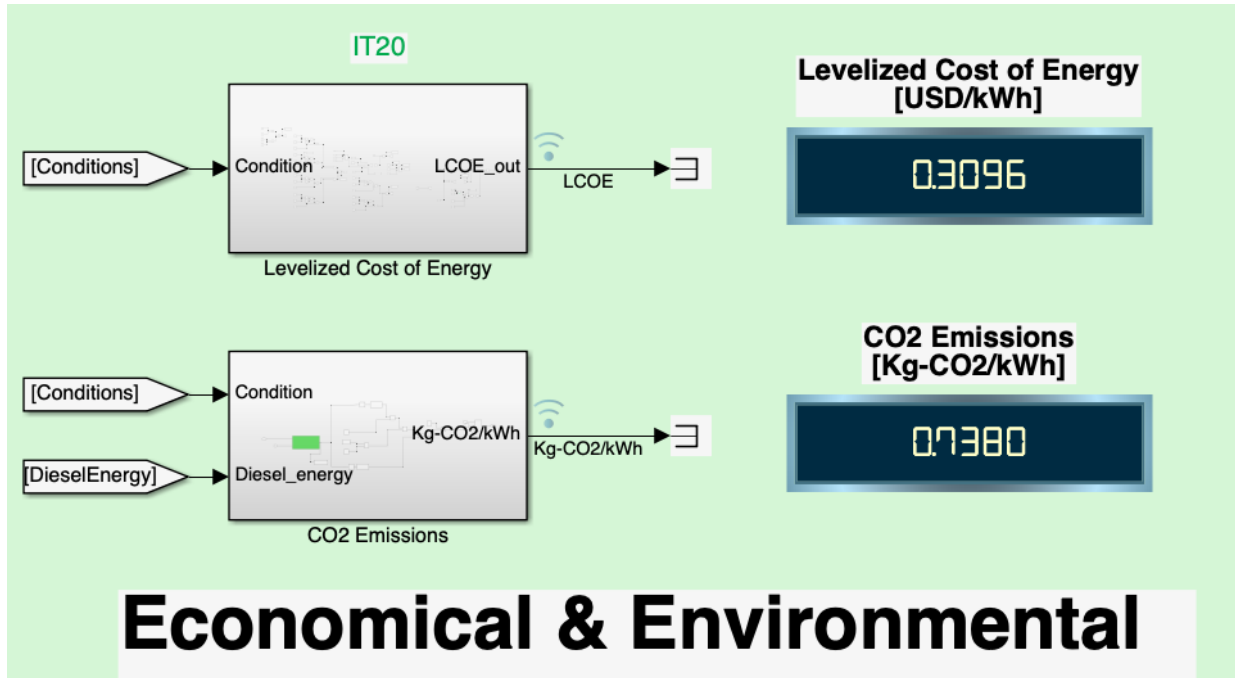


Figure 42: The Economical and Environmental Metrics Displayed.

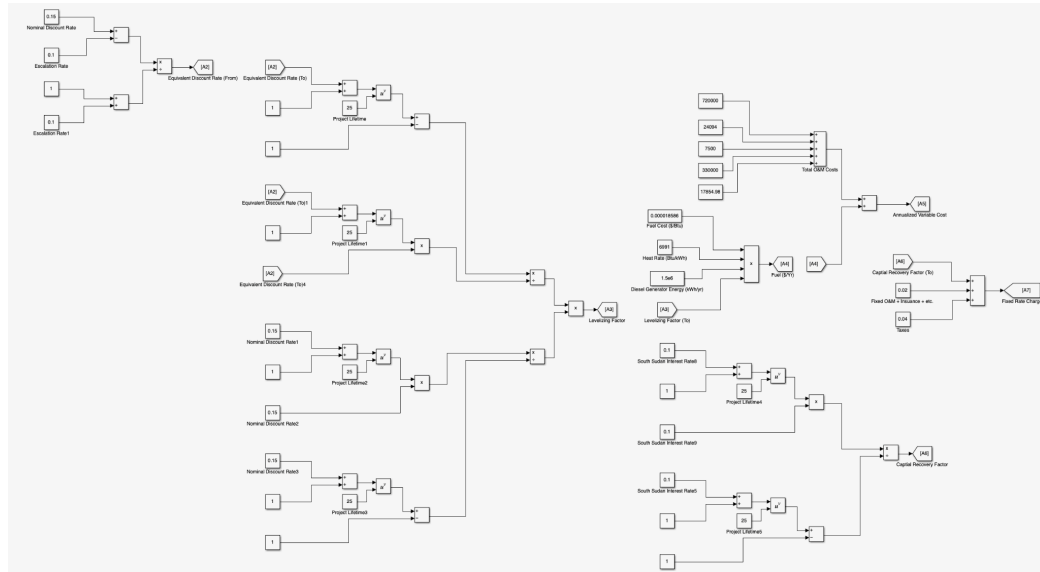


Figure 43: The first part of an internal look of the set of equations used to calculate the LCOE of the MG.

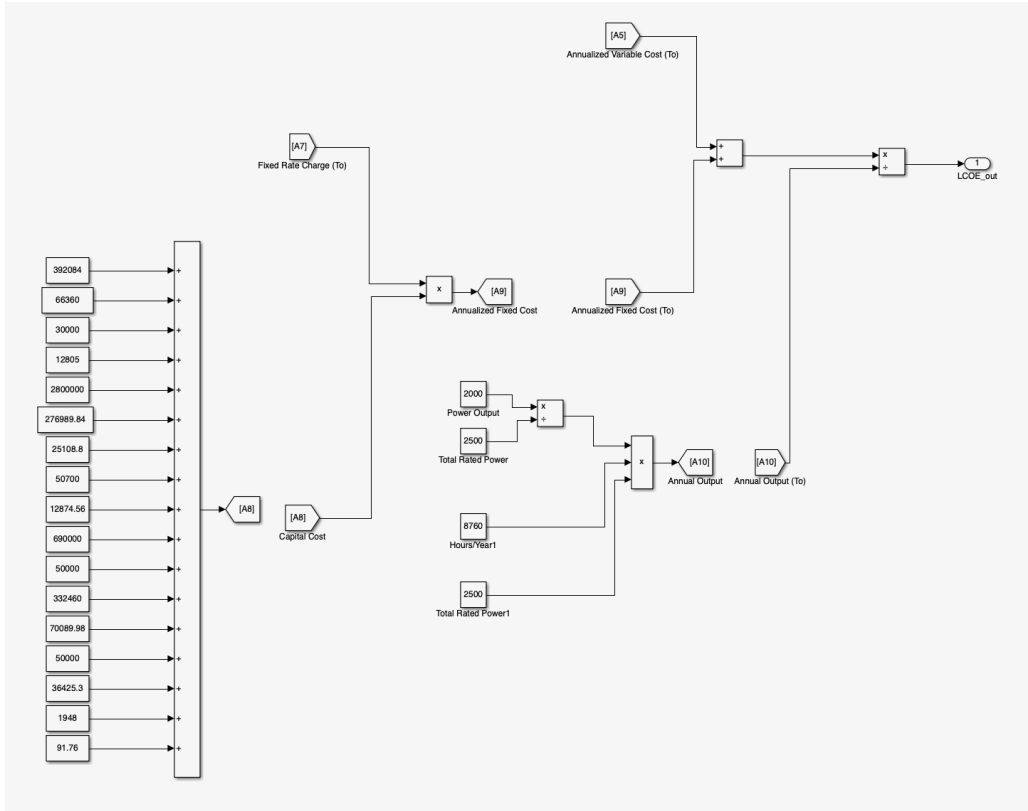


Figure 44: The second part of an internal look of the set of equations used to calculate the LCOE of the MG.

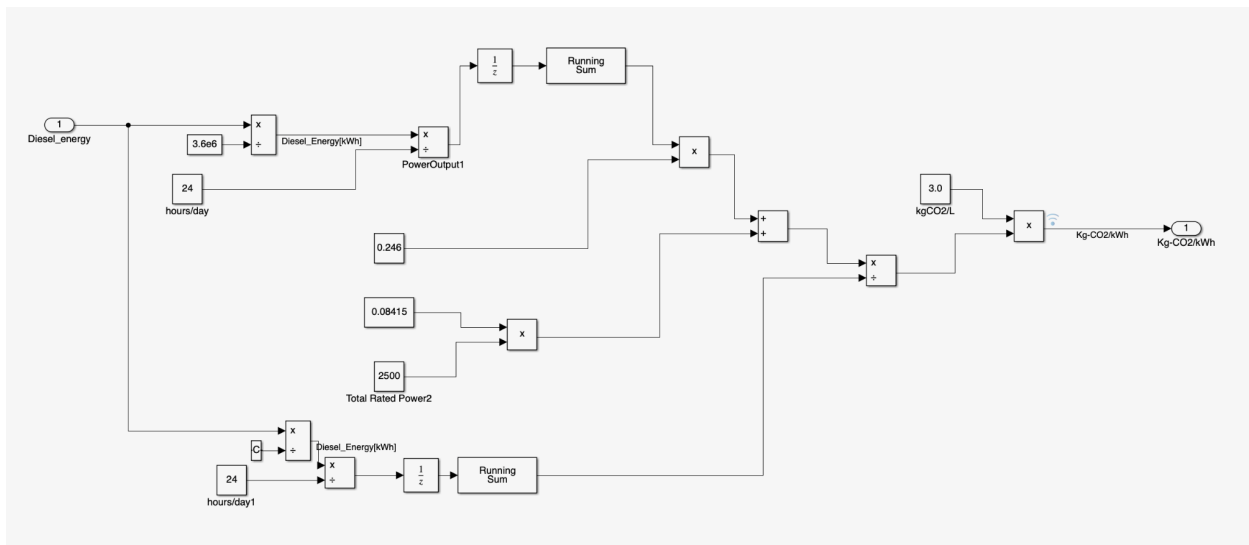


Figure 45: An internal look into the set of equations used to calculate the amount of CO<sub>2</sub> in kilograms per kilo-watt-hours.

# Economical Optimization

The total capital cost was calculated by finding installation, equipment, shipping costs, and the 20% import tax for all the components and other expenditures required to construct the MG. These components and expenditures include PV system costs, wind system costs, battery system costs, diesel generator costs, general system costs, and infrastructure and permitting costs.

## 4.1) PV Solar

In order to understand standard values and costs, NREL's "U.S. Solar Photovoltaic System and Energy Storage Cost Benchmarks" document was inspected [68]. The PV solar system should be rated for 1.4 MW as per HOMER Pro recommendations; thus, according to Neo Virtus solar design engineering team, the industry standards suggest panels between 350 W and 500 W for the size of this system [176]. *Jinko Solar 475-Watt 24V Monocrystalline Solar Panel JKM475N-60Hs* were selected for the system due to their convenience, compatibility with weather conditions, and reliability [177]. With a cost of \$133.48 per panel and a total of 2,948 panels for the 1.4 MW solar array and South Sudan's sales tax of 20% on imported goods entering the country, the total price of the solar panels with shipping would be \$472,199 [178]. The website that had the *Jinko Solar 475W* panels advertised free delivery, thus, shipping costs were omitted for these panels.

In Africa, solar panel installation costs range from \$1.9/kW to \$5.9/kW according to IRENA [179]. This estimation includes electrical and structural balance of the system (cabling, conduits, grounding, racking, etc). Using a range of \$2/W for the installation cost, the total installation cost was calculated to be \$2,800,000.

The *SMA Sunny Tripower CORE2s* 110 kW were selected as we aimed to keep decent DC to AC ratio calculations less than 1.4 as per industry standards, according to the Neo Virtus Engineering Solar design team [180]. With the total system capacity of 1.4 MW and each inverter rated at 110 kW AC output, 13 inverters would be required to handle the system load. Each inverter supports up to a 165 kWp DC input, which is more than enough capacity for the connected *Jinko Solar 475 W* panels. A significant advantage of these inverters is their integration of 12 independent MPPTs per unit. This function proves beneficial because no external component installation is necessary, and the simulations validate their utility. Every MPPT module supports two strings, which enables the inverter to manage 24 strings in total. The system's safety and maintenance abilities improve through the addition of DC disconnects, which enable targeted isolation of parts while keeping the rest of the array operational.

Compatibility with South Sudan's electrical infrastructure emerged as a vital consideration for these inverters, as they work with a frequency of 50 Hz and the standard 400V three-phase AC, which is in line with the country's specifications [224]. The inverters can function across a voltage range between 320V and 460V, which enables them to adjust to MG power variations. The inverters also have a superior degree of compatibility with the solar panels

selected. For instance, under cold conditions, the panels' adjusted Voc reaches 47.36 V, and under hot conditions their Vmp reaches 33.43 V (both values remain inside the inverters' MPPT voltage range of 500-800V).

The system achieves optimal string sizing with 15–16 panels per string while maintaining operation within the efficient range of the inverters despite temperature fluctuations. To achieve reliable performance throughout the full year, South Sudan needs systems that can adapt to temperature variations. Using a calculation of maximum AC output from all inverters determined the required switchboard size. The maximum output of 158.8 A for each inverter leads to a collective current output of 2,064.4 A when all 13 inverters work together. The required switchboard capacity reached approximately 2,600 A when a standard safety margin of 25% was used to manage potential surges and meet electrical code requirements. The selected switchboard possesses a 6,300 A capacity and costs \$30,000 before import tax to ensure safe operation and accommodate future expansions [181].

To meet safety requirements, the system could include 13 safety switches or similar disconnects, one for each inverter [182]. These disconnects allow for safe isolation of individual inverters during maintenance and cost \$985 each, resulting in a total base cost of \$12,805 + taxes. Furthermore, the system also incorporates a buck/boost converter (*ABB PCS100 ESS*) to facilitate integration with battery storage. This converter ensures stable voltage regulation and efficient bidirectional energy flow between the PV system and BSS. The converter costs \$50,000 before tax

## 4.2) Wind

For the wind system, the wind turbine costs \$32,000 with an installation cost of \$21.19 /W and a shipping cost of \$5,950 for a 20-foot shipping container [183], [184], [185] et al. The total cost of the wind turbine system is \$308,765.81.

The 100 kW DC Power Supply AC/DC Converter rectifier for the wind system costs \$10,500. Assuming \$100 per cubic meter for the shipping costs, with a volume of 2.288 cubic meters, the shipping cost is \$228.80 [186], [185]. There is limited information available on the installation costs and rectifier lifetime. With the 20% import tax, the cost of the rectifier is approximately \$12,874. The lifetime of the equipment is important to know because it adds to the cost of the project. The MG has a lifetime of 25 years, if products only have lifetimes of 10–15 years they will need to be replaced and this will add to the overall cost.

The *RedPrime* 200kW, 850V, 400A DC-DC Converter for the wind system has an estimated cost of \$10,000 [187]. This is an estimated price because the *RedPrime* converter does not have a listed price, thus the estimated price is derived from a similar converter that ranges from \$3,000 to \$10,000 [188]. This converter was not chosen because it did not quite match the specifications needed. There is limited information on the installation cost for this converter. Because the lifetime is approximately 20 years, two converters will need to be bought. The shipping cost comes to be approximately \$462 per converter [189]. With the import tax, this brings the total price to \$25,108.8.

For a 100 kW wind turbine system, four 30 kW inverters would cost \$17,600.00 [190]. 8 converters would be needed for the duration of the MG system because they only last for 15–20 years. The shipping would cost \$7,050 for a 20-foot shipping container, with limited information on installation costs, and an import tax of 20%, the total cost comes to \$50,700 [185], [191].

#### 4.3) Battery

The 6.8 MW lithium-ion battery for the MG would cost \$782,000 with a cost of \$115/kWh [192]. The cost is based on lithium-ion battery packs, as in an ESS several packs of lithium-ion batteries are needed in order to meet the power and energy requirements of the MG. The lifetime of the lithium-ion battery is 15–20 years [193]. With this lifetime, the lithium-ion batteries would need to be replaced towards the end of their lifespan in order to ensure the adequate power and energy are met while also maintaining the safety of the ESS.

#### 4.4) Diesel Generator

The 1000 kW diesel generator for the MG costs \$120,000, with an installation cost of \$150/kW, and a shipping cost of \$7,050 [194], [195], [185]. The lifetime of the diesel generator is approximately 20,000 to 40,000 hours which equates to 20–25 years, assuming the generator does not run continuously [196]. This is expected in our system as it is designed to have a high renewable penetration, running mostly on PV solar. Overall, with the import tax, the total cost of the diesel generator in the MG system is \$332,460.

#### 4.5) General System

General system costs include control costs, distribution line capacitor costs, distribution line costs, and smart meter costs.

Distribution line capacitors cost \$1,675.32 for a 100 kVAR capacitor [197]. Assuming a power factor of 0.9, and rating of 2500 kW for the MG, using equation 4 the reactive power of the system is 1210.8 kVAR. Thus, 26 distribution line capacitors are needed, because they only have a lifetime of 11–15 years. 26 are needed instead of only 13, costing \$43,558.32 to account for the 25 year duration of the project [198]. The installation cost is \$600 per 100 kVAR [199]. There is limited information on shipping costs from Thailand (where these capacitors are made) to South Sudan. Using \$7,050, the shipping cost from China to South Sudan, the total cost, including the 20% import tax, of the distribution line capacitors is \$70,089.98 [185].

The PoC camps in Juba, South Sudan have a total of 9,214 households. However, this amount of smart meters is unrealistic; thus, there will be a smart meter for every inverter, for a total of 13 inverters. The smart meters only last 5–7 years, so at least 5 sets are needed [200]. Assuming 1 smart meter per inverter at a price of \$441.00 per smart meter, and installation cost of \$100 per smart meter, for a low complexity installation, and a shipping cost of \$389.42 with the import tax, the total cost of the smart meters are \$36,425.30 [201], [202], [203] et al.

$$Equation \#4: Q = S*(1-0.9^2)^{\frac{1}{2}}$$

The infrastructure costs for the MG include permitting costs, construction costs, and Land Acquisition Costs. The permitting procedures and associated costs totals \$1,948 (see Table 7). Construction costs were based on the installation costs for the PV solar system, battery system, diesel generator, and wind turbines. The land acquisition cost is \$16 per hectare. This figure is derived from how much Nile Trading and Development (NTD) paid per hectare for land in South Sudan [203]. Assuming 22,257.7 m<sup>2</sup>/ MW for the solar array, 4 acres for a 100 kW wind turbine, and 1 hectare for the diesel generator, battery system, and other facilities, the total cost for 5.7348 hectares is \$91.7568 [73], [204], [205].

No.	Procedures	Time to Complete	Associated Costs
1	Request and obtain a site map	14 days	\$31
2	Obtain approval of the building plans	14 days	\$198
3	Receive on-site inspection by the Ministry of Housing, Physical Planning and Environment	1 day	\$143
4	Request and obtain building permit	7 days	\$152
5	Receive on-site inspection by the Payam	1 day	\$69
6	Request to have the plot and the building surface pegged	30 days	\$57
7	Receive inspection by the Ministry of Housing, Physical Planning and Environment - I	1 day	no charge

8	Receive inspection by the Ministry of Housing, Physical Planning and Environment - II	1 day	no charge
9	Receive inspection by the Ministry of Housing, Physical Planning and Environment - III	1 day	no charge
10	Receive inspection by the Ministry of Housing, Physical Planning and Environment - IV	1 day	no charge
11	Receive inspection by the Ministry of Housing, Physical Planning and Environment - V	1 day	no charge
12	Receive inspection by the Ministry of Housing, Physical Planning and Environment - VI	1 day	no charge
13	Receive inspection by the Ministry of Housing, Physical Planning and Environment - VII	1 day	no charge
14	Receive inspection by the Payam once the excavation is completed	1 day	no charge

15	Receive inspection by the Payam once the roofing is completed	1 day	no charge
16	Receive inspection by the Payam once the drainage is completed	1 day	no charge
17	Request and receive final inspection by the Payam	1 day	no charge
18	Obtain certificate of completion from the Payam	1 day	\$42
19	Obtain certificate of completion from the Ministry of Housing, Physical Planning and Environment	1 day	no charge
20	Receive fire safety inspection	1 day	\$86
21	Apply for water and sewage connection	1 day	no charge
22	Receive inspection for water and sewage connection	1 day	no charge
23	Obtain water and sewage connection	48 days	\$1,170

Table 7: Various construction permit costs in South Sudan [206].

## 4.6) Cost Analysis

The annualized fixed cost is the total cost of components summed into a single total that is multiplied by the fixed charge rate (FCR) and rated power of the system. The capital cost is the cost of all the components in the system. The FCR incorporates the interest on loans and acceptable returns for investors, fixed O&M cost, charges, and taxes. As shown in equation 5, FCR depends on the cost of capital and varies with interest rate. The rated power of the plant refers to the power produced by the system under ideal conditions. RHOME has a rated power of 2,500 kW.

*Equation #5:*

$$\text{Annualized Fixed Cost } (\$/\text{yr}) = P_R(\text{kW}) * \text{Capital Cost} (\$/\text{kW}) * \text{FCR} (\%/\text{yr})$$

The FCR is the combined percentage of the capital recovery factor (CRF), fixed O&M, insurance, property taxes, and corporate taxes. The fixed O&M, insurance and property taxes are set to 2% and the corporate taxes are set to 4%. The CRF is the annual loan payment on \$1 borrowed for n years at an interest rate of i. The project life-time is 25 years with an interest rate of 10%. This would make the CRF 11.0168% which would make the FCR 17.0168%. The annualized fixed cost of the MG system totalled \$1,095,371.

*Equation #6:*

$$\text{FCR} = \text{CRF} + (\text{Fixed O\&M, Insurance, and Property Taxes}) + (\text{Corporate Taxes})$$

$$\text{Equation #7: CRF} = \frac{i(1+i)^n}{[(1+i)^n - 1]}$$

The annualized variable cost depends on the annual fuel demand, unit cost of fuel, the O&M rate for the actual operations of the system and the annual energy of the system. Annual energy depends on the rated power of the system and its capacity factor (CF). CF shows how often the system is working at its full rated power, which depends on the rated power of the system and the actual power that the system produces. The actual power that our system produces is 584 kW, which means the CF is 0.2336. Our annual energy is 5,120,000 kWh/yr.

The O&M costs for the PV solar are \$24,374 per year (\$17.21 per kW per year), a total of \$7500 per year for the wind system, \$19,550 for the lithium-ion batteries, \$35,000 for the diesel generator, and, \$1,300 for the distribution line capacitors [68], [199], [207], [208], [209].

*Equation #8:*

$$\text{Variable costs } (\$/\text{yr}) = [\text{Fuel} + \text{O\&M}] (\$/\text{kWh}) * \text{Annual energy} (\text{kWh}/\text{yr})$$

$$\text{Equation #9: Annual energy } (\text{kWh}/\text{yr}) = P_R(\text{kW}) * 8760 \text{h/yr} * \text{CF}$$

$$Equation \#10: CF = \frac{Actual\ Power\ (kW)}{P_R\ (kW)}$$

The total cost of fuel produced by the diesel generators is multiplied by the heat rate (Btu/kWh), fuel cost \$/Btu and levelizing factor (LF). The fuel cost refers to the cost of diesel fuel in South Sudan, which is \$0.000018586/Btu. Through the simulations of the system, it was found that the amount of energy that the diesel generator produces is 1,040,000 kWh/yr).

*Equation #11:*

$$Fuel(\$/yr) = Energy(kWh/yr) * Heat\ rate(Btu/kWh) * Fuel\ cost(\$/Btu) * LF$$

The heat rate refers to the thermal efficiency of the system,  $\eta$  which is the thermal input (Btu) required to deliver 1 kWh of electrical output. The heat rate of the system is 9,144.37 (Btu/kWh). The diesel generator would burn through 125 L/hr at a rpm of 1500 at a capacity of 500 kW [210]. The electrical output is 1,706,071 Btu/hr for 500 kW using the conversion of 1000 kW for 3,412,000 Btu/hr [222]. The heat per liter is 36,579 Btu and the generator produces 3,412,000 Btu of heat per hour. Using equation 14, this means that the system has a thermal efficiency of 37.31%.

$$Equation \#12: Heat\ rate\ (Btu/kWh) = \frac{3412\ (Btu/kWh)}{\eta}$$

$$Equation \#13: Fuel\ Consumption\ (L/hr) * Heat\ per\ Liter\ (Btu/L) = Heat\ Generated\ (Btu/hr)$$

$$Equation \#14: \eta = Electrical\ Output\ (Btu/hr) / Heat\ Generated\ (Btu/hr)$$

The LF depends on an estimate of the escalation rate of the fuel price and the discount factors, which levelizes the cost of fuel over the lifetime. The escalation rate ( $e$ ) is the pricing increase of a particular product in a location. The escalation rate can be calculated using equation 17. With the escalation rate assumed to be 10% and the nominal discount rate ( $d$ ) is 15% the equivalent discount rate is  $d'$  which is 0.04545. With the nominal discount rate, equivalent discount, and the lifetime of our project, the LF of 2.283.

*Equation #15:*

$$\text{Levelizing Factor (LF)} = \left[ \frac{(1+d)^n - 1}{d(1+d)^n} \right] * \left[ \frac{d(1+d)^n}{(1+d)^n - 1} \right]$$

$$\text{Equation #16: } d' = \frac{d-e}{1+e}$$

$$\text{Equation #17: } e = \left( \frac{P_2 - P_1}{P_1} \right)^{\frac{12}{10}}$$

Because the energy produced by the diesel generators is 1,040,000 kWh/yr, the heat rate of 9144.37 Btu/kWh, fuel cost of \$0.000018586/Btu, and a LF of 2.283 a fuel cost of \$259,882.62/yr is obtained. When considering all the components that require O&M, it was found that the total cost of O&M would be \$76,479/yr. This would make the annualized variable cost \$416,411.

The LCOE is calculated by combining the annual fixed cost and the annual variable cost and dividing the annual output of the system. The LCOE is the average cost of electricity generation over the lifetime of a system. It incorporates all costs such as O&M, fuel, construction, etc. With an annual fixed cost of \$1,095,371, an annual variable cost of \$482,000, and an annual output of 5,120,000 kWh/yr yields a LCOE of \$0.2977/kWh. The LCOE varies in the simulation based on the changes in fuel cost, which are subject to different simulation conditions.

$$\text{Equation #18: } \text{LCOE } (\$/\text{kWh}) = \frac{[\text{Annual fixed cost} + \text{Annual variable cost}] (\$/\text{yr})}{\text{Annual output } (\text{kWh}/\text{yr})}$$

$$\text{Equation #19: } \text{Annual output } (\text{kWh}/\text{yr}) = 8760 \text{ h/yr} * CF$$

South Sudan's economy lacks stability, thus, fuel prices can vary drastically due to its high inflation. In this way, the escalation rate was calculated to be 84.95 % based on a fuel price change over a 10-month period [219], [220]. Incorporating this figure into the fuel cost calculations would significantly increase the LF, thereby fuel cost, and the LCOE as a whole assuming a project timeline of 25 years. For the LCOE to remain practical, the assumption was made that South Sudan's economy and government were stable enough for this project to be realistic; this assumed an escalation rate of 10%. Another assumption made was a fixed O&M rate, insurance rate, etc. of 2% and a rate of 4% for taxes for the project to remain realistic [222]. It was also assumed that the installation costs of each of the power sources and battery would cover the construction cost of the MG.

# Results

## 5.1) High-level Results

### Parameters

The HOMER Pro's simulation conditions include a diesel generator, PV Solar and a wind turbine as the renewable sources, and a 1 MWh-Li-ion battery storage system. Values of \$500/kW with a fuel cost of \$2/L will be used in cost calculations for the diesel generator. The PV capital cost will be \$3000/kW, with the battery costing \$600,000 per battery. These values have been informed by previous research and analysis for location specific rates on Section 1. The simulation will optimize a scenario to meet a demand of 7000kWh per day with a community load profile. This means that the load used in the simulation will be what a typical community of people uses in a day. Finally, the project will have a discount rate of 6.0%.

- **Discount Rate:** The discount rate is the interest rate used to calculate the present value of future cash flow from a project or investment [\[211\]](#).
- **Present Value:** is the current value of a future sum of money or stream of cash flows [\[212\]](#).
- **Future Cash Flow:** the projected income and expenses a company expects to have [\[213\]](#).
- **Interest Rate:** the proportion of a loan that is charged as interest to the borrower [\[214\]](#).
- **Interest:** money paid regularly at a particular rate for the use of money lent, or for delaying the repayment of a debt [\[215\]](#).

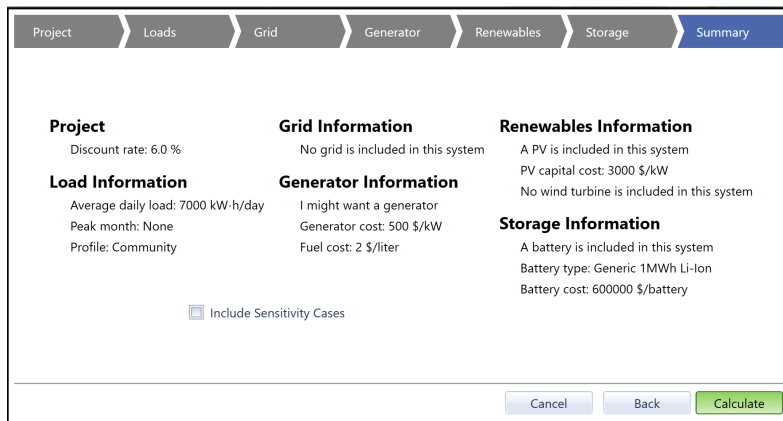


Figure 46: Summary of parameters that will be used to simulate an MG.

## System Schematic

The system in Figure 47 was the proposed simplified view of the IMG provided by HOMER Pro. The system has a diesel generator, a wind turbine, and the electric load all connected to the AC bus. The converter is bidirectional and connects the AC and DC buses. Additionally, the PV solar array and the lithium-ion battery are connected to the DC bus with the battery being bidirectional, allowing for charging and discharging.

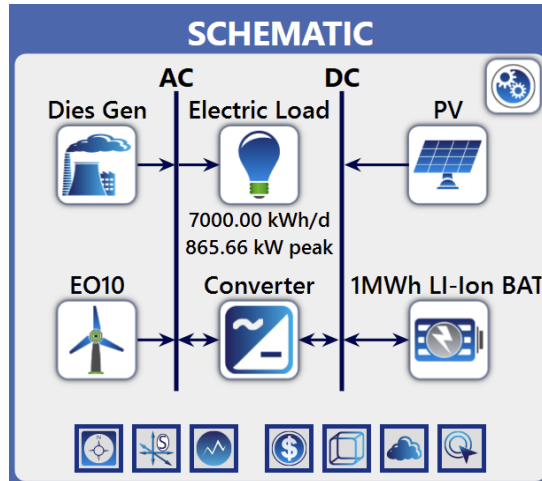


Figure 47: HOMER Pro MG system schematic.

## Cost Summary

Along with MG schematics, HOMER Pro is able to create detailed economic and electrical assessments. Given the input parameters, HOMER Pro determined the capital cost, replacement cost, O&M cost, fuel cost, money back from salvage, and total cost for each of the following components: diesel generator, wind turbine, lithium-ion battery, PV solar array, and converter. It was also able to provide an amount of kWh/yr and a detailed analysis of what each power source would be able to deliver. HOMER Pro concluded that the total system cost is approximately \$9,868,937.55 with the LCOE being \$0.3247 per kWh.

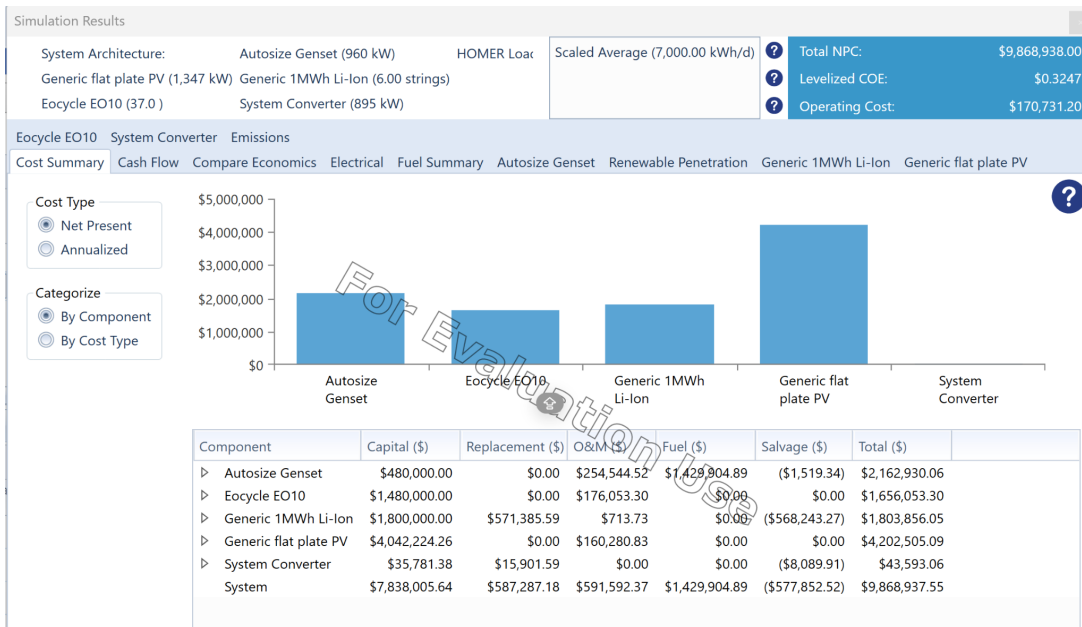


Figure 48: HOMER Pro Cost Data.

## Electrical

According to HOMER Pro, the specified system would produce a total of 3,520,659 kWh/yr, with the load requiring a total of 2,555,000 kWh/yr; thus an excess of 787,815 kWh/yr. It also calculated that such a system would have an average renewable penetration of around 92% per year. The results of the HOMER Pro simulation yield monthly electrification production data, showing the various levels of production throughout the year for each generation source.

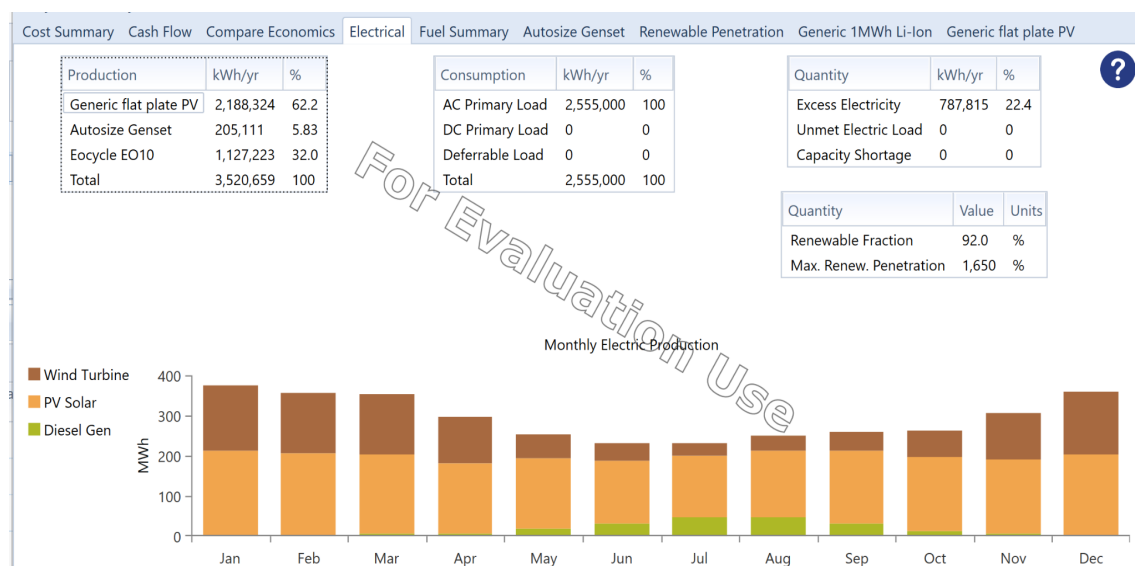


Figure 49: Summary of power per source production, monthly energy per source production, and renewable penetration in the islanded MG.

## Renewable Penetration

As shown in Figure 46, HOMER Pro outputs data on capacity based metrics, including the ratio of nominal renewable capacity over the total nominal capacity. This value ends up being 64.1%. Similarly, the ratio of the usable renewable capacity over the total capacity is 53.2%. Furthermore, some energy-based metrics are explored. These include the total renewable production as a ratio with the load and generation, which come out to be 130% and 94.2% respectively. Some of the peak values reflect the system's ability to run entirely with renewable energy. On days with best power generation suitability, the simulation showcases a 100% renewable output divided by total generation.

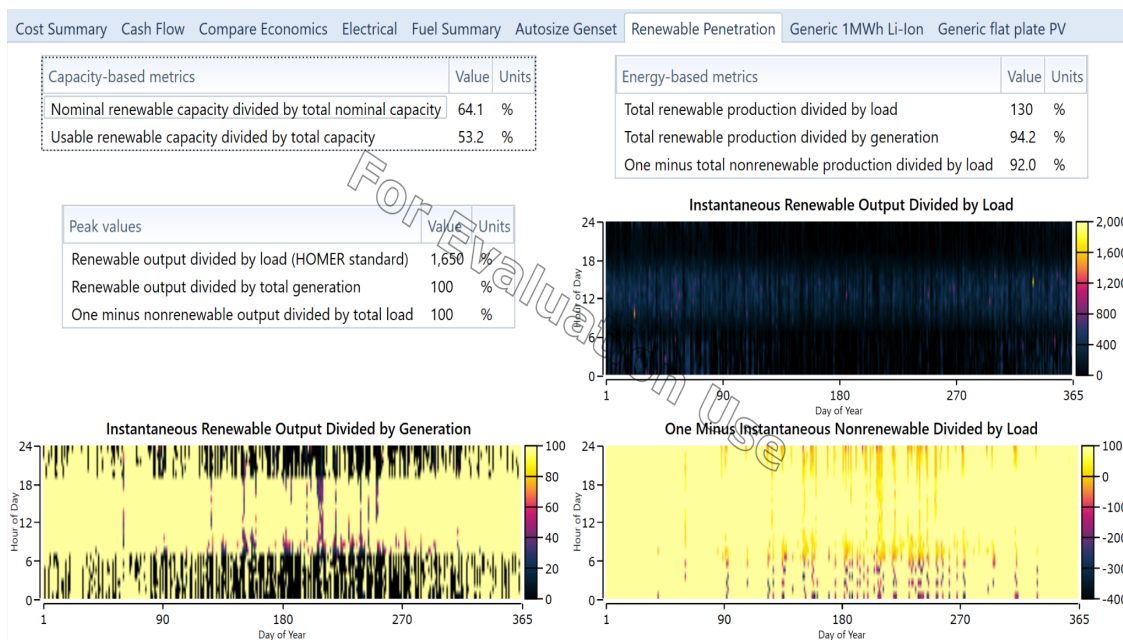


Figure 50: HOMER Pro renewable penetration data.

## 5.2) Low-Level RHOME Results

### 5.2.1) Excellent Conditions

The first scenario analyzed in the simulation was under excellent weather conditions. This simulation considers the best possible irradiance and wind patterns identified in the specific location in Juba, South Sudan. These conditions allow for zero diesel generator power output. The battery is assumed to have a higher initial charge and power available which supports the MG to meet the entire demand of the community solely with renewable energy sources, as shown in Figure 51. The PV peaks around 1.347 MW, which is almost 96% of the expected maximum power output. The wind output starts almost at its peak of 100kW and ranges in between 40kW and 60kW, supporting the overall system in a meaningful way. The battery follows a semi-inverted pattern to the PV, compensating for whenever there is more or less power available and charging between t = 10 hr and t = 15 hrs.

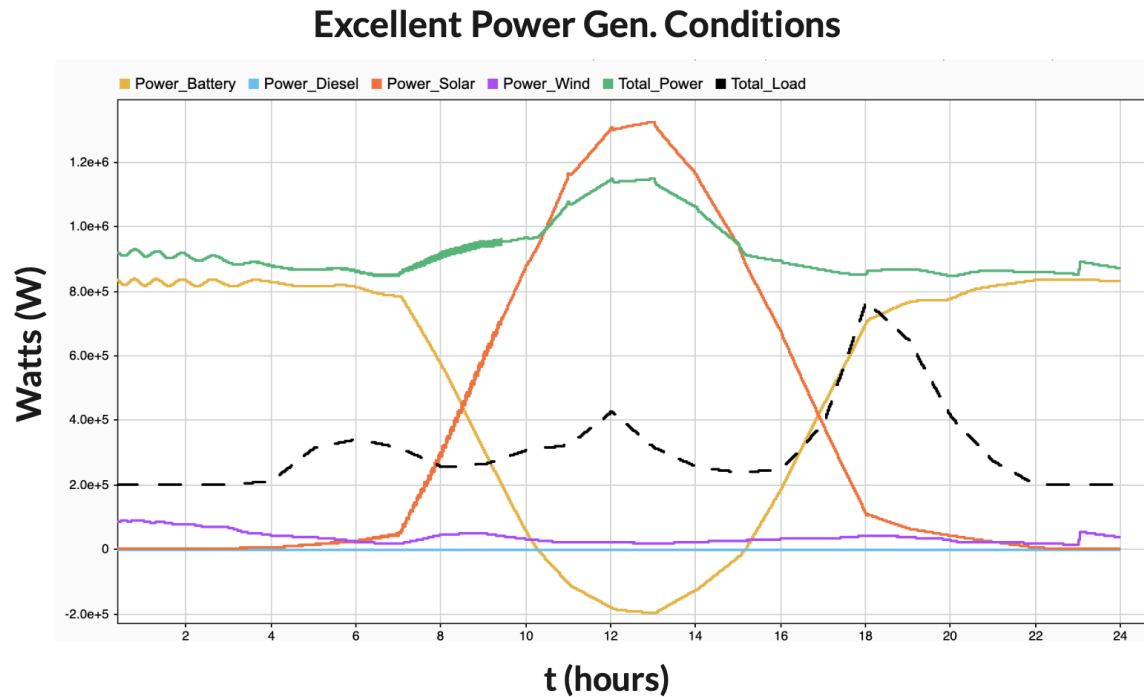


Figure 51: The power output for each power source under excellent conditions, total power output, and the total load measured in watts over a 24-hour period.

## Dashboard

In the dashboard, it is worth noting how during excellent conditions, the MG is able to achieve 100% renewable penetration as well as 0 kg-CO<sub>2</sub> emissions, which is critical to align with our project goals of sustainability and clean energy. The energy produced is considerably higher than what the community demand requires, providing up to 3 times as much energy. The system frequency stays stable at 50 Hz, since it is regulated by the grid-forming controller rather than by the diesel generator. The absence of diesel energy results in an LCOE of 0.221 \$/kWh.

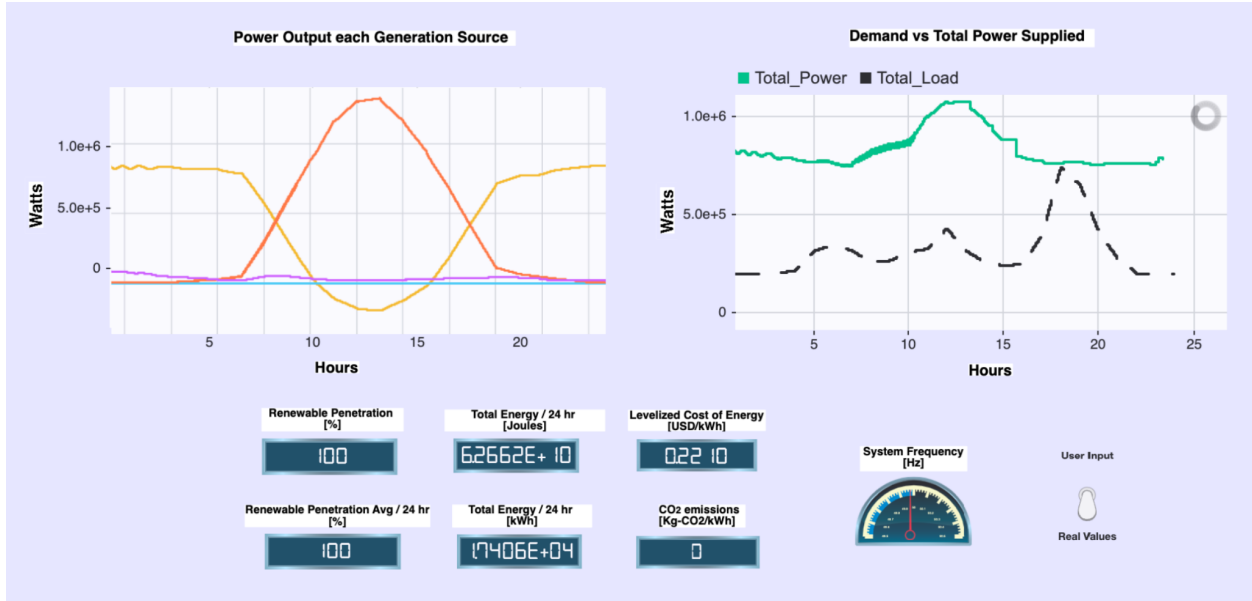


Figure 52: The GUI of the power output for each generation source under excellent conditions, demand vs total power supplied, renewable penetration, average renewable penetration for a 24-hour period, the total energy in Joules and kilo-watt-hours, LCOE, CO<sub>2</sub> emissions, and frequency.

## PV/Battery Voltage and Current

In terms of the PV/Battery voltage and current, the voltage stays mostly constant at 400 VAC, where the current amplitude and phase change more drastically to accommodate for the MPPT pulses.

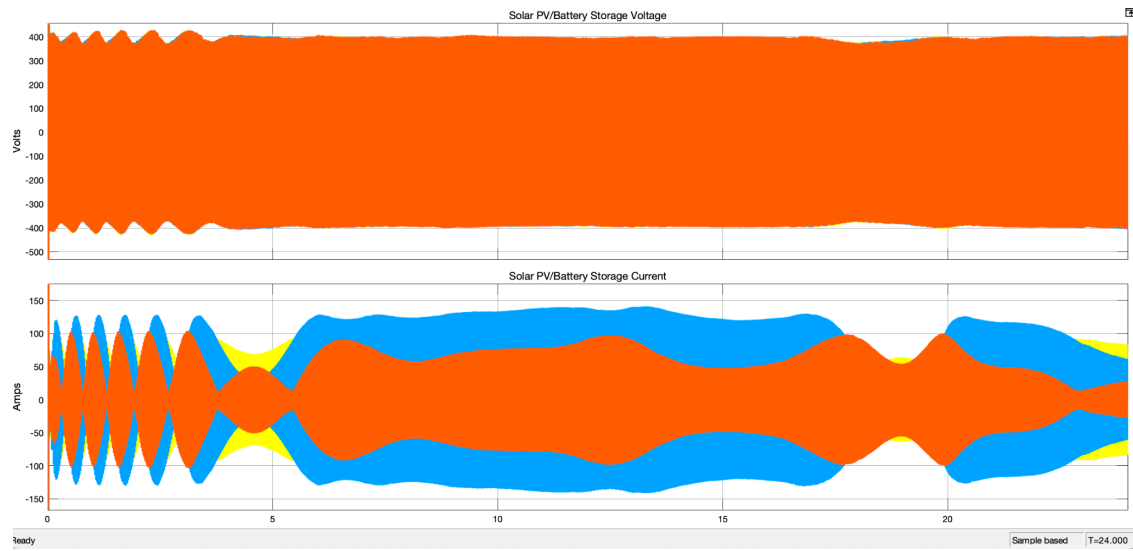


Figure 53: The voltage and current of the PV/Battery Storage system for the duration of the simulation under excellent conditions.

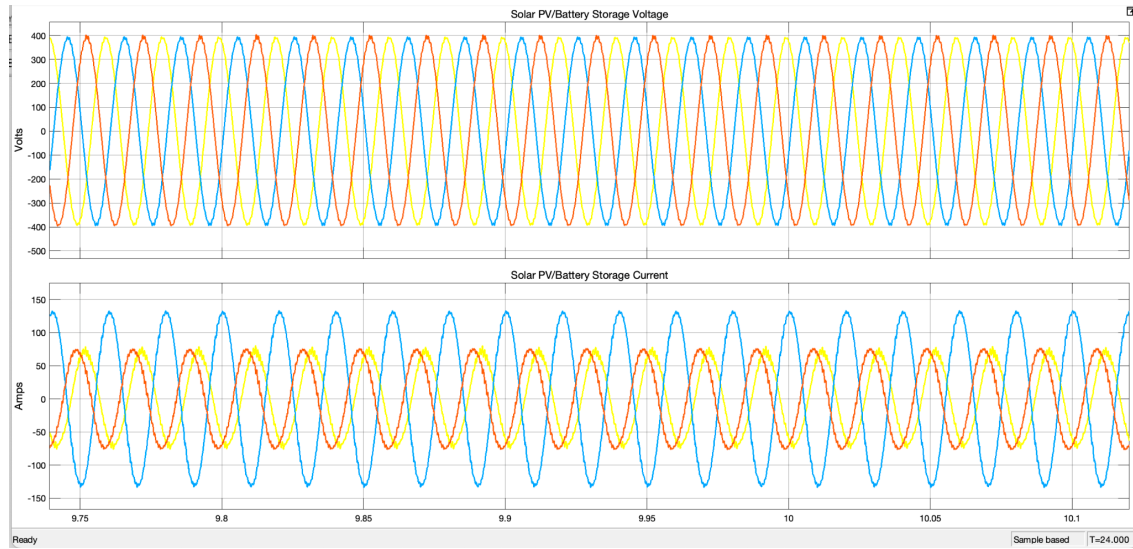


Figure 54: A close up of the current and voltage of the PV/Battery Storage system under excellent conditions.

## Wind Voltage and Current

Similar to the PV/Battery, the wind voltage remains constant at 400 VAC, which is crucial for reliability as the current shifts according to the pitch angle information received.

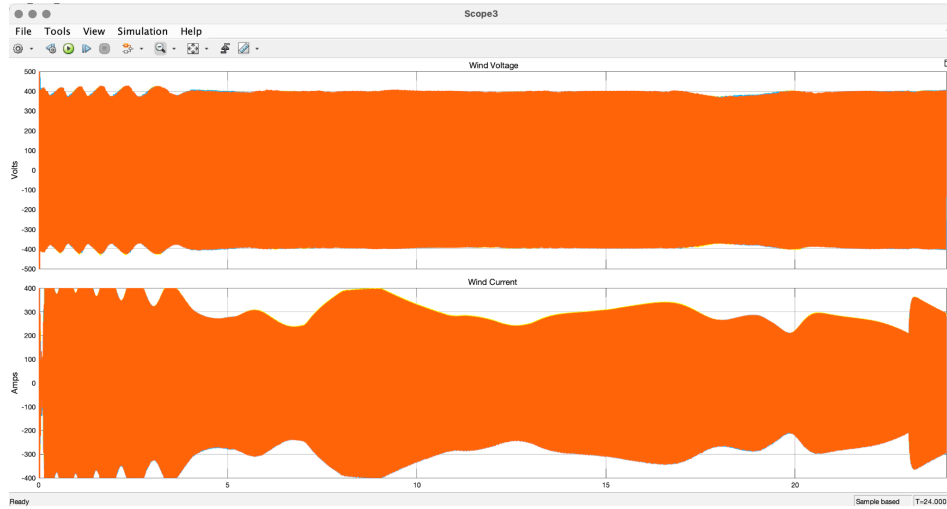


Figure 55: The voltage and current of the Wind system for the duration of the simulation under excellent conditions.

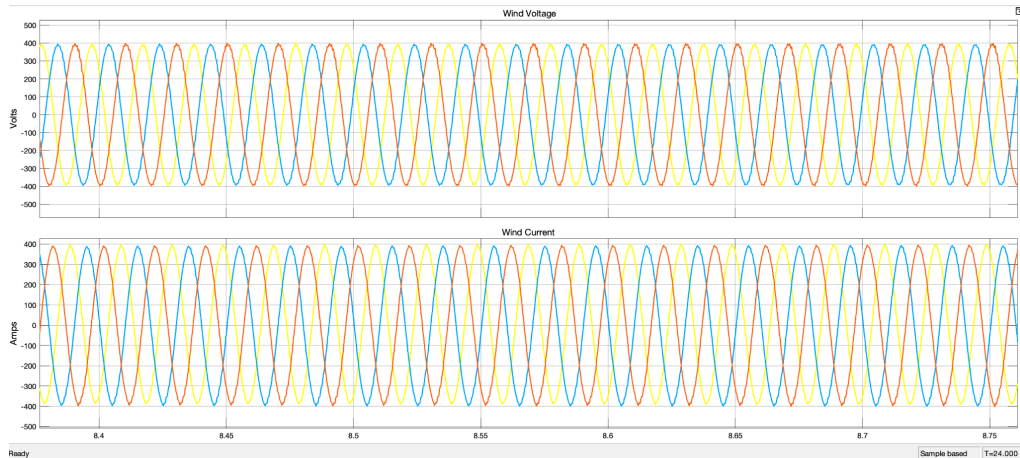


Figure 56: A close up of the current and voltage of the Wind system for the simulation under excellent conditions.

## Energy Produced

The energy produced in Joules by every power source is congruent with the expected results for each generation source. Since the diesel generator is turned off all the time, it outputs 0 J. The PV system produces a total of  $3.11 \times 10^{10}$  J, while the wind energy achieves a total of  $2.96 \times 10^9$  J. The battery achieves a total of  $3.60 \times 10^{10}$  J.

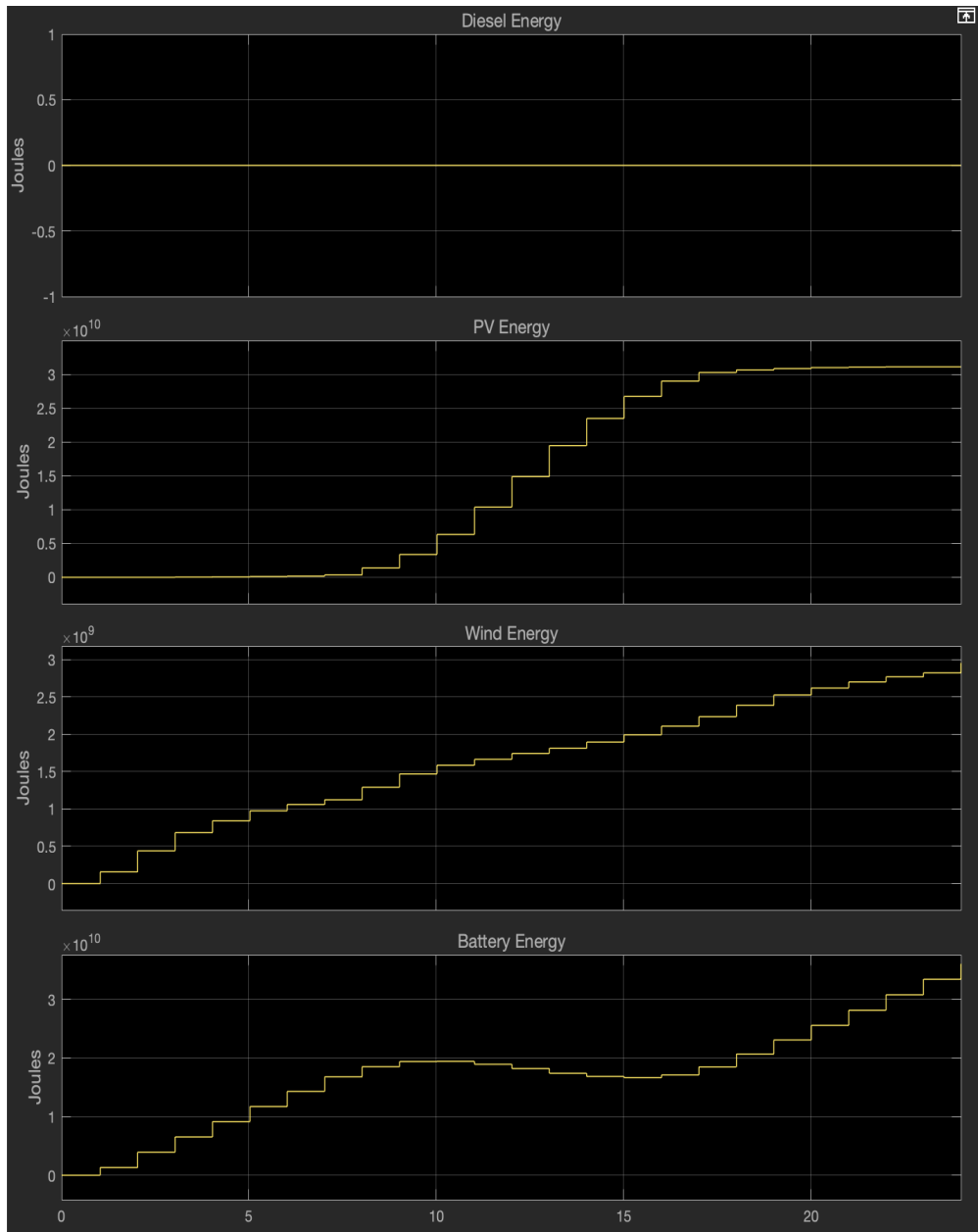


Figure 57: A measure of the total energy in joules of each power source under excellent conditions.

### 5.2.2) Typical Conditions

Under typical power generation conditions, the average community load is met and exceeded with PV solar, wind, diesel, and battery power, as shown in Figure 58. There is a lower amount of irradiance, which means that diesel power is required to adequately meet the load of the MG.

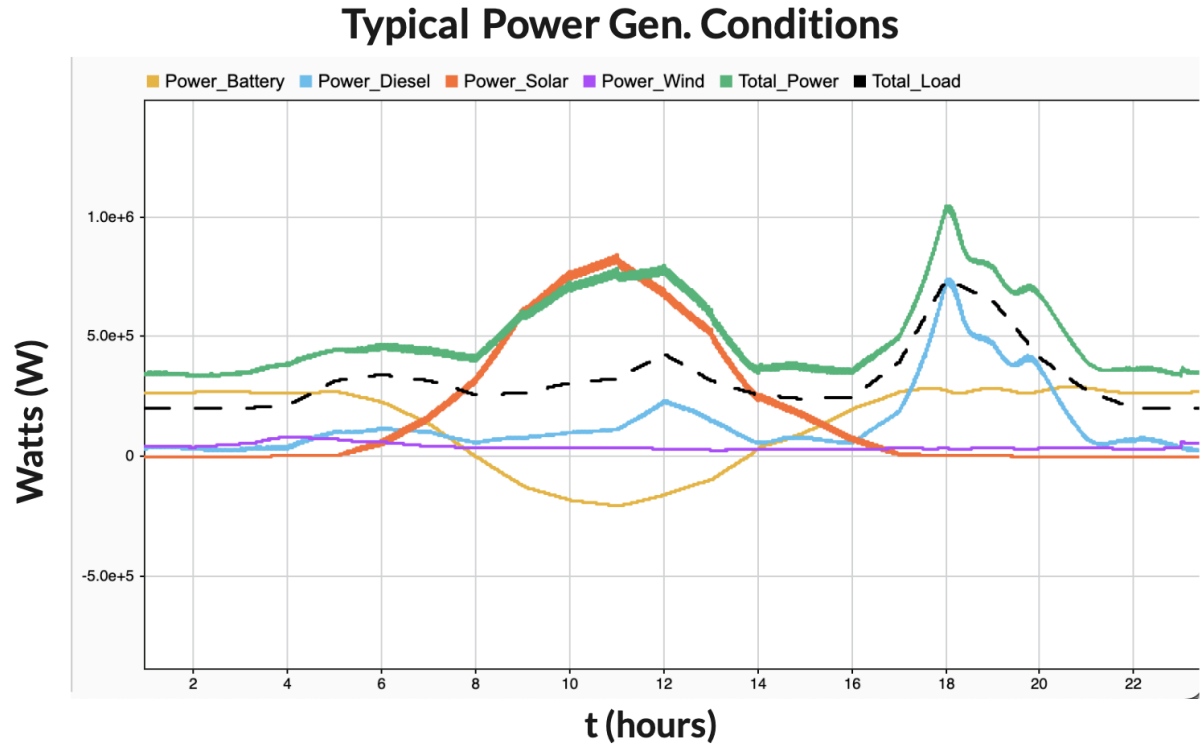


Figure 58: The power output for each power source under typical conditions, total power output, and the total load measured watts over a 24-hour period.

## Dashboard

Despite this use of diesel power, the average renewable penetration remains at 77% for a 24-hour period, as shown in Figure 59. The system frequency remains stable at approximately 50.04 Hz. The LCOE is calculated by assuming the energy produced for a typical day, 12,007 kWh, is the same for the entire year. In this way, the LCOE is \$0.3096/kWh. The CO<sub>2</sub> emissions under these conditions are 0.738 kg-CO<sub>2</sub>/kWh of generator operation.

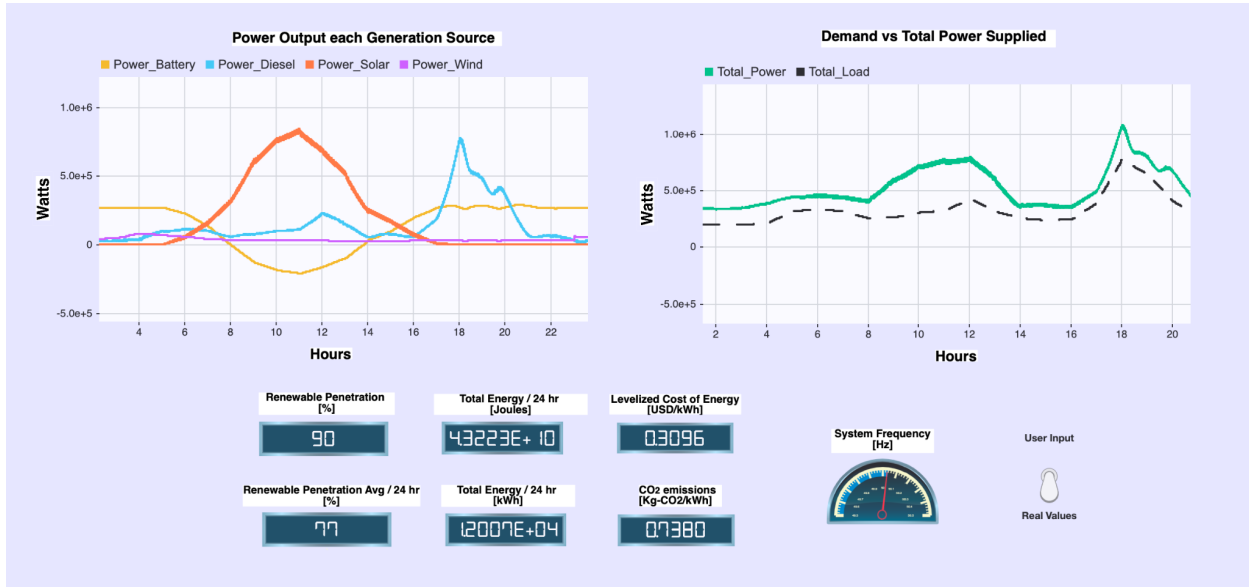


Figure 59: The GUI of the power output for each generation source under typical conditions, demand vs total power supplied, renewable penetration, average renewable penetration for a 24-hour period, the total energy in Joules and kilo-watt-hours, LCOE, CO<sub>2</sub> emissions, and frequency.

## PV/Battery Voltage and Current

As shown in Figures 60 and 61, the solar and battery voltage remains relatively constant at 400 VAC throughout the duration of the simulation. The varying current reflects the power output of that source.

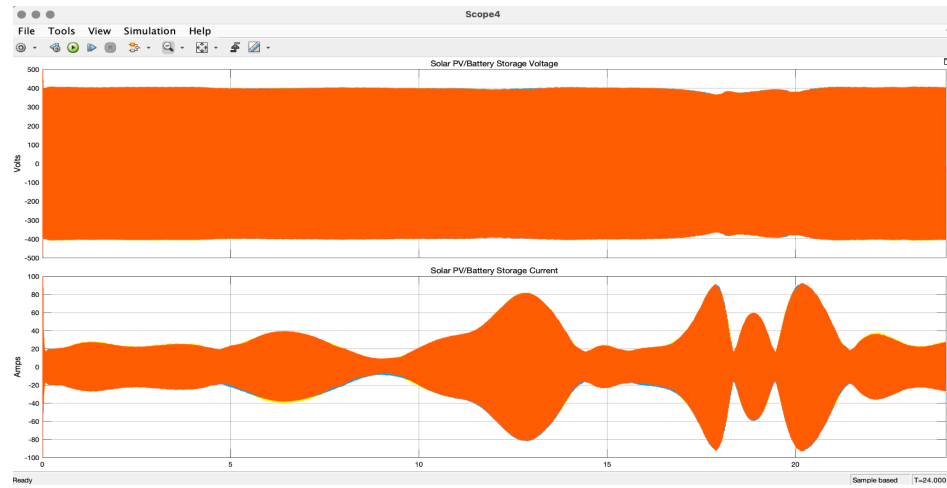


Figure 60: The voltage and current of the PV/Battery Storage system for the duration of the simulation under typical conditions.

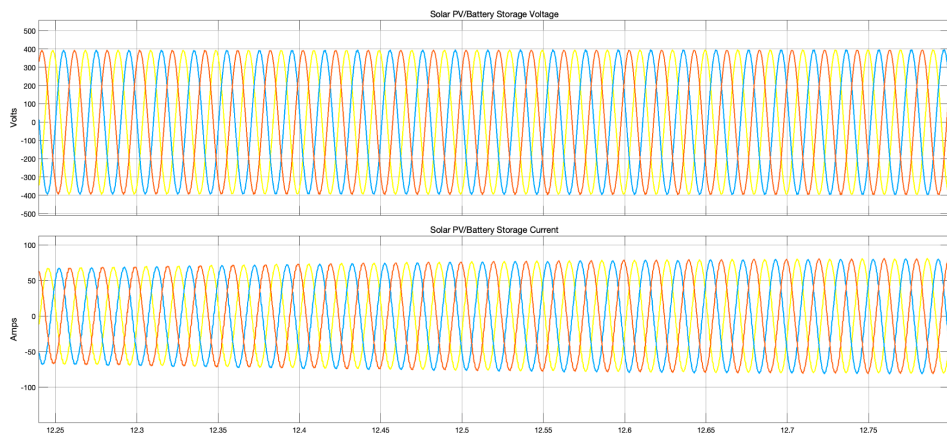


Figure 61: A close up of the current and voltage of the PV/Battery Storage system under typical conditions.

## Wind Voltage and Current

As shown in Figures 62 and 63, the wind voltage remains relatively constant at 400 VAC throughout the duration of the simulation with a change in current, which reflects the change in power output of that source.

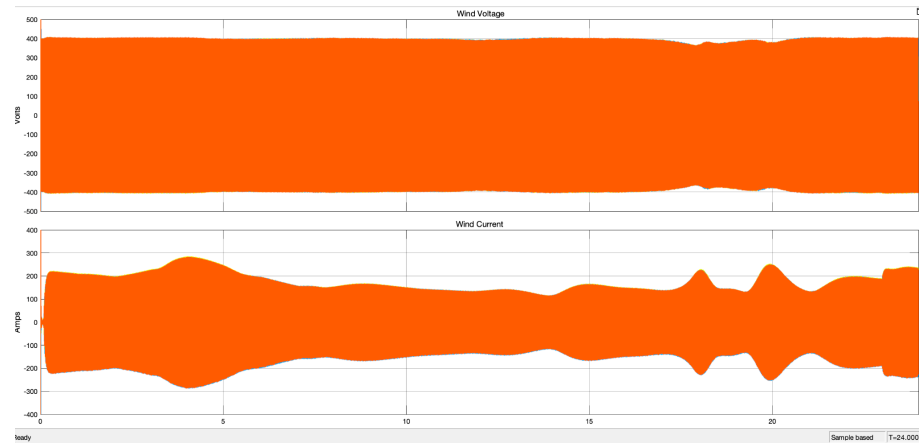


Figure 62: The voltage and current of the Wind system for the duration of the simulation under typical conditions.

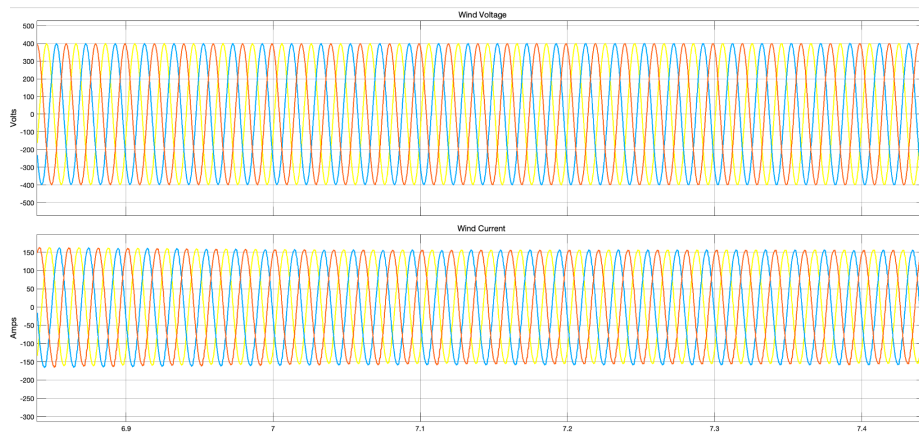


Figure 63: A close up of the current and voltage of the Wind system for the duration of the simulation under typical conditions.

## Energy Produced

As shown in Figure 64, PV solar produces the most energy, followed by the diesel generator, then the battery, and the wind. Thus, under typical power generation conditions, renewable energy sources remain dominant.

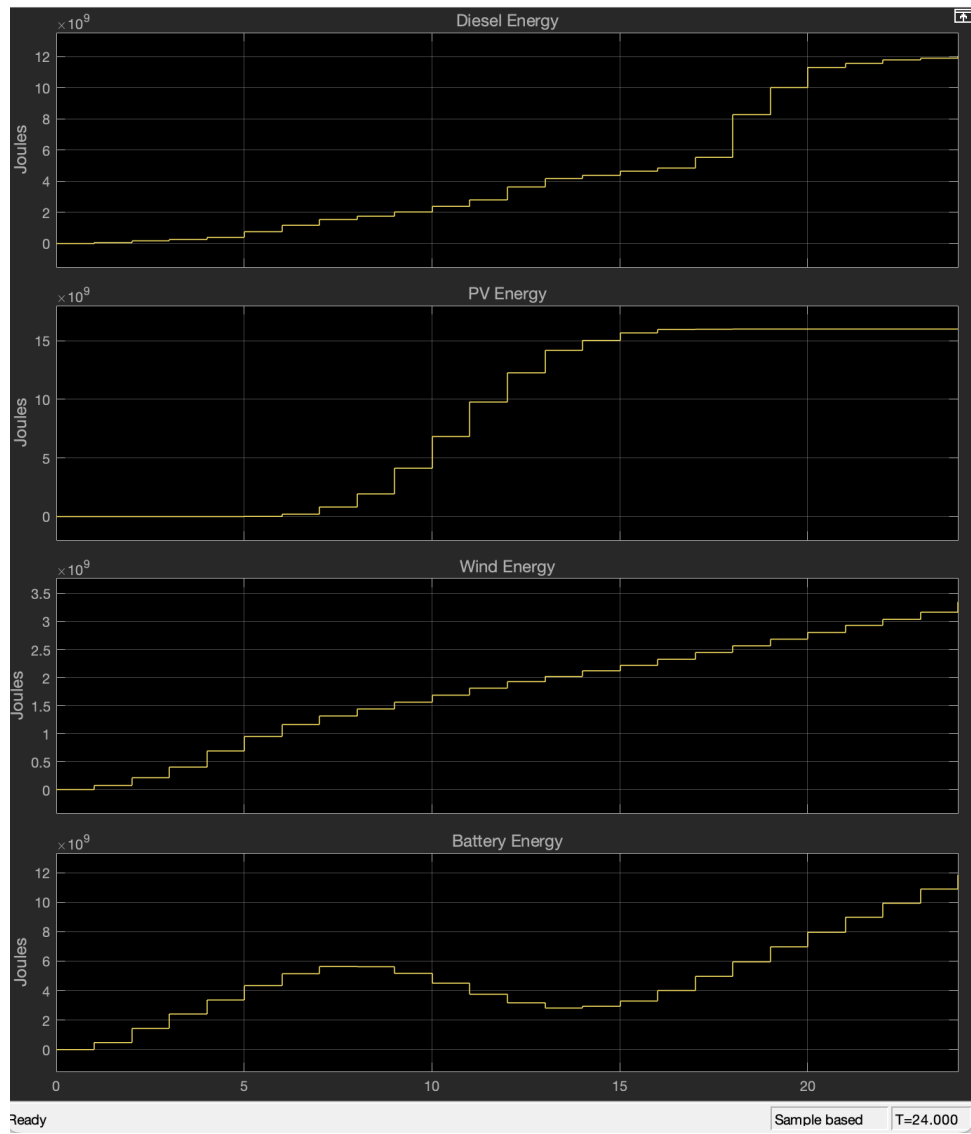


Figure 64: A measure of the total energy in joules of each power source under typical conditions.

### 5.2.3) Worst Conditions

Under the worst power generation conditions, the average load is still met with the battery power and diesel being the main contributors to the power produced as shown in Figure 65. The irradiance is low in this simulation, resulting in a peak irradiance of around  $150 \text{ Wh/m}^2$  and the wind speeds are negligible as under  $3\text{m/s}$ , the turbine is unable to produce any wind energy. This requires the diesel energy to be the main contributor in this simulation, with battery power making up the difference between the diesel and the load, around  $200 \text{ kW per hour}$ . The results of these weather conditions show that the MG design can still meet all necessary load requirements with the worst possible conditions in Juba, South Sudan, with only a minor decrease in renewable penetration.

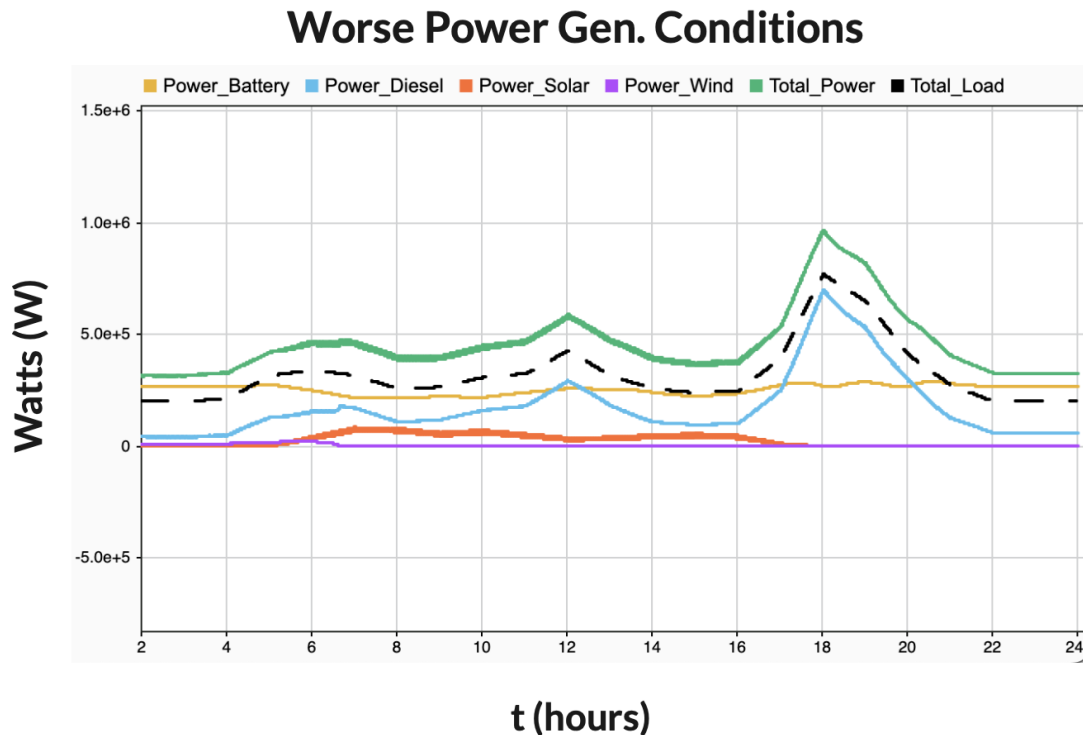


Figure 65: The power output for each power source under worst conditions, total power output, and the total load measured over a 24-hour period.

## Dashboard

Despite the fact that these conditions rely heavily on diesel, for a majority of the simulation, the battery power is producing more than the generator, resulting in an average renewable penetration of 67% over the 24-hour period, as seen in Figure 66. The system frequency stays stable at 50Hz and the LCOE results in 0.3279 \$/kWh. The CO<sub>2</sub> emissions during the worst conditions is 0.7380 kg-CO<sub>2</sub>/kWh.

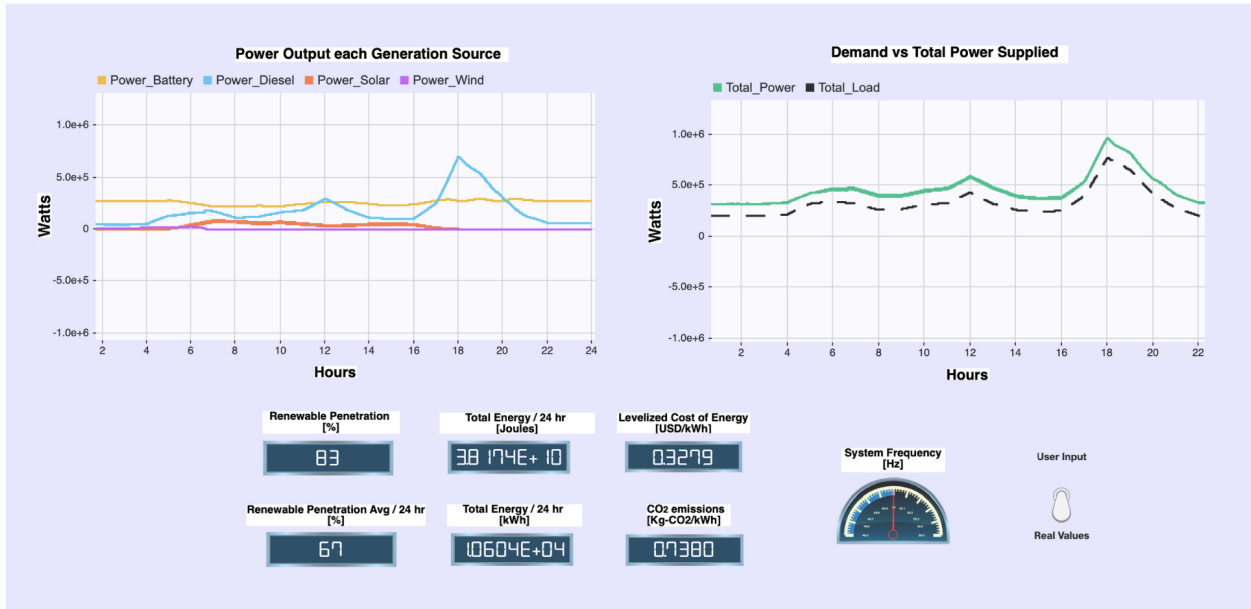


Figure 66: The GUI of the power output for each generation source under worst conditions, demand vs total power supplied, renewable penetration, average renewable penetration for a 24-hour period, the total energy in Joules and kilo-watt-hours, LCOE, CO<sub>2</sub> emissions, and frequency.

## PV/Battery Voltage and Current

The voltage output for the wind and solar remains constant at 400 VAC while those renewables are active, and the current is varying according to the MPPT pulses.

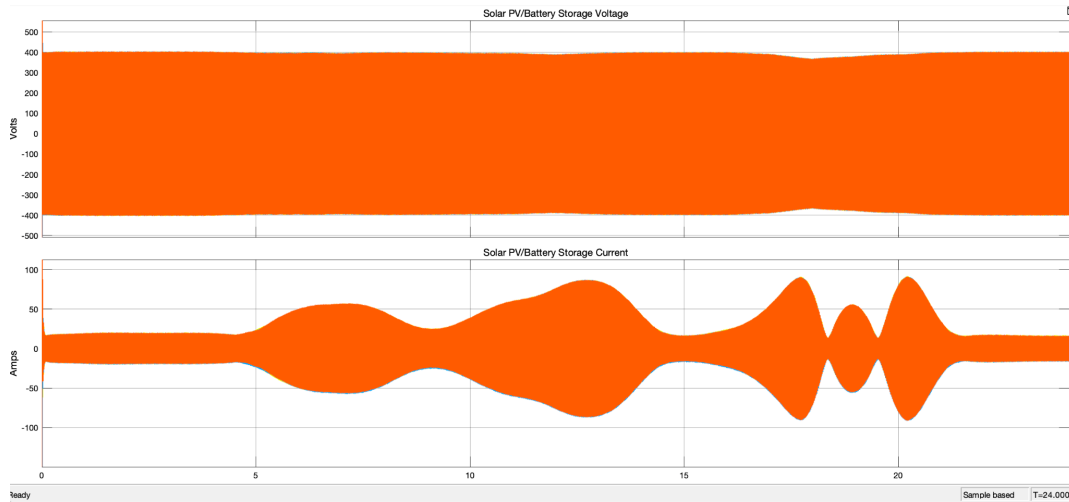


Figure 67: The voltage and current of the PV/Battery Storage system for the duration of the simulation under worse conditions.

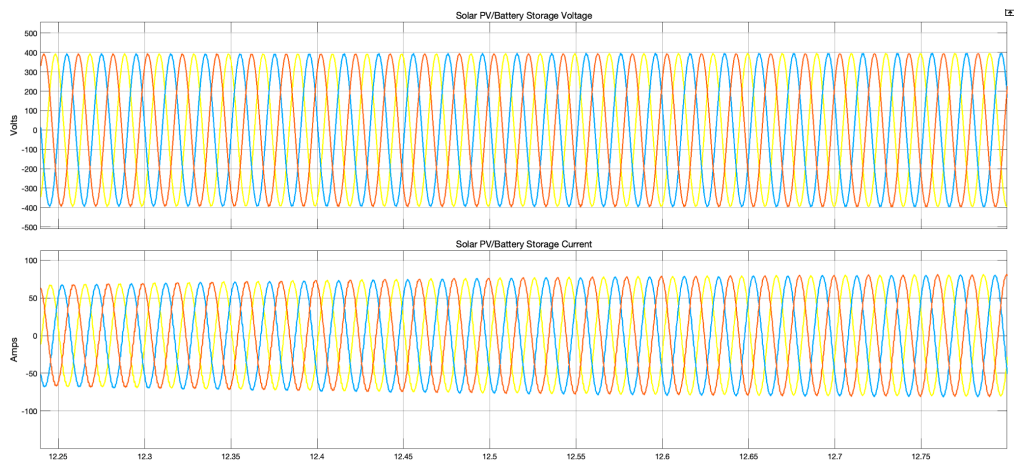


Figure 68: A close up of the current and voltage of the PV/Battery Storage system for the duration of the simulation under worse conditions.

## Wind Voltage and Current

As shown in Figures 69 and 70, the wind voltage remains relatively constant at 400 VAC throughout the duration of the simulation with a change in current, which reflects the change in power output of that source.

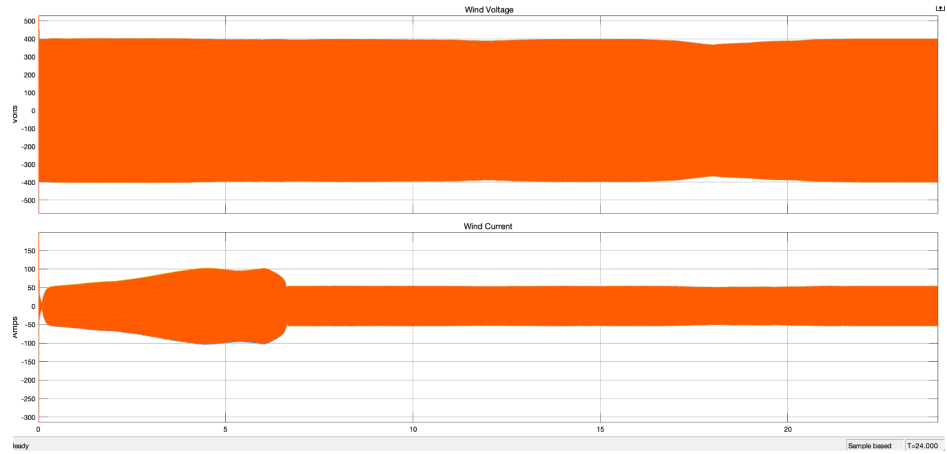


Figure 69: The voltage and current of the Wind system for the duration of the simulation under the worst conditions.

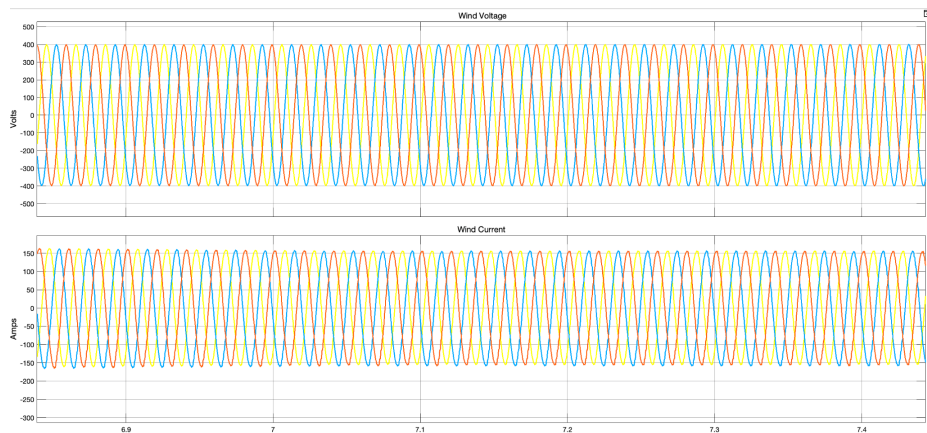


Figure 70: A close up of the current and voltage of the Wind system under the worst conditions.

## Energy Produced

The energy produced in Joules by every power source is shown below. The diesel generator is the main power source under the worst conditions and outputs  $1.44 \times 10^{10}$  J. The PV energy reaches a total of  $3.41 \times 10^9$  J, and the wind turbine generates a total energy of  $2.32 \times 10^8$  J during the entire run. The battery produces a total energy of  $2.12 \times 10^{10}$  J.

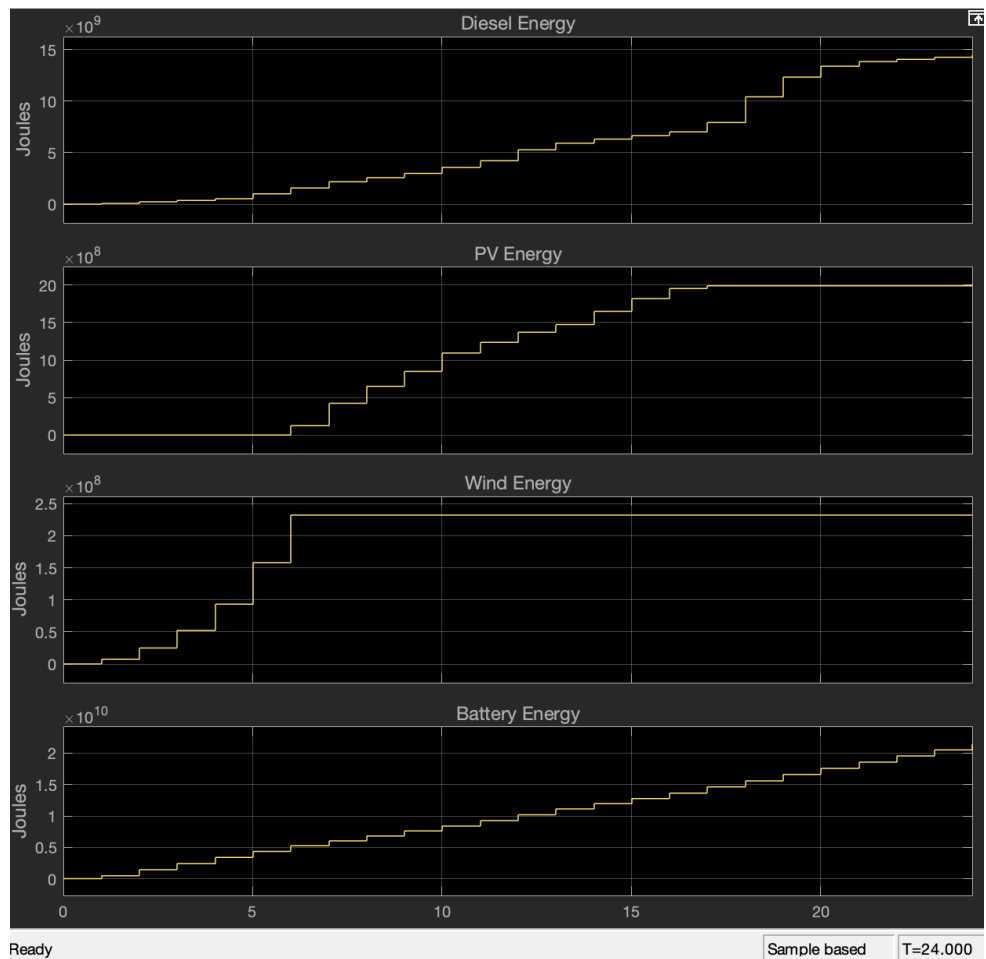


Figure 71: A measure of the total energy in joules of each power source under typical conditions.

#### 5.2.4) User-input

For a user-input example, we decided to test the simulation on a day with good irradiance, bad wind, and a high temperature. With a user-input scenario of an irradiance of 1200 Wh/m<sup>2</sup>, 4 m/s for the wind speed, and an average temperature of at 39° C we can see that solar, battery, and diesel are able to meet the average load. In Figure 72, you are able to see that the solar peaks at around 1.1MW which is able to provide the load and charge the battery between t = 7 hr and t = 16 hr. With the wind speed being 4 m/s, it is too slow for the turbine to produce a sufficient amount of energy. Under these conditions, solar and battery alone are unable to meet the load, which means diesel power is required.

### User Input: Good irradiance, bad wind, & high temp

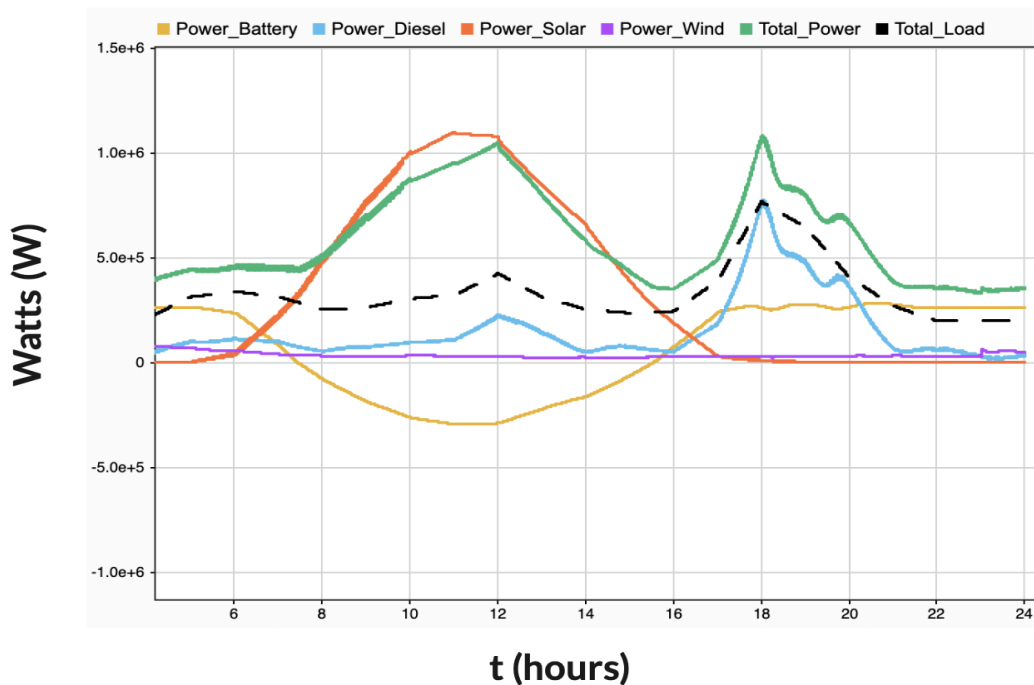


Figure 72: The power output for each power source under user input conditions, total power output, and the total load measured watts over a 24-hour period

## Dashboard

In the dashboard, under these user input conditions, the MG is able to achieve 70% average renewable penetration as well as 0.7380 kg-CO<sub>2</sub>/kWh of emissions over the 24-hour period. The system frequency remains stable at 50.04 Hz. The MG was able to generate 13,309kW over the 24-hour time period. The resulting LCOE was 0.3096 \$/kWh which relies on the amount of diesel that was being used under the user specific conditions.

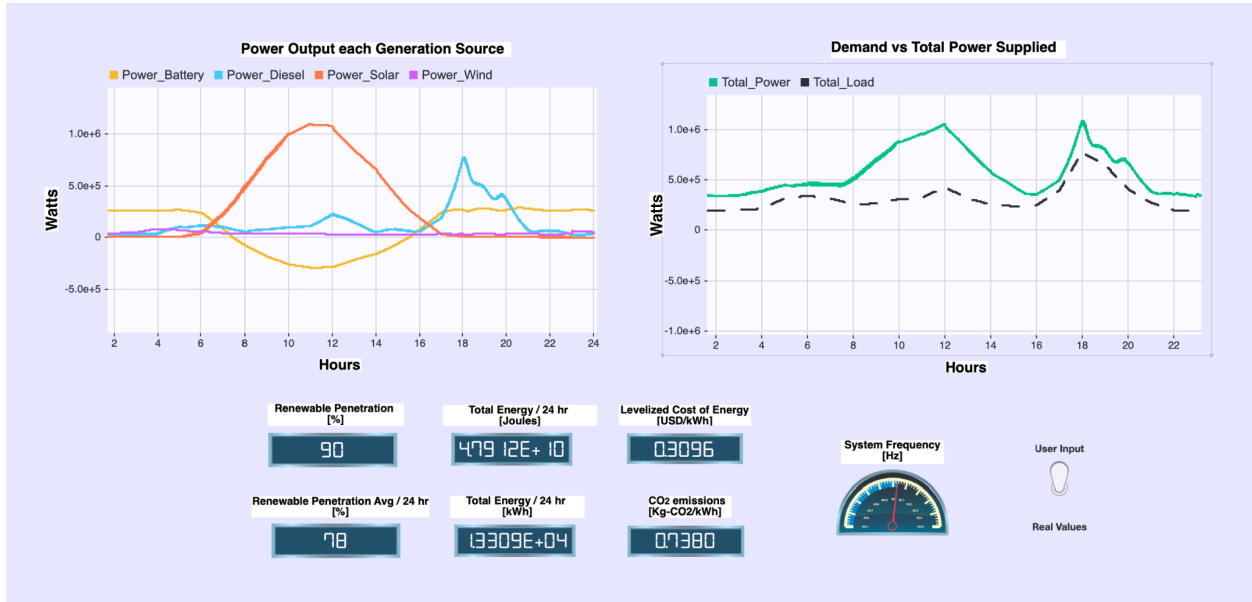


Figure 73: The GUI of the power output for each generation source under user-input conditions, demand vs total power supplied, renewable penetration, average renewable penetration for a 24-hour period, the total energy in Joules and kilo-watt-hours, LCOE, CO<sub>2</sub> emissions, and frequency.

## PV/Battery Voltage and Current

In Figures 74 and 75, the voltage remains constant around 400VAC and the current is changing depending on the power output of the source in accordance to the MPPT pulses.

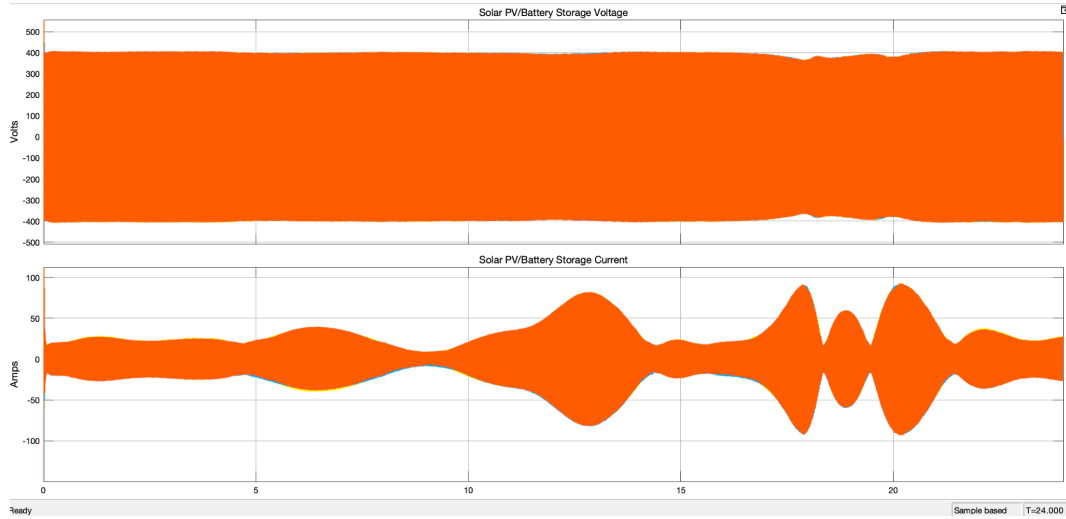


Figure 74: The voltage and current of the PV/Battery Storage system for the duration of the simulation under low wind speed, high irradiance, and high temperature.

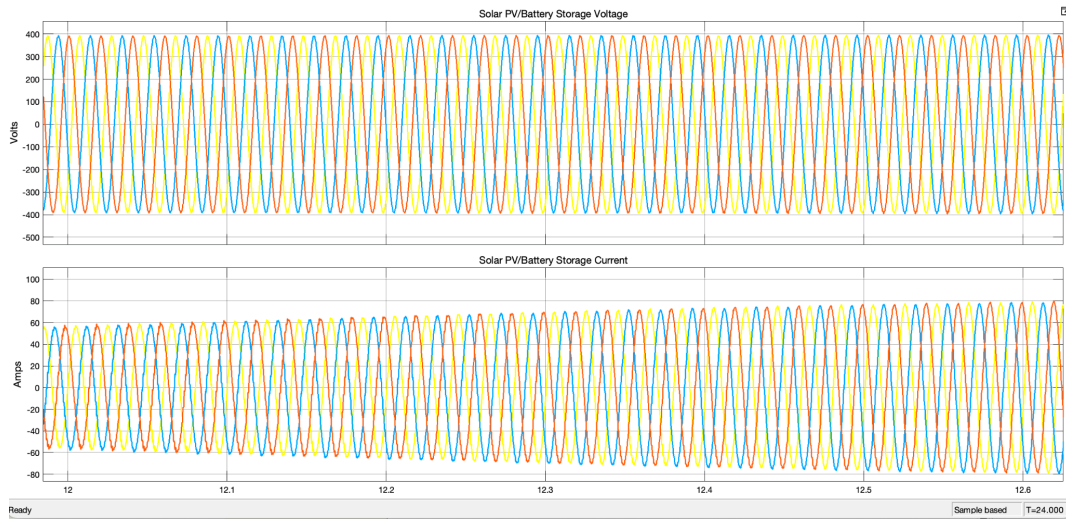


Figure 75: A close up of the current and voltage of the PV/Battery Storage system for the duration of the simulation under low wind speed, high irradiance, and high temperature.

## Wind Voltage and Current

In Figures 76 and 77, the voltage remains constant around 400VAC and the current is changing depending on the power output of the source.

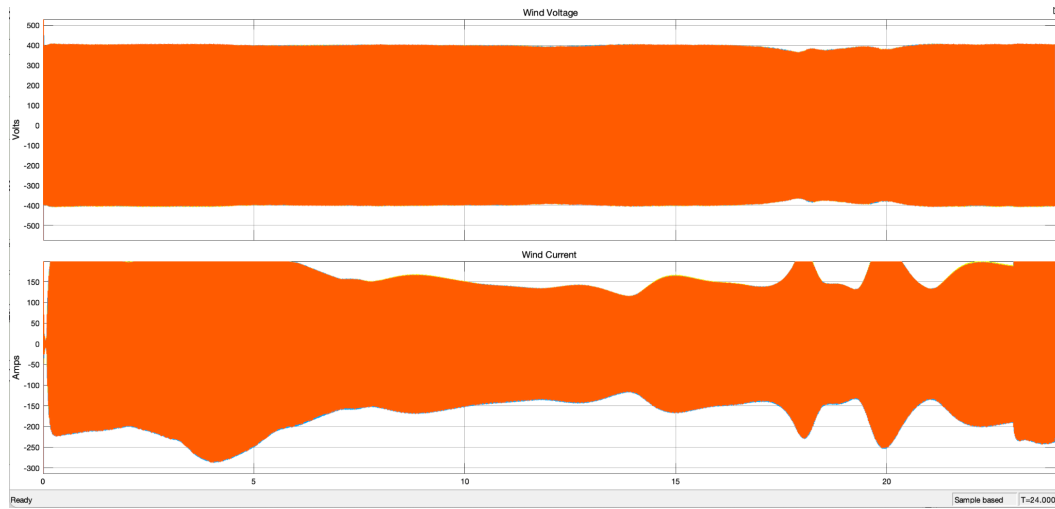


Figure 76: The voltage and current of the Wind system for the duration of the simulation under low wind speed, high irradiance, and high temperature.

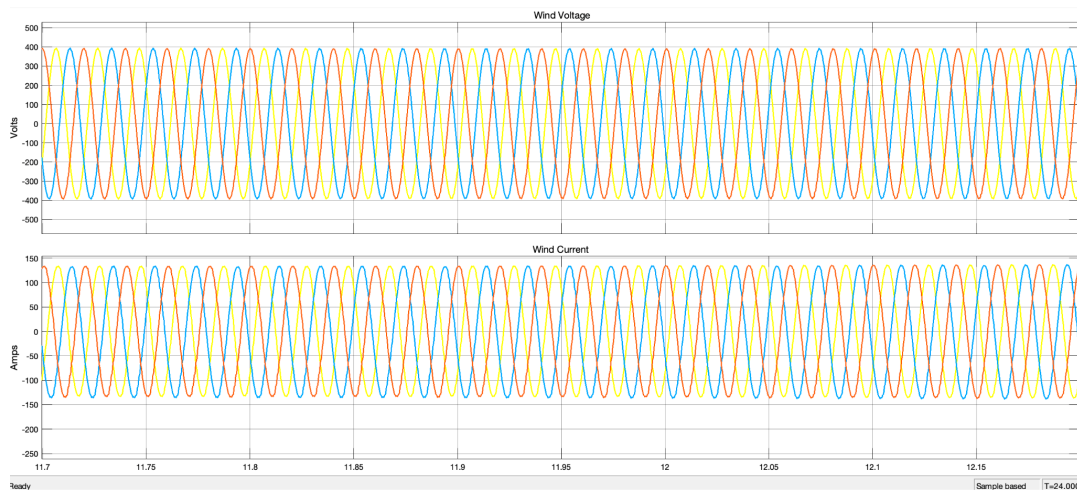


Figure 77: A close up of the current and voltage of the Wind system under low wind speed, high irradiance, and high temperature.

## Energy Produced

In Figure 78, the energy produced in Joules is shown for the solar, diesel, battery, and wind under these user input conditions. The PV solar produces  $2.5 \times 10^{10}$  J, diesel produces  $12 \times 10^9$  J, the wind turbine produces  $3.25 \times 10^9$  J and the battery produces  $7 \times 10^9$  J.

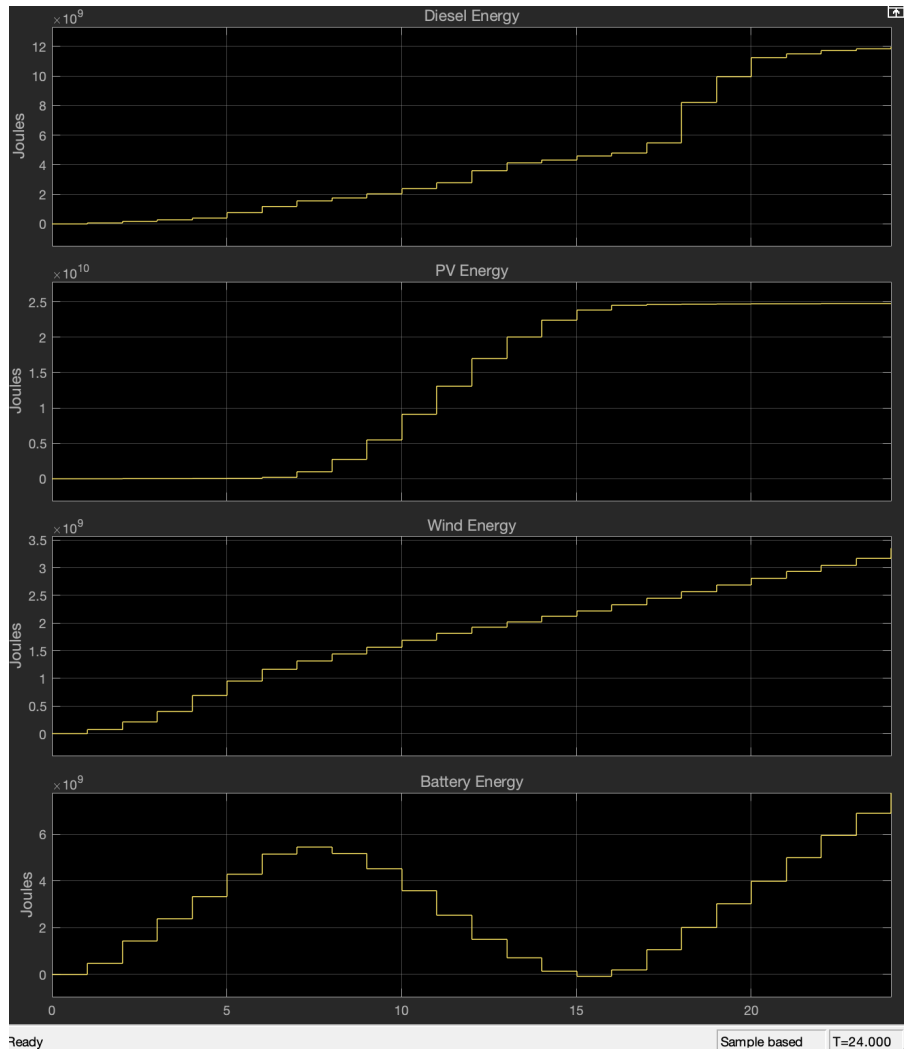


Figure 78: A measure of the total energy in joules of each power source under typical conditions.

# Analysis & Discussion

## 6.1) Economics

A critical goal of this project was to create a HOMER Pro simulation of a MG as a basis for a IMG in Simulink, and design the IMG in Simulink to be more cost-effective than the one in HOMER Pro. The results of the two simulations are shown in Table 8.

	HOMER Pro	RHOME
LCOE (\$/kWh)	0.3247	0.2977
Total O&M Operating Cost (\$)	591,287	1,911,975
Generator Capital Cost (\$)	480,000	332,460
Fuel Cost (\$)	1,429,904	10,125,000
PV Solar Capital Cost (\$)	4,042,224	3,403,197
6 MWh Lithium-ion Battery Cost (\$)	1,800,000	842,000
System Convertor Cost (\$)	35,781	12,874
Total System Cost (\$)	7,838,005	5,101,885
Net Present Cost (\$)	9,291,086	17,138,860

Table 8: HOMER Pro vs RHOME cost metrics comparison.

It should be noted that salvage cost and replacement cost do not appear in Table 8 because salvage cost was not considered in the costs for the RHOME system and replacement costs are a part of the capital costs for each system. These costs are included in the NPC for the HOMER Pro system. The replacement and salvage costs are \$587,287.18 and \$577,852.52 respectively, yielding a NPC of \$9,868,938.55. Omitting the salvage costs brings down the NPC to \$9,291,086. Following this logic of adding all the costs in the table for the RHOME simulation, the NPC is \$17,138,860. This difference in cost is primarily due to the limits of the RHOME simulation. In the simulation, the diesel generator always follows the variable load; in an actual MG system, the diesel generator would contend with a lesser portion of the total load. This would reduce the total energy produced in a year and therefore the fuel cost.

Assuming a total fuel cost approximation of \$1,429,904.89 for the RHOME system would yield a \$8,443,764.24 NPC and a LCOE of \$0.2754. Considering this assumption, the NPC makes the RHOME system superior to the HOMER Pro system. It is also important to consider that the LCOE calculations for RHOME are different from the LCOE calculations of the HOMER Pro, and that these differences may have associated errors. It should also be noted that, in consideration for project feasibility, subsidies will likely need to be granted by the South Sudanese government or another organization such as the UN. This would further lower the price of diesel fuel from \$10,125,000 to something closer to the \$1,429,904.89 obtained from HOMER Pro.

Despite the difference in NPC between the systems, the LCOE for the RHOME system is superior to that of the HOMER Pro system. The economic analysis of the RHOME system also includes a greater amount of components.

The equipment, installation, shipping cost, and import tax for each component were considered in the RHOME system, while HOMER Pro only provided general estimations. These components were also selected from websites where they were sold, while installation costs were estimated based on data and standard industry practices. Overall, with subsidies for fuel, relatively stable economic conditions in South Sudan, and a similarity to the HOMER Pro simulation cost estimations, a MG in Juba South Sudan is economically feasible.

## 6.2) Electrical

With regard to HOMER Pro, the equipment used was rated for the same amount of power. A 100kW wind turbine, 1.4MW PV solar array, a 6MWh capacity Li-ion battery and a 1MW diesel generator. However, there are some slight differences in how the battery was simulated. The battery in Simulink is one large battery cell while in HOMER Pro, it is modelled as many battery cells in one large battery pack.

Despite these differences, the simulations with excellent, typical, and the worst conditions all meet the required load, granting tier 2 energy access to 25,000 people. The following sections compare each energy resource across the three weather conditions. The renewable penetration and CO<sub>2</sub> emissions for each condition are also contrasted. The final section includes an analysis on how the power generation for each resource differs from the results of the HOMER Pro simulation.

### 6.2.1) Solar

The PV array is the main power source in the MG and covers a majority of the load in excellent and typical conditions. During the worst conditions, there is not nearly enough solar power to supply the load, thus other resources must cover the losses. With excellent weather conditions, the irradiance peaks over 1000 Wh/m<sup>2</sup>, resulting in a peak solar power of 1.397MW, just under the rated value of 1.4MW. On a typical day, the solar power peaks at 800kW with an irradiance of 900 Wh/m<sup>2</sup>, while under the worst conditions, it peaks at around 100kW with an irradiance of 200 Wh/m<sup>2</sup>.

The total solar power over 24 hours for each weather condition is 8.64 MW, 6.71 MW, and 946kW, with total energy values of 31.1 GJ, 24.2 GJ, and 3.41 GJ respectively. Between the excellent and typical conditions, the irradiance decreases by around 100 Wh/m<sup>2</sup>, while the peak power drops to about 75 percent. Showcasing a significant decrease in power relative to the decrease in irradiance.

#### 6.2.2) Wind

Wind power supplements the MG while irradiance and demand is low. During excellent and typical conditions, the wind peaks at around 100kW, its rated power, in the early morning before the sun comes up. This wind power along with the battery sustains the MG, providing enough energy to fully cover the load during the nighttime. However, under the worst conditions, the wind power peaks around 25kW and shuts off after about 6.5 hours of running. This is a result of not adequate wind speeds to keep the wind turbine active. When the wind speed falls below approximately 3m/s, the wind turbine stops turning, and therefore stops producing energy.

#### 6.2.3) Battery

The battery power, under excellent conditions, is higher than the typical and worst conditions. This is because it is assumed that the day before the simulated day would also have excellent conditions, resulting in a higher initial SOC for the battery. The behavior of the battery in this simulation mirrors the PV power. The battery is on overnight in tandem with the wind turbine to manage the nighttime load. Once the day starts and solar power starts being produced, the battery produces less and less energy until solar power is sufficient to supply the whole MG load. At this point, the battery starts charging in order to have enough stored energy to last until the following morning. The total amount of power output by the battery under excellent weather conditions is 10MW, while during typical and worst conditions, the power output is 2.24MW and 5.9MW respectively. Naturally, during the worst conditions, the main renewable power source is the battery, forcing it to be discharging energy for a majority of the day. The reason excellent conditions force the battery to be used more than under typical conditions is because the diesel generator is not active under excellent conditions, and it is the battery that makes up for that demand.

#### 6.2.4) Diesel Generator

Under excellent conditions, the diesel generator is turned off, allowing the renewable sources to match the load. During typical and worst conditions, the generator is turned on and is structured to follow a variable load, having the renewable sources make up the difference between the variable and total load. On a typical day, the diesel generator produces 12GJ of energy while on a day with the worst conditions, it produces 14GJ. These values result in total power output of around 3MW and 4MW respectively. All the excess power from renewables is used to charge the battery, while the diesel generator focuses directly on handling the load.

### 6.2.5) Renewable Penetration

The power from the battery is considered a renewable source in the RHOME model because the battery is only charged from renewable sources and not by the diesel generator. Renewable penetration is an instantaneous measurement and changes over the course of the simulation. Therefore, the average renewable penetration over 24 hours will be used for this analysis. The average renewable penetration for the three weather conditions are 100%, 77%, and 67% respectively.

During excellent conditions, the diesel generator is turned off, meaning only renewable sources are used to produce power, resulting in 100% renewable penetration throughout the simulation.

With typical conditions, the diesel generator is on, but most of the power is still produced from solar energy and the battery. The only time when diesel is the main power source is around 6 pm when there is a spike in the demand. This results in an instantaneous renewable penetration of 28%; however, throughout most of the day, the MG is powered by renewable sources, resulting in an average renewable penetration of 77%.

Under the worst weather conditions, the diesel generator is the main energy source, along with the power stored in the battery. These conditions result in an average renewable penetration of 67%. This number is expected because for the majority of the day, the battery is producing more power than the diesel generator. The only section of the day when the diesel overtakes the battery power, is between the hours of 5pm-8pm, where the load spikes and the diesel increases to cover the load.

### 6.2.6) Carbon Emission

The CO<sub>2</sub> emissions are measured in kg-CO<sub>2</sub>/kWh and are measured over the course of the 24-hour simulation. Naturally, during excellent conditions when there is no diesel, there are also no CO<sub>2</sub> emissions. Under typical and worst conditions, the diesel generator follows the same variable load which results in the same value of 0.738 kg-CO<sub>2</sub>/kWh.

### 6.2.7) Overall Resource Comparison

In relation to the simulation found using HOMER Pro, the RHOME MG system produced a larger total amount of power over the course of the year. The distribution of the power generation of each source is listed below in Table 9.

	HOMER Pro (kWh/yr)	RHOME (kWh/yr)
Diesel Generator	205,111	1,040,000
Wind Turbine	1,127,223	318,000
PV Solar	2,188,324	2,450,000
Total	3,520,659	3,810,000

Table 9: HOMER Pro vs RHOME resource power generation comparison.

The amount of solar power generated from both simulations is approximately the same with the HOMER Pro simulation reaching just over 2,000,000 kWh/yr while the RHOME simulation produced just shy of 2,500,000 kWh/yr. The major difference is the use of diesel and the effectiveness of the wind turbine. The use of the diesel generator in the HOMER Pro model was restricted to only during the summer months when there was a decrease in both wind and solar power. However, in the RHOME model, the diesel is used to counteract the daily variable load. This results in its use during days with typical and the worst weather conditions, accounting for approximately 85% of days throughout the year. The wind turbine power is another main difference between the two simulations. One reason for this is that HOMER Pro uses a different method to optimize the wind power. The RHOME system matches the voltage of each power source to the optimal voltage for PV solar since that resource is the main source of power in the system. This results in the loss of some power for the wind turbine. Another reason is that the model in Simulink accounts for more realistic power efficiency losses throughout the system, lowering the total power of the wind turbine further. Overall, the RHOME system produces more power than shown in the HOMER Pro simulation at the cost of higher diesel use.

### 6.3) Reliability

The RHOME system has been able to demonstrate an ability to adapt to varying power generation suitability conditions: excellent, typical, and worst, while still maintaining reliable functionality throughout the year. This section contrasts the outputs from these conditions and provides meaningful insights into the MG's performance under different scenarios and its overall reliability.

Renewable penetration reaches 100% under excellent conditions, with solar and wind being responsible for meeting the entire load demand. The diesel generator remains off during the entire time in these cases, which results in zero CO<sub>2</sub> emissions and a highly competitive LCOE of \$0.22/kWh. Moreover, the total energy produced over 24 hours is 17,406 kWh, which showcases the capacity of the system to operate entirely on renewables during periods of high solar irradiance and decent wind availability. This highlights the MG's sustainability and cost efficiency capabilities when renewable resources are abundant, which was a core objective since the beginning of this project.

In typical conditions, which represent about 80% of the year, renewable penetration averages 77%. Solar and wind contribute significantly but require additional power from the diesel generator in order to meet variable load demands. The use of diesel increases CO<sub>2</sub> emissions to 0.738 kg-CO<sub>2</sub>/kWh, while LCOE rises to \$0.3096\$/kWh due to higher fuel use. The total energy produced is 12,007 kWh over 24 hours, which reflects a balanced operation between renewables and diesel. This scenario demonstrates that the MG can reliably meet load demands while maintaining moderate environmental impact and operational costs most of the time in the year, with location specific characteristics.

Additionally, during the worst conditions, the renewable penetration drops to 67%, with solar and wind being unable to meet most of the load demand by themselves and having to rely on the diesel generator and assuming a greater initial SOC of battery. The diesel generator here would play a more critical role in ensuring reliability, resulting in similar CO<sub>2</sub> emissions compared to typical conditions despite higher diesel. These values are similar because the diesel output follows variable load profiles in both scenarios in the RHOME simulation, and it's a practical point for future enhancement. In reality, the worst day conditions will result in higher levels of CO<sub>2</sub>/kWh around 0.8 kg-CO<sub>2</sub>/kWh, which is still superior compared to diesel-only systems that emit approximately 0.9–1.1 kg-CO<sub>2</sub>/kWh in South Sudan [139]. The total energy produced is slightly lower at 10,604 kWh over 24 hours due to reduced renewable contributions and increased reliance on diesel.

Considering an annual distribution of power generation conditions of roughly 80% typical, 15% excellent, and 5% worst, the RHOME simulation achieves an average renewable penetration of approximately 78%. Annual CO<sub>2</sub> emissions are driven by diesel usage during typical and worst conditions, averaging 0.738-0.8 kg-CO<sub>2</sub>/kWh for these scenarios. The system is able to maintain competitive costs with an annual average LCOE between \$0.30-\$0.32\$/kWh while reliably meeting load demands throughout the year.

## 6.4) Feasibility

South Sudan's current reliance on diesel generators for electricity has created economic, environmental, and social challenges. Diesel dependency has led to some of the highest energy costs in that region, having prices over \$2/kWh in conflict zones due to fuel scarcity, black market activity, and high transportation costs [125]. Furthermore, degradation to the environment and human living conditions from diesel emissions and unreliable power delivery have made the nation's energy crisis even worse. By contrasting diesel-only systems with hybrid renewable systems, it is very reasonable to infer that transitioning to a hybrid system is not only viable but essential for addressing South Sudan's energy access challenges; additionally providing a feasible opportunity to scale a solution to deliver reliable power to remote locations around the world.

The economic collapse caused by hyperinflation has made diesel even less viable as a primary energy source. Between 2015 and 2017, South Sudan's consumer price index increased by over 2,100% making diesel fuel unaffordable basically for everyone there [139]. Hybrid systems like what RHOME proposes would alleviate this issue by leveraging abundant solar and wind resources available in the region (which have also seen dramatic cost reductions globally). Furthermore, reducing diesel dependency would likely help to stabilize energy costs and improve affordability for households and institutions.

Diesel-only systems are too expensive for most people in South Sudan, mainly caused by high operational costs driven by volatile fuel prices and inefficiencies. According to simulation results from RHOME's model, hybrid systems achieve an annual average LCOE of around 30–32¢/kWh, compared to the higher values for diesel-only systems previously referenced. During excellent renewable conditions, the LCOE drops further to 22¢/kWh as solar and wind fully meet the demand without requiring diesel backup. In contrast, the hybrid system reduces emissions to an annual average of 0.738 kg-CO<sub>2</sub>/kWh based on RHOME simulation outputs. During excellent conditions, emissions drop to zero as renewables fully meet load demand.

Diesel-only systems are more prone to supply chain disruptions caused by insecurity, poor infrastructure, and fluctuating currency values, leading to unreliable power delivery while hybrid systems ensure reliability through diversified generation sources [139]. RHOME simulation results show that the hybrid system achieves an annual renewable penetration of approximately 78%, with diesel serving as a backup during typical and worst conditions. During excellent conditions, renewables fully meet load demand without diesel support, demonstrating sustainability and reliability under favorable scenarios. Under typical conditions, solar and wind contribute significantly but require supplemental power from the diesel generator to meet variable load demands. Even under the worst conditions, where renewable penetration drops further, diesel ensures uninterrupted power delivery, which means that these systems are not only feasible but also more cost-effective and environmentally friendly.

## 6.5) Potential Enhancements

While working on the RHOME system, there are some sections that could be improved upon. Some improvements would be more sophisticated controls and management systems of different components in order to improve efficiency, resilience, and sustainability. Other improvements can be made on the realistic aspects of the MG. In order for the data to properly reflect real world values, the simulation conditions must also be able to change, and the system must be able to adjust to these changes dynamically. In order to properly reflect accurate data, the RHOME system must utilize real-time data to optimize energy usage, improve efficiency and maximize the power output.

For the RHOME system, in order to more accurately represent the diesel usage and CO<sub>2</sub> emissions data, the control logic for when the diesel generator could dynamically turn on and off instead of following the variable load. Ideally, depending on the energy that is produced by the renewables, the diesel generator should be used as a backup that will provide energy when the renewables can not meet the load. If the RHOME system could take in real-time data such as irradiance, wind speed, temperature, and power demand, it ideally would be able to determine when the diesel generator needs to be used. If the controls were enhanced, the diesel generator would be able to be used as a backup source and the amount of fuel and CO<sub>2</sub> emissions can be greatly reduced.

RHOME currently has a BMS that will discharge the battery when solar is unable to provide enough power for the load. The management system will also charge the battery when solar exceeds the amount of energy needed for the load. The current, voltage and SOC of the battery are monitored by the management system. It is also possible to add further practicality by monitoring more data, such as temperature in the battery pack system. By monitoring the temperature, it would be possible to control the charge and discharge of the battery even further by making sure the battery isn't discharging at high temperatures in order to reduce the chance of any potential damage. When considering the SOC of the battery, it's realistic to add limits that ensure that the battery doesn't discharge under a certain SOC or charge over a certain SOC to maintain the lifetime of the battery. Battery storage systems tend to use multiple cells in packs of batteries, and a BMS can make sure that all cells are charging and discharging evenly, which maximizes battery life and performance. These improvements focus on maximizing the battery life and performance through incredibly detailed charge and discharge conditions, while also monitoring crucial battery parameters.

The simulation uses conditions that are set at the beginning of the simulation and are unable to change them while the simulation is running. By incorporating the ability to change these conditions during the simulation, it is plausible to more accurately predict the changes in the conditions over a 24-hour period. This would simulate the MG's ability to take in real time data and its ability to adjust the components to improve efficiencies and power output.

By comparing the specification between real components and the RHOME model, it would better inform the feasibility of the MG.

During the RHOME simulations, there were difficulties with extreme conditions that were set before the simulation was run. When the conditions provided do not result in enough total power to cover the load, errors occur in the simulation.

## 6.6) Consideration of Public Health and Other Factors

### Global considerations

The environmental benefits of the implementation of a project similar to RHOME extend beyond CO<sub>2</sub> reduction. Diesel generators produce local air pollution that disproportionately affects densely populated areas such as internally displaced persons camps near Bentiu and Malakal, as well as the one analyzed by the RHOME simulation in Juba [125]. Transitioning to hybrid systems with storage solutions would help eliminate these risks while providing clean and reliable power.

### Public health

South Sudan's electrification rate is among the lowest globally at just 8.4% with most households relying on expensive and polluting fuels like kerosene or firewood for lighting [216]. The hybrid system offers several social benefits. The RHOME MG proposal would lead to improved access to clean electricity for households and institutions such as hospitals and schools.

### Public welfare

Reduced dependence on costly diesel fuel would free resources for other essential needs. Enhanced quality of life through reliable power for lighting, refrigeration, and communication could be achieved. Renewable energy systems can also create long-term infrastructure that supports peace building efforts by reducing economic tensions tied to fossil fuel dependency [139].

### Cultural considerations

With the construction of any project around the world, it is important to consider the cultural beliefs and practices of an area. Land would be purchased for the MG before any construction takes place, and an environmental and social impact assessment (ESIA) should be conducted [217]. The ESIA would address potential unfavorable social and environmental impacts and their solutions.

### Social considerations

The construction and maintenance of the MG would promote steady jobs within the area, and most likely increase the population and social activity of the area. The renewable energy is also intended to benefit all residents of the area, therefore it would not incite any conflict since there would be no competition over who is subjected to the renewable energy.

## Economic considerations

A MG is a massive project to be funded, and the companies responsible for all the components and construction would benefit largely. The purchase of energy is also an everlasting expense for people, so there will always be a constant flow of money within this project. The people would also be saving significant amounts of their money, which could help boost the economy through new business ventures and expenditures.

## Public safety

Most aspects of a MG come with safety risks, thus the protection of the people is the main priority. The MG would be placed far enough from civilization, so that if any damage were to occur, the people would not be harmed. A wind turbine also would need clearance from any other construction in the unfortunate circumstance that it falls over.

## 6.7) Recognizing Ethical and Professional Responsibilities

IEEE provides a set of ethical guidelines that were followed throughout the duration of this project. Under Section 7.8 IEEE Code of Ethics, we recognize and commit ourselves to the three ethical standards established [\[218\]](#). We upheld the highest standards of integrity, responsible behavior, and ethical conduct in professional activities. We accomplished this through using credible online sources and referencing them appropriately. We also reached out to experts in the respective field to ensure reliable and realistic data. We treated all persons fairly and with respect through patience and understanding. We exhibited kind behavior towards each other throughout the project, where nobody felt singled out or subjected to harassment. Lastly, we chose a project that would provide benefits to many people, with the thought that the people's lives can be changed for the best. We strongly encourage others to incorporate these standards if they decide to replicate or implement the project in real life.

# Conclusion

The journey to develop the Renewable Hybrid Optimized Microgrid Energy (RHOME) model began with a seemingly simple but incredibly complex question: can renewable energy systems provide reliable power to remote communities? Through countless hours of modeling, simulations, research, and analysis, it has been crystal clear that the answer is a promising ‘yes!’ (though certainly not without challenges). By combining high-level and low-level simulation approaches, we were able to create the initial stages of a tool that bridges theoretical modeling with practical implementation considerations for real impact. Our results suggest that a hybrid system with the conditions that lay out incorporating solar PV, wind, battery storage, and diesel backup can achieve up to 78% renewable penetration annually, which represents a significant improvement over conventional diesel-only systems prevalent in remote underdeveloped locations. The consistent reliable system’s performance under various conditions was certainly surprising and showcases the potential impact if we are able to intelligently harness the vast amount of renewable energy resources at our disposal. During excellent weather conditions in our MG model can fully meet load demands with renewable resources, in typical and worst-case scenarios, the system maintained reliable power delivery thanks to MG specific power management strategies we developed through trial and error of different conditions and relying on the data. From an economic perspective, the hybrid MG system appears as a strongly competitive option with LCOEs between \$0.22-\$0.32/kWh. While this isn't as inexpensive as grid-connected power in developed regions, it represents a meaningful improvement over the \$0.40/kWh costs of diesel-only generation that many remote communities currently endure. The environmental benefits were encouraging as well. The simulations showed CO<sub>2</sub> emissions reduced from typical diesel-generator levels (0.8-1.1 kg-CO<sub>2</sub>/kWh) to an average of 0.738 kg-CO<sub>2</sub>/kWh with our hybrid approach. It's clearly not perfect but it's a step in the right direction. We believe our interactive simulation offers value beyond just the numbers and the ability to visualize how different components interact in real-time helps demystify MG technology for those who might implement similar systems in real life. We hope our work provides a practical starting point for engineers, policymakers, and community leaders considering renewable MGs as solutions for energy access challenges. There's still much work to be done. Our model has limitations, particularly in regards to real time power distribution controls to perfectly control non renewable vs renewable resources mix and long-term battery configurations. Future research could enhance these aspects while exploring financing mechanisms that make initial capital costs more manageable for resource-constrained communities, including targeted UN economical support mechanisms. In closing, we've learned that renewable MGs aren't just technically possible, they're increasingly practical solutions for communities living beyond the reach of traditional power grids. By sharing our findings and methodology, we hope to contribute, even in a small way, to expanding sustainable energy access where it's needed most.

## References

- [i] World Bank, "Access to electricity (% of population) - South Sudan," World Bank, 2023. Available: <https://data.worldbank.org/indicator/EG.ELC.ACCTS.ZS?locations=SS>.
- [ii] U.S. Department of Energy, "The U.S. Department of Energy's Microgrid Initiative," U.S. Department of Energy. Available: <https://www.energy.gov/sites/prod/files/2016/06/f32/The%20US%20Department%20of%20Energy's%20Microgrid%20Initiative.pdf>.
- [iii] Duke Energy, "Three Types of Microgrids," Duke Energy. Available: <https://energyservices.duke-energy.com/resources/three-types-of-microgrids/>.
- [1] A. McGrath and A. Gomstyn "What is a microgrid?" *IBM*, Available: <https://www.ibm.com/topics/microgrid>.
- [2] R. Broderick, B. Garcia, S. Horn, and M. Lave, "Microgrid Conceptual Design Guidebook" Sandia National Laboratories, March 2022. Available: [Microgrid Conceptual Design Guidebook | March 2022](#).
- [3] National Renewable Energy Laboratory, "Microgrids," *NREL*, Available: <https://www.nrel.gov/grid/microgrids.html>.
- [4] ScienceDirect, "Islanded Microgrid," *ScienceDirect*, Available: <https://www.sciencedirect.com/topics/engineering/islanded-microgrid>.
- [5] M. Siira, "Interconnection, interoperability for integration in the smart grid," *CSE Magazine*, Mar. 2014. Available: <https://www.csemag.com/articles/interconnection-interoperability-for-integration-in-the-smart-grid/>.
- [6] Transmission and Distribution Committee of the IEEE Power and Energy Society, "IEEE Guide for Distributed Energy Resources Management Systems (DERMS) Functional Specification," IEEE Apr. 2021. Available: <https://ieeexplore.ieee.org/stamp/stamp.jsp?tp=&arnumber=9447316&tag=1>
- [7] IEEE Standards Association, "How to Manage Distributed Energy Resources More Effectively," *IEEE Beyond Standards*, July 2021. Available: <https://standards.ieee.org/beyond-standards/how-to-manage-distributed-energy-resources-more-effectively/>.

[8] U.S. Department of Energy, "Microgrid Program Strategy," *Office of Electricity*, Available: <https://www.energy.gov/oe/microgrid-program-strategy>.

[9] SMA Solar Technology AG, "Solar Inverters," *SMA*, Available: <https://www.sma.de/en/products/solar-inverters>.

[10] SolarEdge Technologies, "PV Inverter," *SolarEdge*, Available: <https://www.solaredge.com/products/pv-inverter/>.

[11] National Renewable Energy Laboratory, "Power Electronics and Inverters," *NREL*, Available: <https://www.nrel.gov/grid/power-electronics-inverters.html>.

[12] Schneider Electric, "Telemetry and Remote SCADA Systems," *Schneider Electric*, Available: <https://www.se.com/us/en/product-category/6000-telemetry-and-remote-scada-systems/>.

[13] DNP Users Group, "New Standard Communication Model Enables Grid Operators to Enhance Performance, Value of Distributed Energy Resources," Electric Power Research Institute, DNP, Mesa, and Sunspec, Jan. 2019. Available: [https://www.dnp.org/Portals/0/Public%20Documents/PR%201112%20App%20Note%20Press%20Release\\_2019-01-14\\_FINAL.pdf](https://www.dnp.org/Portals/0/Public%20Documents/PR%201112%20App%20Note%20Press%20Release_2019-01-14_FINAL.pdf).

[14] International Electrotechnical Commission, "Find out more about IEC 61850," *IEC*, Available: <https://iec61850.dvl.iec.ch>.

[15] Siemens, "Grid Control," *Siemens*, Available: <https://www.siemens.com/us/en/products/energy/grid-software/operation/grid-control.html>.

[16] Digi International, "Digi ConnectPort X2 Gateway," *Digi*, Available: <https://hub.digi.com/support/products/digi-xbee/digi-connectport-x2-gateway/>.

[17] The Things Industries, "Laird Sentrius Gateway," *The Things Industries*, Available: <https://www.thethingsindustries.com/docs/gateways/models/laird-sentrius/>.

[18] A. Elgargouri, M. M. Elfituri and M. Elmusrati, "IEC 61850 and smart grids," *2013 3rd International Conference on Electric Power and Energy Conversion Systems*, Istanbul, Turkey, 2013, pp. 1-6, doi: [10.1109/EPECS.2013.6713080](https://doi.org/10.1109/EPECS.2013.6713080).

[19] M. T. Lawder *et al.*, "Battery Energy Storage System (BESS) and Battery Management System (BMS) for Grid-Scale Applications," in *Proceedings of the IEEE*, vol. 102, no. 6, pp.

1014-1030, June 2014, doi: [10.1109/JPROC.2014.2317451](https://doi.org/10.1109/JPROC.2014.2317451).

[20] Power Sonic, "Battery Energy Storage System Components," *Power Sonic*, Available: <https://www.power-sonic.com/blog/battery-energy-storage-system-components/>.

[21] NorCal Controls, "How Battery Energy Storage Systems (BESS) Integrate with SCADA," *NorCal Controls*, Nov. 2021. Available: <https://blog.norcalcontrols.net/how-battery-energy-storage-systems-bess-integrate-with-scada>.

[22] L. Paulk, "Components of an Energy Storage System," *Energy Toolbase*, July 2023. Available: <https://www.energytoolbase.com/blog/energy-storage/components-of-an-energy-storage-system/>.

[23] Energy Education, "Distribution Grid," *Energy Education*. Available: [https://energyeducation.ca/encyclopedia/Distribution\\_grid#cite\\_ref-prime\\_2-0](https://energyeducation.ca/encyclopedia/Distribution_grid#cite_ref-prime_2-0).

[24] R. Ivins, "What Are Relays, CTs, & PTs?" *Pure Power*, Apr. 2023. Available: <https://www.purepower.com/blog/what-are-relays-cts-pt#:~:text=A%20relay%20monitors%20the%20current,Utility's%20grid>.

[25] Eaton, "Fundamentals of Reclosers," *Eaton*, Available: <https://www.eaton.com/us/en-us/products/medium-voltage-power-distribution-control-systems/reclosers/reclosers--fundamentals-of-reclosers.html#:~:text=A%20recloser%20is%20an%20automatic,such%20as%20a%20short%20circuit>.

[26] Eaton, "Fundamentals of Circuit Breakers," *Eaton*, Available: <https://www.eaton.com/us/en-us/products/electrical-circuit-protection/circuit-breakers/circuit-breakers-fundamentals.html#:~:text=A%20circuit%20breaker%20is%20an,protective%20relays%20detect%20a%20fault>.

[27] KateR, "What is the Difference Between Rectifiers and Converters?" *Visicomm Industries*, Mar. 2024. Available: <https://50hz.com/what-is-the-difference-between-rectifiers-and-converters/#:~:text=What%20Are%20Converters?,functions%20of%20converters%20beyond%20rectification>.

[28] E. Csanyil, "What is Distribution Substation and its main components," *Electrical Engineering Portal*, Feb. 2018 Available: <https://electrical-engineering-portal.com/distribution-substation>.

[29] Rabert T., "Essential Components of an Electrical Substation," *Forum Electrical.com*, Available:

<https://forumelectrical.com/essential-components-of-an-electrical-substation/#htoc-13-capacitor-bank>.

[30] Cummins, "Microgrid Control," *Cummins*, Available:  
<https://www.cummins.com/generators/microgrid-control>.

[31] J. Carson, "What Are the Main Components of SCADA Systems?" *Pacific Blue Engineering*, Available:  
<https://pacificblueengineering.com/what-are-main-components-scada-systems/>.

[32] Eltel Networks, "The Role of Geographic Information System (GIS) in the Electric Power Industry," *Eltel Networks*, Available:  
<https://www.eltenetworks.pl/pl-en/blog/2024/role-geographic-information-system-gis-electric-power-industry/#:~:text=In%20addition%2C%20the%20use%20of,maintain%20and%20use%20paper%20documentation>.

[33] Md Shafiullah, Syed Masiur Rahman, Md. Golam Mortoja, Baqer Al-Ramadan, "Role of Spatial Analysis Technology in Power System Industry: An Overview," *Renewable and Sustainable Energy Reviews*, vol. 66, pp. 584–595, Dec. 2016.  
<https://doi.org/10.1016/j.rser.2016.08.017>

[34] Wi-SUN Alliance, "Field Area Networks (FAN)," *Wi-SUN Alliance*, Available:  
[https://wi-sun.org/fan/#:~:text=FAN%20\(Field%20Area%20Networks\)%20provide,Wi%2DSUN%20Alliance%20member%20companies](https://wi-sun.org/fan/#:~:text=FAN%20(Field%20Area%20Networks)%20provide,Wi%2DSUN%20Alliance%20member%20companies).

[35] Wikipedia, "Backhaul (telecommunications)," *Wikipedia*, Available:  
[https://en.wikipedia.org/wiki/Backhaul\\_\(telecommunications\)](https://en.wikipedia.org/wiki/Backhaul_(telecommunications)).

[36] Tata Communications, "What is a core network and how does it work" *Tata Communications*, Nov. 2024. Available:  
<https://www.tatacommunications.com/knowledge-base/network-core-network-explained/>.

[37] Cloudflare, "What is a Subnet?" *Cloudflare*, Available:  
<https://www.cloudflare.com/learning/network-layer/what-is-a-subnet/>.

[38] Amazon Web Services, "What is a WAN (Wide Area Network)?" *Amazon Web Services*, Available:  
[https://aws.amazon.com/what-is/wan/#:~:text=A%20wide%2Darea%20network%20\(WAN,and%20their%20uses%20and%20benefits](https://aws.amazon.com/what-is/wan/#:~:text=A%20wide%2Darea%20network%20(WAN,and%20their%20uses%20and%20benefits).

[39] Cisco Systems, "Field Area Network (FAN) 2.0," *Cisco Systems*. Available:  
<https://www.cisco.com/c/en/us/td/docs/solutions/Verticals/Utilities/FAN/2-0/CU-FAN-2-DIG/CU>

[-FAN-2-DIG1.html#65859.](#)

- [40] Cisco Systems, "1000 Series Connected Grid Routers," *Cisco Systems*, Feb. 2021. Available: [https://www.cisco.com/c/en/us/products/collateral/routers/1000-series-connected-grid-routers/datasheet\\_c78-696278.html](https://www.cisco.com/c/en/us/products/collateral/routers/1000-series-connected-grid-routers/datasheet_c78-696278.html).
- [41] S. E. Eyimaya and N. Altin, "Microgrids: definitions, architecture, and control strategies," in *Power Electronics Converters and Their Control for Renewable Energy Applications*, A. Fekik, M. Ghanes, and H. Denoun, Eds. Academic Press, 2023. <https://doi.org/10.1016/B978-0-323-91941-8.00008-1>.
- [42] National Renewable Energy Laboratory (NREL), "Energy storage for microgrids: Benefits and technical insights," *NREL*, Jan. 2013. <https://www.nrel.gov/docs/fy13osti/58703.pdf>.
- [43] M. Marzband, F. Azarinejadian, M. Savaghebi and J. M. Guerrero, "An Optimal Energy Management System for Islanded Microgrids Based on Multiperiod Artificial Bee Colony Combined With Markov Chain," in IEEE Systems Journal, vol. 11, no. 3, pp. 1712-1722, Sept. 2017, doi: [10.1109/PSCE.2011.5772451](https://doi.org/10.1109/PSCE.2011.5772451).
- [44] National Renewable Energy Laboratory (NREL), "Microgrid controls: Advancements, challenges, and future directions," *NREL*, Apr. 2022. <https://www.nrel.gov/docs/fy22osti/80583.pdf>.
- [45] "IEEE Guide for Smart Grid Interoperability of Energy Technology and Information Technology Operation with the Electric Power System (EPS), End-Use Applications, and Loads," in IEEE Std 2030-2011 , vol., no., pp.1-126, 10 Sept. 2011, doi: 10.1109/IEEESTD.2011.6018239: [10.1109/TPWRS.2006.873018](https://doi.org/10.1109/TPWRS.2006.873018).
- [46] E. -K. Lee, R. Gadh and M. Gerla, "Energy Service Interface: Accessing to Customer Energy Resources for Smart Grid Interoperation," in IEEE Journal on Selected Areas in Communications, vol. 31, no. 7, pp. 1195-1204, July 2013, doi: [10.1109/JSAC.2013.130704](https://doi.org/10.1109/JSAC.2013.130704).
- [47] Tesla, "Opticaster: Tesla's real-time energy optimization software," Tesla, 2024. Available: <https://www.tesla.com/support/energy/tesla-software/opticaster>.
- [48] Schweitzer Engineering Laboratories, "Power management solutions," SEL, 2024. Available: <https://selinc.com/engineering-services/power-management/>.
- [49] ComAp, "InteliNeo 6000: Microgrid controller," ComAp, 2024. Available: <https://na.comap-control.com/products/controllers/microgrid-controllers/intelineo/intelineo-6000/>.

- [50] M. Uddin, H. Mo, D. Dong, S. Elsawah, J. Zhu, and J. M. Guerrero, "Microgrids: A review, outstanding issues and future trends," *Energy Strategy Reviews*, vol. 49, p. 101127, 2023. Available: <https://doi.org/10.1016/j.esr.2023.101127>.
- [51] T. Adefarati and R. C. Bansal, "Reliability, economic and environmental analysis of a microgrid system in the presence of renewable energy resources," *Appl. Energy*, vol. 236, pp. 1089–1114, Feb. 2019. doi: [10.1016/j.apenergy.2018.12.050](https://doi.org/10.1016/j.apenergy.2018.12.050).
- [52] M. Issa, H. Ibrahim, R. Lepage, and A. Ilinca, "A review and comparison on recent optimization methodologies for diesel engines and diesel power generators," *Energy and Power Engineering*, vol. 11, no. 3, pp. 103-116, 2023. doi: [10.4236/epe.2023.113009](https://doi.org/10.4236/epe.2023.113009).
- [53] Z. N. Ndalloka, H. V. Nair, S. Alpert, and C. Schmid, "Solar photovoltaic recycling strategies," *Solar Energy*, vol. 270, p. 112379, 2024. doi: [10.1016/j.solener.2024.112379](https://doi.org/10.1016/j.solener.2024.112379).
- [54] International Renewable Energy Agency (IRENA), *Renewable Capacity Highlights 2024*, IRENA, Mar. 2024. Available: [https://www.irena.org/-/media/Files/IRENA/Agency/Publication/2024/Mar/IRENA\\_RE\\_Capacity\\_Highlights\\_2024.pdf](https://www.irena.org/-/media/Files/IRENA/Agency/Publication/2024/Mar/IRENA_RE_Capacity_Highlights_2024.pdf).
- [55] U.S. Department of Energy, "Photovoltaics," Energy.gov. Available: <https://www.energy.gov/eere/solar/photovoltaics>.
- [56] Sandia National Laboratories, "Irradiance & Insolation," PVPMC. Available: <https://pvpmc.sandia.gov/modeling-guide/1-weather-design-inputs/irradiance-insolation/>.
- [57] J. Vickerman, "What is solar irradiance and how is it measured?," RatedPower. Available: <https://ratedpower.com/glossary/solar-irradiance/>.
- [58] Feleke, S., Anteneh, D., Pydi, B., Satish, R., El-Shahat, A., & Abdelaziz, A. Y. (2023). Feasibility and Potential Assessment of Solar Resources: A Case Study in North Shewa Zone, Amhara, Ethiopia. *Energies*, 16(6), 2681. <https://doi.org/10.3390/en16062681>
- [59] U.S. Department of Energy, "Solar Energy Supply Chain Report," U.S. Department of Energy, Washington, D.C., Feb. 2022. Available: <https://www.energy.gov/sites/default/files/2022-02/Solar%20Energy%20Supply%20Chain%20Report%20-%20Final.pdf>.
- [60] National Institute of Building Sciences, "Photovoltaics," Whole Building Design Guide (WBDG). Available: <https://www.wbdg.org/resources/photovoltaics>.

- [61] U.S. Department of Energy, "Solar Performance and Efficiency," Energy.gov, [Online]. Available: <https://www.energy.gov/eere/solar/solar-performance-and-efficiency>.
- [62] Enel X, "Solar Panel Efficiency: what is it?" Enel X. Available: <https://corporate.enelx.com/en/question-and-answers/are-solar-panels-energy-efficient>.
- [63] B. Layton, "A Comparison of Energy Densities of Prevalent Energy Sources in Units of Joules Per Cubic Meter," Drexel University. Available: [https://drexel.edu/~media/Files/greatworks/pdf\\_sum10/WK8\\_Layton\\_EnergyDensities.ashx](https://drexel.edu/~media/Files/greatworks/pdf_sum10/WK8_Layton_EnergyDensities.ashx).
- [64] T. Farmer, "How much does Solar Farm Cost?," homeguide. Available: <https://homeguide.com/costs/solar-farm-cost>. [Accessed: 17-Feb-2025].
- [65] J. Marsh, "Solar Farms: What are they and how much do they cost?," EnergySage. Available: <https://www.energysage.com/community-solar/solar-farms-start-one/>.
- [66] L. Bongard, "How Much Does a Solar Farm Cost to Install?" Angi. Available: <https://www.angi.com/articles/cost-solar-farm.htm>.
- [67] Eyeradio, "Gov't to Install \$150 Million Hyper Solar Power in Juba." Available: [https://www.eyeradio.org/govt-to-install-150-million-hyper-solar-power-in-juba/#google\\_vignette](https://www.eyeradio.org/govt-to-install-150-million-hyper-solar-power-in-juba/#google_vignette).
- [68] V. Ramasamy, J. Zuboy, E. O'Shaughnessy, D. Feldman, J. Desai, M. Woodhouse, P. Basore, & R. Margolis, "U.S. Solar Photovoltaic System and Energy Storage Cost Benchmarks, With Minimum Sustainable Price Analysis: Q1 2022," NREL. Available: <https://www.nrel.gov/docs/fy22osti/83586.pdf>.
- [69] O. Benny, "Solar Project Types: Utility-Scale, Commercial, Residential," Targray. Available: <https://www.targray.com/media/articles/solar-project-types#:~:text=The%20most%20common%20types%20of.corporate%20organizations%20and%20industrial%20plants>.
- [70] International Renewable Energy Agency (IRENA), "Renewable Power Generation Costs in 2022," IRENA, Aug. 2023. Available: <https://www.irena.org/Publications/2023/Aug/Renewable-Power-Generation-Costs-in-2022>.
- [71] R. Kennedy, "Solar LCOE now 29% lower than any fuel fossil option, says EY," PV Magazine, Dec. 8, 2023. [Online]. Available: <https://www.pv-magazine.com/2023/12/08/solar-lcoe-now-29-lower-than-any-fuel-fossil-option-says-ey/>.

[72] Lazard, "Lazard's Levelized Cost of Energy Analysis," Lazard, Apr. 2023. Available: <https://www.lazard.com/media/2ozoovyg/lazards-lcoeplus-april-2023.pdf>.

[73] S. Ong, C. Campbell, P. Denholm, R. Margolis, & G. Heath, "Land-Use Requirements for Solar Power Plants in the United States," NREL, Jul. 2013. Available: <https://www.nrel.gov/docs/fy13osti/56290.pdf>.

[74] PVcase team, "Solar Plant Design Guide: The Basics," PVcase. Available: <https://pvcase.com/blog/solar-plant-design-guide-the-basics/>.

[75] BAI Group LLC, "11 Civil Engineering Considerations for Developing a Large Solar Array," BAI Group LLC. Available: <https://baigroupllc.com/11-civil-engineering-considerations-for-developing-a-large-solar-array/>.

[76] ESA Solar, "Solar Farms: What Are They & How Do They Work?" ESA Solar, Aug. 2018. <https://esa-solar.com/solar-farms-what-are-they-how-do-they-work/#:~:text=How%20long%20does%20it%20take,for%202%20to%203%20decades>.

[77] Coldwell Solar, "How Much Investment Do You Need for a Solar Farm?" Coldwell Solar, [Online]. Available: <https://coldwellsolar.com/commercial-solar-blog/how-much-investment-do-you-need-for-a-solar-farm/#:~:text=2,,three%20to%20four%20times%20yearly>.

[78] N. Santhanam, "Timelines of a MW Solar Project Installation in India," Solar Mango, Dec. 2015. Available: <https://www.solarmango.com/2015/12/14/timelines-of-a-mw-solar-project-installation-in-india/>.

[79] Solair World, "How Long Does It Take to Build a Solar Power Plant?" Solair World. Available: <https://solairworld.com/how-long-does-it-take-to-build-a-solar-power-plant/>.

[80] OYA Renewables, "How Long Does It Take to Develop and Construct a Solar Farm?" OYA Renewables. Available: <https://oyarenewables.com/faq/how-long-does-it-take-to-develop-and-construct-a-solar-farm/>.

[81] Amatrol, "Solar Energy Training," Amatrol. Available: <https://amatrol.com/product/program-solar-technology/>.

[82] NREL, "Concentrating Solar Power," NREL. Available: <https://www.nrel.gov/research/re-csp.html>.

[83] International Renewable Energy Agency (IRENA), "Concentrating Solar Power," IRENA, Jan. 2013. Available:  
<https://www.irena.org/-/media/Files/IRENA/Agency/Publication/2013/IRENA-ETSAP-Tech-Brief-E10-Concentrating-Solar-Power.pdf>.

[84] Solar Power Authority Staff, "High-Temperature Solar Thermal Technology: An Overview and Evaluation," Solar Power Authority. Available:  
<https://www.solarpowerauthority.com/high-temperature-solar-thermal/>.

[85] Solar Power Engineering, "NREL: This parabolic trough 73% efficient," Solar Power World. Available:  
<https://www.solarpowerworldonline.com/2010/09/nrel-says-skyfuels-parabolic-troughs-are-73-efficient/>.

[86] M. Radovic, "Chapter 4: Efficiency of Energy Conversion," Penn State University. Available: <https://personal.ems.psu.edu/~radovic/Chapter4.pdf>.

[87] NREL, "Consider Installing High-Pressure Boilers with Backpressure Turbine-Generators," NREL, Jan. 2006. Available: <https://www.nrel.gov/docs/fy06osti/39324.pdf>.

[88] Bureau of Meteorology, "Solar Energy," Australian Government. Available:  
<https://www.sws.bom.gov.au/Educational/2/1/12>.

[89] J. Burkhardt, G. Heath, C. Turchi, "Life Cycle Assessment of a Parabolic Trough Concentrating Solar Power Plant and the Impacts of Key Design Alternatives," *Environmental Science & Technology*, vol. 45, Feb. 2011, doi: [10.1021/es1033266](https://doi.org/10.1021/es1033266).

[90] U.S. Department of Energy, "Solar Parabolic Trough," U.S. Department of Energy, 2009. Available: [https://www1.eere.energy.gov/ba/pba/pdfs/solar\\_trough.pdf](https://www1.eere.energy.gov/ba/pba/pdfs/solar_trough.pdf).

[91] Australian Academy of Science, "Concentrating solar thermal." Available:  
<https://www.science.org.au/curious/technology-future/concentrating-solar-thermal#:~:text=The%20fact%20that%20the%20system%20only%20needs,can%20be%20stored%20in%20a%20moltene%20salt>.

[92] A. Ahmad, O. Prakash, R. Kausher, G. Kumar, S. Pandey, and S. M. M. Hasnain, "Parabolic trough solar collectors: A sustainable and efficient energy source," *Mater. Sci. Energy Technol.*, vol. 7, pp. 99-106, 2024. Available: <https://doi.org/10.1016/j.mset.2023.08.002>.

[93] National Renewable Energy Laboratory, "2023 Concentrating Solar Power," *Annual Technology Baseline (ATB)*, 2023. Available:  
[https://atb.nrel.gov/electricity/2023/concentrating\\_solar\\_power#PDK6P7LE](https://atb.nrel.gov/electricity/2023/concentrating_solar_power#PDK6P7LE).

- [94] P. Kurup, S. Glynn, and S. Akar, "Manufacturing Cost Analysis of Advanced Parabolic Trough Collector," NREL, 2020. Available: <https://www.nrel.gov/docs/fy21osti/77829.pdf>.
- [95] Solar Energy International (SEI), "SEI Solar Professionals Certificate Program," SEI. Available: <https://www.solarenergy.org/sei-solar-professionals-certificate-program/>.
- [96] Solar Energy International (SEI), "Solar Training Tools, Techniques, Operation & Maintenance (Online)," Solar Energy International, [Online]. Available: <https://www.solarenergy.org/courses/solar-training-tools-techniques-operation-maintenance-online/>.
- [97] Climate Central, "A Decade of U.S. Wind Growth, 2024," Climate Central. Apr. 2024. Available: <https://www.climatecentral.org/climate-matters/a-decade-of-us-wind-growth-2024>.
- [98] Center for Sustainable Systems, University of Michigan, "Wind Energy Factsheet," Center for Sustainable Systems. Available: <https://css.umich.edu/publications/factsheets/energy/wind-energy-factsheet>.
- [99] W. Cao, N. Xing, Y. Wen, X. Chen, and D. Wang, "New adaptive control strategy for a wind turbine permanent magnet synchronous generator (PMSG)," *Inventions*, vol. 6, no. 1, p. 3, 2021. [Online]. Available: <https://doi.org/10.3390/inventions6010003>.
- [100] U.S. Environmental Protection Agency, "Renewable Energy Fact Sheet: Wind Turbines," U.S. Environmental Protection Agency, Aug. 2013. Available: [https://www.epa.gov/sites/default/files/2019-08/documents/wind\\_turbines\\_fact\\_sheet\\_p100i18k.pdf](https://www.epa.gov/sites/default/files/2019-08/documents/wind_turbines_fact_sheet_p100i18k.pdf).
- [101] WeatherGuard Wind, "Wind Turbine Cost: How Much? Are They Worth It in 2025?" WeatherGuard Wind, Jun. 2024. Available: <https://weatherguardwind.com/how-much-does-wind-turbine-cost-worth-it/>.
- [102] HomeGuide, "How much does a wind turbine cost," HomeGuide. Available: <https://homeguide.com/costs/wind-turbine-cost>.
- [103] T. Bridgewater, "Review Biomass for Energy," *J. Sci. Food Agric.*, vol. 86, pp. 1755–1767, 2006. Available: <https://scijournals.onlinelibrary.wiley.com/doi/pdf/10.1002/jsfa.2605>.
- [104] U.S. Department of Energy, "Biomass Resources," U.S. Department of Energy. Available: <https://www.energy.gov/eere/bioenergy/biomass-resources>.
- [105] M. A. Helal, N. Anderson, Y. Wei, and M. Thompson, "A Review of Biomass-to-Bioenergy Supply Chain Research Using Bibliometric Analysis and Visualization," *Energies*, vol. 16, no. 3, p. 1187, 2023. Available: <https://doi.org/10.3390/en16031187>.

[106] U.S. Department of Energy, "Microhydropower systems," U.S. Department of Energy. Available: <https://www.energy.gov/energysaver/microhydropower-systems>.

[107] R. Syahputra and I. Soesanti, "Renewable energy systems based on micro-hydro and solar photovoltaic for rural areas: A case study in Yogyakarta, Indonesia," *Energy Reports*, vol. 7, pp. 472-490, 2021, doi: [10.1016/j.egyr.2021.01.015](https://doi.org/10.1016/j.egyr.2021.01.015).

[108] U.S. Department of Energy, "Geothermal basics," U.S Department of Energy. Available: <https://www.energy.gov/eere/geothermal/geothermal-basics>.

[109] A. Rezaee Jordehi, "Scheduling heat and power microgrids with storage systems, photovoltaic, wind, geothermal power units and solar heaters," *Journal of Energy Storage*, vol. 41, 2021, art. no. 102996, ISSN 2352-152X, <https://doi.org/10.1016/j.est.2021.102996>.

[110] U.S. Department of Energy, "How lithium-ion batteries work," U.S Department of Energy. Available: <https://www.energy.gov/energysaver/articles/how-lithium-ion-batteries-work>.

[111] Thundersaid Energy, "Lithium-ion batteries: energy density?" Available: <https://thundersaidenergy.com/downloads/lithium-ion-batteries-energy-density/>.

[112] Bioenno Power, "The pros and cons of lithium-ion batteries: A deep dive." Available: <https://www.bioennopower.com/blogs/news/the-pros-and-cons-of-lithium-ion-batteries-a-deep-dive?srsltid=AfmBOopFaoiKEmt-AOJkvwzd5V6mGrY6Hpd84WZKSx8HUEcd6rm5cCVs>.

[113] Polinovel, "Energy Density vs Power Density: What's Their Differences?" Polinovel Group. Available: <https://www.polinovelgroup.com/energy-density-vs-power-density-differences/>.

[114] Choose Solar, "What is the typical lifespan of Lithium-ion battery?" Choose Solar Australia. Available: <https://www.choosesolar.com.au/typical-lifespan-lithium-ion-battery/>.

[115] DNK Power, "Myth or Fact: Lithium-ion batteries self-discharge after being fully charged," DNK Power. Available: <https://www.dnkpower.com/myth-or-fact-lithium-ion-batteries-self-discharge/>.

[116] University of Michigan, "Tips for extending the lifetime of lithium-ion batteries," *Michigan News*. Available: <https://news.umich.edu/tips-for-extending-the-lifetime-of-lithium-ion-batteries/>.

[117] Tektronix, "Lithium-ion battery maintenance guidelines," *Tektronix*. Available: <https://www.tek.com/en/documents/technical-brief/lithium-ion-battery-maintenance-guidelines>.

[118] Battery University, "BU-808c: Coulombic and energy efficiency with the battery," *Battery University*. Available:  
<https://batteryuniversity.com/article/bu-808c-coulombic-and-energy-efficiency-with-the-battery>.

[119] Lawn Love, "How much does a Lithium-ion battery cost in 2025?" *Lawn Love*. Available:  
<https://lawnlove.com/blog/lithium-ion-battery-cost/#hours>.

[120] National Renewable Energy Laboratory, "Pumped Storage Hydropower," *NREL Annual Technology Baseline 2022*. Available:  
[https://atb.nrel.gov/electricity/2022/pumped\\_storage\\_hydropower#LJT3875Dv](https://atb.nrel.gov/electricity/2022/pumped_storage_hydropower#LJT3875Dv).

[121] Fuel Cell and Hydrogen Energy Association, "Fuel Cells," *FCHEA*. Available:  
<https://www.fchea.org/fuelcells>.

[122] CAS, "Lithium-ion batteries vs Hydrogen fuel cells: Which are more promising?," *CAS Insights*. Available:  
<https://www.cas.org/resources/cas-insights/lithium-batteries-hydrogen-fuel-cells#:~:text=Lithium%20Dion%20batteries%20vs%20Hydrogen,be%20used%20in%20the%20future>.

[123] A.G. Olabi, T. Wilberforce, M. Ramadan, M.A. Abdelkareem, A.H. Alami, "Compressed air energy storage systems: Components and operating parameters – A review," *Journal of Energy Storage*, vol. 34, 2021, 102000, ISSN 2352-152X,  
<https://doi.org/10.1016/j.est.2020.102000>.

[124] International Energy Agency, "Access to electricity," *SDG7: Data and Projections*. Available: <https://www.iea.org/reports/sdg7-data-and-projections/access-to-electricity>.

[125] E. Chen, F. McCrone, and D. Mozersky, "Renewable energy and the United Nations: A Green Spark for Peace in South Sudan." *Stimson Center*, Feb. 13, 2023. Available:  
[https://www.stimson.org/wp-content/uploads/2023/02/Stimson\\_RenewableEnergy\\_Feb13-1.pdf](https://www.stimson.org/wp-content/uploads/2023/02/Stimson_RenewableEnergy_Feb13-1.pdf).

[126] World Bank, "World Bank support for renewable energy projects," *World Bank*, Mar. 2023. Available:  
<https://documents1.worldbank.org/curated/en/099224503082327543/pdf/P17889107ed356060831d0a278ac8c3e34.pdf>.

[127] NASA Langley Research Center, "Power Data Access Viewer," *NASA*, 2023. Available:  
<https://power.larc.nasa.gov/data-access-viewer/>.

[128] S. Feleke, D. Anteneh, B. Pydi, R. Satish, A. El-Shahat, and A. Y. Abdelaziz, "Feasibility and potential assessment of solar resources: A case study in North Shewa Zone, Amhara,

Ethiopia," *Energies*, vol. 16, no. 6, p. 2681, 2023. Available: <https://doi.org/10.3390/en16062681>.

[129] RECOSS, "Technologies we are promoting," *RECOSS.org*. Available: <https://www.recooss.org/technologies-we-are-promoting/>.

[130] International Organization for Migration (IOM), "South Sudan — Population Count, Juba IDP Camp 1, August 2024," *Displacement Tracking Matrix*. Available: <https://dtm.iom.int/reports/south-sudan-population-count-juba-idp-camp-1-august-2024?close=true>.

[131] U.S. Energy Information Administration (EIA), "Where wind power is harnessed," *Energy Explained*. Available: <https://www.eia.gov/energyexplained/wind/where-wind-power-is-harnessed.php>.

[132] ESMAP, "Multi-Tier Framework for Energy Access," *The World Bank*. Available: [https://www.esmap.org/mtf\\_multi-tier\\_framework\\_for\\_energy\\_access](https://www.esmap.org/mtf_multi-tier_framework_for_energy_access).

[133] IOM, "South Sudan — Bentiu IDP Camp Population Count — August 2024," *Displacement Tracking Matrix*. Available: <https://dtm.iom.int/reports/south-sudan-bentiu-idp-camp-population-count-august-2024?close=true>.

[134] IOM, "South Sudan — Bentiu PoC Site Population Count — October 2020," *Displacement Tracking Matrix*. Available: <https://dtm.iom.int/reports/south-sudan-%E2%80%94-bentiu-poc-site-population-count-october-2020>.

[135] Enel Green Power, "Energy Access Tiers," *Enel Green Power*. Available: <https://www.enelgreenpower.com/learning-hub/gigawhat/search-articles/articles/2023/01/energy-access-tiers>.

[136] International Organization for Migration (IOM), "Photo story: Flood response in Bentiu, South Sudan," *IOM*. Available: <https://eastandhornofafrica.iom.int/stories/photo-story-flood-response-bentiu-south-sudan>.

[137] Topographic Map, "Bentiu," *Topographic Map*. Available: <https://en-us.topographic-map.com/map-vczf51/Bentiu/?center=9.10976%2C29.71416>.

[138] J.V. Sutcliffe and Y.P. Parks, "The Hydrology of the Nile: Chapter 6," 1999, *IAHS*. Available: <https://iahs.info/uploads/dms/16942.chapter6.pdf>.

[139] D. Mozersky and D. Kammen, "South Sudan's Renewable Energy Potential: A Building Block for Peace," *United States Institute of Peace*, Jan. 2018. Available: <https://www.usip.org/sites/default/files/2018-01/sr418-south-sudans-renewable-energy-potential-a-building-block-for-peace.pdf>.

[140] United Nations Peacekeeping, "The Green Bentiu Initiative: Pakistani Peacekeepers Encourage Planting Hope Amid Climate Shocks," *United Nations Peacekeeping*. Available: <https://peacekeeping.un.org/en/green-bentiu-initiative-pakistani-peacekeepers-encourage-planting-hope-amid-climate-shocks>.

[141] A. Finn, J. Goltz, M. Saidi, and A. Sharma, "Job Outcomes in the Towns of South Sudan: Jobs, Recovery, and Peace Building in Urban South Sudan - Technical Report I," *World Bank Group Jobs*, 2020. Available: <https://openknowledge.worldbank.org/server/api/core/bitstreams/28a9e2be-cd66-5d85-92ef-150411b578e5/content>

[142] United Nations Peacekeeping, "South Sudan: Protection of civilians sites are transitioning into internally displaced persons camps," *UN Peacekeeping*. Available: <https://peacekeeping.un.org/en/south-sudan-protection-of-civilians-sites-are-transitioning-internally-displaced-persons-camps>.

[143] Central Intelligence Agency, "South Sudan," *The World Factbook*. Available: <https://www.cia.gov/the-world-factbook/countries/south-sudan/#:~:text=Since%20independence%2C%20South%20Sudan%20has,political%20conflict%2C%20and%20communal%20violence>.

[144] Conflict Sensitivity Resource Facility, "Wau County Profile," *CSRF South Sudan*. Available: [https://www.csrf-southsudan.org/county\\_profile/wau/#:~:text=An%20additional%20primary%20road%20runs>this%20road%20network%20is%20unknown](https://www.csrf-southsudan.org/county_profile/wau/#:~:text=An%20additional%20primary%20road%20runs>this%20road%20network%20is%20unknown).

[145] Africa Energy Portal, "South Sudan: Agreement with Cairo for the Wau Dam Feasibility Study," *Africa Energy Portal*, Jun. 2021. Available: <https://africa-energy-portal.org/news/south-sudan-agreement-cairo-wau-dam-feasibility-study#:~:text=The%20Wau%20Dam%20will%20improve,delivering%2064%20GWh%20per%20year>.

[146] International Organization for Migration (IOM), " Understanding Multidimensional Fragility in South Sudan," *IOM South Sudan*, 2023. Available: [https://southsudan.iom.int/sites/g/files/tmzbdl1046/files/documents/2023-11/20231120\\_multi\\_dimensional\\_fragility\\_ss\\_report.pdf](https://southsudan.iom.int/sites/g/files/tmzbdl1046/files/documents/2023-11/20231120_multi_dimensional_fragility_ss_report.pdf).

[147] A. Q. Jakhrani, A. R. H. Rigit, A. -K. Othman, S. R. Samo and S. A. Kamboh, "Estimation of carbon footprints from diesel generator emissions," 2012 International Conference on Green and Ubiquitous Technology, Bandung, Indonesia, 2012, pp. 78-81, doi: [10.1109/GUT.2012.6344193](https://doi.org/10.1109/GUT.2012.6344193).

[148] V. Ramanathan and Y. Feng, "Air pollution, greenhouse gases and climate change: Global and regional perspectives," *Atmospheric Environment*, Volume 43, Issue 1, 2009, Pages 37-50, ISSN 1352-2310, <https://doi.org/10.1016/j.atmosenv.2008.09.063>.

- [149] Ø. Skarstein, & K. Uhlen, "Design Considerations with Respect to Long-Term Diesel Saving in Wind/Diesel Plants." *Wind Engineering*, 13(2), 72–87, 1989, <http://www.jstor.org/stable/43749369>
- [150] HOMER Energy, "HOMER Pro Microgrid Software for Designing Optimized Hybrid Power Systems," *HOMER Energy by UL Solutions*. Available: <https://homerenergy.com/products/pro/index.html>.
- [151] K. Schneider, K. Balasubramaniam, D. Fobes, A. Moreira, V. Donde, B. Palmintier, T. Kuruganti, M. E. Ropp, and C. Liu, "Microgrid R&D Program White Papers," *Pacific Northwest National Laboratory*, Mar. 2021. Available: <https://www.energy.gov/sites/default/files/2022-09/2-T&D%20Co-simulation%20of%20Microgrid%20Impacts%20and%20Benefits.pdf>.
- [152] A. Rousis, D. Tzelepis, I. Konstantelos, C. Booth, and G. Strbac, "Design of a Hybrid AC/DC Microgrid Using HOMER Pro: Case Study on an Islanded Residential Application. *Inventions*, 3(3), 55, Aug. 2018. <https://doi.org/10.3390/inventions3030055>
- [153] HOMER Energy, "Levelized Cost of Energy," *HOMER Pro Documentation*, 2022. Available: [https://homerenergy.com/products/pro/docs/3.15/levelized\\_cost\\_of\\_energy.html](https://homerenergy.com/products/pro/docs/3.15/levelized_cost_of_energy.html).
- [154] S. Bracco, F. Delfino, P. Laiolo, L. Pagnini, and G. Piazza, "Evaluating LCOE in sustainable microgrids for smart city applications," *E3S Web of Conferences*, E3S Web of Conferences, Volume 1, 2019 <https://doi.org/10.1051/e3sconf/201911303006>.
- [155] U.S. Department of Energy, "Levelized Cost of Energy (LCOE)," *DOE Office of Indian Energy*. Available: <https://www.energy.gov/sites/prod/files/2015/08/f25/LCOE.pdf>.
- [156] T. Reber, S. Booth, D. Cutler, X. Li and J. Salasovich, "Tariff Considerations for Microgrids in Sub-Saharan Africa" *NREL*, Feb. 2018. Available: <https://www.nrel.gov/docs/fy18osti/69044.pdf>.
- [157] Afaq Alqimam Company, "Return on Investment in Energy Efficiency Projects," *LinkedIn*. Available: <https://www.linkedin.com/pulse/return-investment-energy-efficiency-projects-afaq-alqimam-company/>.
- [158] HOMER Energy, "Return on Investment," *HOMER Pro Documentation*. Available: [https://homerenergy.com/products/pro/docs/3.15/return\\_on\\_investment.html](https://homerenergy.com/products/pro/docs/3.15/return_on_investment.html).
- [159] HOMER Energy, "Renewable Penetration Metrics," *HOMER Pro Documentation*. Available: [https://homerenergy.com/products/pro/docs/3.15/renewable\\_penetration\\_metrics.html](https://homerenergy.com/products/pro/docs/3.15/renewable_penetration_metrics.html).

- [160] MathWorks, "Simscape Electrical," *MathWorks*. Available: <https://www.mathworks.com/products/simscape-electrical.html>.
- [161] R. Nanmaran, K. Mohan, R. Sindhuja, S. Srimathi, G. Gulothungan, R. Ramasamy, "Developing Simulink Model of Microgrid Energy Management System and Optimizing Electricity Cost Using Linear Optimization Approach," in *Computing Technologies for Sustainable Development*, Sivakumar, P.D., Ramachandran, R., Pasupathi, C., Balakrishnan, P., Eds., vol. 2362, *Communications in Computer and Information Science*, Springer, Cham, 2025, pp. 45-56. [https://doi.org/10.1007/978-3-031-82386-2\\_6](https://doi.org/10.1007/978-3-031-82386-2_6).
- [162] T. Prabaksorn, R. T. Naayagi and S. S. Lee, "Modelling and Simulation of Microgrid in Grid-Connected Mode and Islanded Mode," *2020 2nd International Conference on Electrical, Control and Instrumentation Engineering (ICECIE)*, Kuala Lumpur, Malaysia, 2020, pp. 1-8, doi: [10.1109/ICECIE50279.2020.9309649](https://doi.org/10.1109/ICECIE50279.2020.9309649).
- [163] MathWorks, "Subsystems," *MathWorks*. Available: <https://www.mathworks.com/help/simulink/subsystems.html>.
- [164] A. Zhang, J. Yang, Y. Luo, and S. Fan , "Forecasting the progression of human civilization on the Kardashev Scale through 2060 with a machine learning approach," *Scientific Reports*. Available: <https://www.nature.com/articles/s41598-023-38351-y>
- [165] C. Sagan, "Carl Sagan's Cosmic Connection: An Extraterrestrial Perspective." <https://books.google.com/books?id=IL57o9YB0mAC&pg=PA156#v=onepage&q&f=false>
- [166] J. LeSage, "Systems-level Microgrid Simulation from Simple One-line Diagram," *MATLAB Central File Exchange*, MathWorks, 2020. Available: <https://www.mathworks.com/matlabcentral/fileexchange/67060-systems-level-microgrid-simulation-from-simple-one-line-diagram>.
- [167] MathWorks, "SynchronousMachinePUStruct," *MATLAB Documentation*, MathWorks, 2025. Available: <https://www.mathworks.com/help/sps/powersys/ref/synchronousmachinepustandard.html>.
- [168] MathWorks, "AC1A Excitation System," *MATLAB Documentation*, MathWorks, 2025. Available: [https://www.mathworks.com/help/sps/powersys/ref/ac1aexcitationsystem.html?searchHighlight=AC1A%20Excitation%20System&s\\_tid=srchtitle\\_support\\_results\\_1\\_AC1A%20Excitation%20System](https://www.mathworks.com/help/sps/powersys/ref/ac1aexcitationsystem.html?searchHighlight=AC1A%20Excitation%20System&s_tid=srchtitle_support_results_1_AC1A%20Excitation%20System).
- [169] MathWorks, "Powergui," *MATLAB Documentation*, MathWorks, 2025. Available:

[https://www.mathworks.com/help/sps/powersys/ref/powergui.html?s\\_tid=srchttitle\\_support\\_results\\_1\\_powergui](https://www.mathworks.com/help/sps/powersys/ref/powergui.html?s_tid=srchttitle_support_results_1_powergui).

[170] MathWorks, "Transfer Fcn," *MATLAB Documentation*, MathWorks, 2025. Available: [https://www.mathworks.com/help/simulink/slref/transferfcn.html?searchHighlight=Transfer%20Fcn&s\\_tid=srchttitle\\_support\\_results\\_1\\_Transfer%20Fcn](https://www.mathworks.com/help/simulink/slref/transferfcn.html?searchHighlight=Transfer%20Fcn&s_tid=srchttitle_support_results_1_Transfer%20Fcn).

[171] MathWorks, "Connection Port," *Simscape Documentation*, MathWorks, 2025. Available: [https://www.mathworks.com/help/simscape/ref/connectionport.html?searchHighlight=Physical%20Modeling%20Connection%20Port%20block%20for%20subsystems&s\\_tid=srchttitle\\_support\\_results\\_1\\_Physical%20Modeling%20Connection%20Port%20block%20for%20subsystems](https://www.mathworks.com/help/simscape/ref/connectionport.html?searchHighlight=Physical%20Modeling%20Connection%20Port%20block%20for%20subsystems&s_tid=srchttitle_support_results_1_Physical%20Modeling%20Connection%20Port%20block%20for%20subsystems).

[172] MathWorks, "Transport Delay," *Simulink Documentation*, MathWorks, 2025. Available: [https://www.mathworks.com/help/simulink/slref/transportdelay.html?searchHighlight=Transport%20Delay&s\\_tid=srchttitle\\_support\\_results\\_1\\_Transport%20Delay](https://www.mathworks.com/help/simulink/slref/transportdelay.html?searchHighlight=Transport%20Delay&s_tid=srchttitle_support_results_1_Transport%20Delay).

[173] J. Aberilla, A. Schmid, and L. Stamford, "Design and Environmental Sustainability Assessment of Small-scale Off-grid Energy Systems for Remote Rural Communities," *Research Gate*, Nov. 2019. <http://dx.doi.org/10.1016/j.apenergy.2019.114004>

[174] MathWorks, "Three-Phase Dynamic Load," *Simscape Power Systems Documentation*, MathWorks, 2025. Available: [https://www.mathworks.com/help/sps/powersys/ref/threephasedynamicload.html?searchHighlight=Three-Phase%20Dynamic%20Load&s\\_tid=srchttitle\\_support\\_results\\_2\\_Three-Phase%20Dynamic%20Load](https://www.mathworks.com/help/sps/powersys/ref/threephasedynamicload.html?searchHighlight=Three-Phase%20Dynamic%20Load&s_tid=srchttitle_support_results_2_Three-Phase%20Dynamic%20Load).

[175] MathWorks, "Mux," *Simulink Documentation*, MathWorks, 2025. Available: [https://www.mathworks.com/help/simulink/slref/mux.html?searchHighlight=Mux&s\\_tid=srchttitle\\_support\\_results\\_1\\_Mux](https://www.mathworks.com/help/simulink/slref/mux.html?searchHighlight=Mux&s_tid=srchttitle_support_results_1_Mux).

[176] Neo Virtus, "Homepage," *Neo Virtus*, 2025. Available: <https://neovirtus.com>.

[177] Kweli, "Jinko Solar 475 Watt 24V Monocrystalline Solar Panel JKM475N-60H," *Kweli Shop*, 2025. Available: <https://kweli.shop/product/jinko-solar-475-watt-24v-monocrystalline-solar-panel-jkm475n-60h/>.

[178] National Revenue Authority, "Financial Act FY 2023/2024," *NRA South Sudan*, 2023. Available: [https://cms.nra.gov.ss/uploads/FINANCIAL\\_Act\\_FY\\_2023\\_2024\\_MAIL\\_97b32cab38.pdf](https://cms.nra.gov.ss/uploads/FINANCIAL_Act_FY_2023_2024_MAIL_97b32cab38.pdf).

[179] International Renewable Energy Agency (IRENA), *Solar PV in Africa: Costs and Markets*,

Africa50, 2016. Available:  
[https://www.africa50.com/fileadmin/uploads/africa50/Documents/Knowledge\\_Center/IRENA\\_Solar\\_PV\\_Costs\\_Africa\\_2016.pdf](https://www.africa50.com/fileadmin/uploads/africa50/Documents/Knowledge_Center/IRENA_Solar_PV_Costs_Africa_2016.pdf).

[180] "SMA Sunny Tripower CORE2 STP 110-60," Europe Solar Store. Available:  
<https://www.europe-solarstore.com/sma-sunny-tripower-core2-stp-110-60.html>

[181] ABB, "System pro E power — Main distribution boards." Available:  
<https://new.abb.com/low-voltage/products/enclosures/main-distribution-boards/system-pro-e-power>.

[182] Siemens, "600 Volt 3 Pole 4-Wire FUSIBLE Safety Switches/Disconnects — Outdoor Heavy," Direct Pivot Parts. Available:  
<https://directpivotparts.com/products/Siemens-600-Volt-3-Pole-4--Wire-FUSIBLE-Safety-SwitchesDisconnects-Outdoor-Heavy-HF362R/HF364R>.

[183] Global Sources, "Wind Turbine Generator 1000W 48V Horizontal Axis Small Wind Generator," Global Sources. Available:  
<https://www.globalsources.com/Wind-electric/Wind-Turbine-1192746823p.htm>.

[184] H. Akuiyibo, "Public-Private Partnerships in Africa: Some Lessons from Kenya's Lake Turkana Wind Power Project," Wilson Center. Available:  
<https://www.wilsoncenter.org/blog-post/public-private-partnerships-in-africa-some-lessons-from-kenyas-lake-turkana-wind-project>.

[185] Hongocean, "HongOcean: Your Gateway to Affordable Freight Shipping from China to Sudan," Hongocean. Available: <https://hongocean.com/ship-from-china-to-sudan/>.

[186] Deming Power, "China 100kW DC Power Supply AC-DC Converter with AC400V Input, DC220V Stabilized Output Voltage," Made-in-China. Available:  
<https://demingpower.en.made-in-china.com/product/MdEtrsQAcUP/China-100kw-DC-Power-Supply-AC-DC-Converter-with-AC400V-Input-DC220V-Stabilized-Output-Voltage.html>.

[187] "DC-DC Converter 200kW 850V," Zeka Labs. Available:  
<https://zekalabs.com/products/non-isolated-high-power-converters/dc-dc-converter-200kw-850v/>

[188] "Deming 200kW Bidirectional DC-DC Converter for Energy Storage Microgrid," Deming Power. Available:  
<https://demingpower.en.made-in-china.com/product/wEIrsBXbZYpR/China-Deming-200kw-Bidirectional-DC-DC-Converter-for-Energy-Storage-Microgrid.html>.

[189] "Shipping Rates from the U.S. to Africa," Nile Cargo Carrier. Available: <https://nilecargocarrier.com/shipping-rates-from-the-u-s-to-africa/>.

[190] "Atess On/Off Grid Hybrid Inverter," Alibaba. Available: [https://www.alibaba.com/product-detail/Atess-On-Off-Grid-Hybrid-Inverter\\_1600311601335.html](https://www.alibaba.com/product-detail/Atess-On-Off-Grid-Hybrid-Inverter_1600311601335.html).

[191] F. Gregor, "When Should I Replace My Solar Inverter?" The Power Facts. Available: <https://thepowerfacts.com/when-should-i-replace-my-solar-inverter/>.

[192] C. Murray, "Lithium-ion battery pack prices fall 20% in 2024 amidst fight for market share," Energy-Storage.news, Dec. 2024. Available: [https://www.energy-storage.news/lithium-ion-battery-pack-prices-fall-20-in-2024-amidst-fight-for-market-share/#:~:text=Global%20average%20lithium-ion%20battery,\(EVs\)%2C%20BloombergNEF%20said.](https://www.energy-storage.news/lithium-ion-battery-pack-prices-fall-20-in-2024-amidst-fight-for-market-share/#:~:text=Global%20average%20lithium-ion%20battery,(EVs)%2C%20BloombergNEF%20said.)

[193] "The complete guide to lithium-ion solar battery lifespan," BSL-BATT, May 2024. Available: <https://www.bsl-battery.com/news/the-complete-guide-to-lithium-ion-solar-battery-lifespan>.

[194] "1MW diesel generator with Cummins diesel engine KTA50-G3," Generators Industrial. Available: <https://www.generatorsindustrial.com/products/1mw-diesel-generator-with-cummins-diesel-engine-kta50-g3>.

[195] "Total Cost of Ownership Diesel vs. Natural Gas Generators," Genset Services. Available: [https://gensetservices.com/wp-content/uploads/2017/11/TCO- diesel\\_vs\\_natural\\_gas\\_generators.pdf](https://gensetservices.com/wp-content/uploads/2017/11/TCO- diesel_vs_natural_gas_generators.pdf).

[196] "What is the life expectancy of industrial generators?" Turnkey Industries, July 2022. Available: <https://turnkey-industries.com/what-is-the-life-expectancy-of-industrial-generators>.

[197] "ABB 100 KVAR 480V VAC 3PH CLMD 83 C488G100-RB640C Open Capacitor 1YR WARRANTY," eBay. Available: <https://www.ebay.com/itm/221376754992>.

[198] "Lifetime Estimation of Capacitors," AIC Tech Inc. Available: [https://www.aictech-inc.com/en/valuable-articles/capacitor\\_troubleshooting02c.html](https://www.aictech-inc.com/en/valuable-articles/capacitor_troubleshooting02c.html).

[199] "Optimal Capacitor Placement Costs Benefits Due to Loss Reductions," ETAP. Available: [https://etap.com/docs/default-source/white-papers/optimal-capacitor-placement-benefits.pdf?sfvrsn=9b37b27f\\_4](https://etap.com/docs/default-source/white-papers/optimal-capacitor-placement-benefits.pdf?sfvrsn=9b37b27f_4).

[200] K.T. Weaver, "Smart Meters Have Life of 5 to 7 Years," Smart Grid Awareness,

29-Oct-2015. Available:  
<https://smartgridawareness.org/2015/10/29/smart-meters-have-life-of-5-to-7-years/>.

[201] "How Much Does an Electric Meter Cost?," Outdoorsiness. Available:  
<https://outdoorsiness.com/2023/09/21/how-much-does-an-electric-meter-cost/>.

[202] "Best Parcel Courier to Juba/Nairobi (Air Freight/Road Freight)," Wakah Logistics, Aug. 2024. Available:  
<https://wakahlogistics.com/best-parcel-courier-to-juba-nairobi-air-freight-road-freight/>.

[203] M. Rhode, "Is South Sudan's Largest Land Deal a Land Grab?," The Oakland Institute. Available: <https://www.oaklandinstitute.org/south-sudans-largest-land-deal-land-grab>.

[204] T. Benn, "How to Start a Wind Farm: The Ultimate Guide," Lumify Energy, July 2024. Available: <https://lumifyenergy.com/blog/how-to-start-a-wind-farm/>.

[205] "World's biggest battery maker unveils higher density, 'nil degradation,' battery packs for grid," RenewEconomy, Apr. 2024. Available:  
<https://reneweconomy.com.au/worlds-biggest-battery-maker-unveils-higher-density-nil-degradation-longer-lasting-battery-packs-for-grid/>.

[206] "Economy Profile of South Sudan," Doing Business, 2020. Available:  
<https://archive.doingbusiness.org/content/dam/doingBusiness/country/s/south-sudan/SSD.pdf>.

[207] "Wind Power Operating Costs," Thunder Said Energy. Available:  
<https://thundersaidenergy.com/downloads/wind-power-operating-costs/>.

[208] "Utility-Scale Battery Storage," NREL Annual Technology Baseline, 2024. Available:  
[https://atb.nrel.gov/electricity/2024/utility-scale\\_battery\\_storage](https://atb.nrel.gov/electricity/2024/utility-scale_battery_storage).

[209] S. Ericson and D. Olis, "A Comparison for Fuel Choice for Backup Generators," NREL, JISEA, Mar. 2019. Available: <https://www.nrel.gov/docs/fy19osti/72509.pdf>.

[210] Parsian Industrial, "KTA50-G3 Diesel Engine Specification," Parsian Industrial, 2023. Available: [https://parsianind.com/uploads/product\\_files/KTA50-G3.pdf](https://parsianind.com/uploads/product_files/KTA50-G3.pdf).

[211] HOMER Energy, "Real discount rate," HOMER Pro, 2023. Available:  
[https://homerenergy.com/products/pro/docs/3.15/real\\_discount\\_rate.html](https://homerenergy.com/products/pro/docs/3.15/real_discount_rate.html).

[212] HOMER Energy, "Net present cost," HOMER Pro, 2023. Available:

[https://homerenergy.com/products/pro/docs/3.15/net\\_present\\_cost.html](https://homerenergy.com/products/pro/docs/3.15/net_present_cost.html).

[213] HOMER Energy, "Cash flow outputs," HOMER Pro, 2023. Available: [https://homerenergy.com/products/pro/docs/3.15/cash\\_flow\\_outputs.html](https://homerenergy.com/products/pro/docs/3.15/cash_flow_outputs.html).

[214] HOMER Energy, "Real discount rate," HOMER Pro, 2023. Available: [https://homerenergy.com/products/pro/docs/3.15/real\\_discount\\_rate.html](https://homerenergy.com/products/pro/docs/3.15/real_discount_rate.html).

[215] C. Banton, "Interest Rates: Types and What They Mean to Borrowers," Investopedia, Feb 2025. Available: <https://www.investopedia.com/terms/i/interestrate.asp>.

[216] The World Bank, "Pathways to Electricity Access Expansion in South Sudan: Off-grid and Mini-grid Market Assessment," 2023. Available: <https://documents1.worldbank.org/curated/en/099062423121021301/pdf/P17522707b8eef0490a6cc033f3f97890a8.pdf>.

[217] International Union for Conservation of Nature (IUCN), "ESMS Environmental and Social Impact Assessment (ESIA) Guidance Note," Mar. 2020. Available: <https://iucn.org/sites/default/files/2022-05/esms-environmental-and-social-impact-assessment-esia-guidance-note.pdf>.

[218] IEEE, "IEEE Policy 7.8: Code of Ethics," IEEE. Available: <https://www.ieee.org/about/corporate/governance/p7-8.html>.

[219] I. Bosco, "EES Orders Fuel Price Cut to SSP 5,700 per Liter," One Citizen Daily, Available: <https://onecitizendaily.com/index.php/2025/01/27/ees-orders-fuel-price-cut-to-ssp-5700-per-liter/>.

[220] Radio Tamazuj, "Juba Transport Fares to Reduce as Government Introduces Subsidized Fuel," Radio Tamazuj, July 2024. Available: <https://www.radiotamazuj.org/en/news/article/juba-transport-fares-to-reduce-as-government-introduces-subsidized-fuel>.

[221] "Automatic Voltage Regulation in Diesel Generators: What to Know," *Sustainable Maintenance*, Nov. 2024. Available: <https://www.sustainablemaintenance.com/2024/11/automatic-voltage-regulation-in-diesel.html>.

[222] G. Masters, "Renewable and Efficient Electric Power Systems, 2nd ed." Hoboken, NJ: John Wiley & Sons, Inc., 2013.

[223] J. Li, "Measuring and Understanding the Output Voltage Ripple of a Boost Converter," Texas Instruments. Available: <https://www.ti.com/lit/an/slva30/slva30.pdf>.

[224] "List of Voltages & Frequencies (Hz) Around the World," *Generator Source*. Available: [https://www.generatorsource.com/Voltages\\_and\\_Hz\\_by\\_Country.aspx](https://www.generatorsource.com/Voltages_and_Hz_by_Country.aspx).